OPTIMAL PARTITIONING OF A SURVEILLANCE SPACE FOR PERSISTENT COVERAGE USING MULTIPLE AUTONOMOUS UNMANNED AERIAL VEHICLES: AN INTEGER PROGRAMMING APPROACH

THESIS

Umar M. Khan, Major, USAF

AFIT-ENS-14-M-16

DEPARTMENT OF THE AIR FORCE
AIR UNIVERSITY

AIR FORCE INSTITUTE OF TECHNOLOGY

Wright-Patterson Air Force Base, Ohio

The views expressed in this thesis are those of the author and do not reflect the official policy or position of the United States Air Force, the United States Department of Defense or the United States Government. This is an academic work and should not be used to imply or infer actual mission capability or limitations.

AFIT-ENS-14-M-16

OPTIMAL PARTITIONING OF A SURVEILLANCE SPACE FOR PERSISTENT COVERAGE USING MULTIPLE AUTONOMOUS UNMANNED AERIAL VEHICLES: AN INTEGER PROGRAMMING APPROACH

THESIS

Presented to the Faculty

Department of Operational Sciences

Graduate School of Engineering and Management

Air Force Institute of Technology

Air University

Air Education and Training Command

in Partial Fulfillment of the Requirements for the

Degree of Master of Science (Operations Research)

Umar M. Khan, BS, MS Ed

Major, USAF

March 2014

AFIT-ENS-14-M-16

OPTIMAL PARTITIONING OF A SURVEILLANCE SPACE FOR PERSISTENT COVERAGE USING MULTIPLE AUTONOMOUS UNMANNED AERIAL VEHICLES: AN INTEGER PROGRAMMING APPROACH

Umar M. Khan, BS, MS Ed
Major, USAF

Approved:

//signed//	24 March 2014
James W. Chrissis, PhD (Chair)	Date
//signed//	24 March 2014
Darryl K. Ahner, PhD (Member)	Date
//signed//	24 March 2014
LTC Brian J. Lunday, PhD (Member)	Date

Abstract

Unmanned aerial vehicles (UAVs) are an essential tool for the battlefield commander in part because they represent an attractive intelligence gathering platform that can quickly identify targets and track movements of individuals within areas of interest. In order to provide meaningful intelligence in near-real time during a mission, it makes sense to operate multiple UAVs with some measure of autonomy to survey the entire area persistently over the mission timeline. This research considers a space where intelligence has identified a number of locations and their surroundings that need to be monitored for a period of time. An integer program is formulated and solved to partition this surveillance space into the minimum number of subregions such that these locations fall outside of each partitioned subregion for efficient, persistent surveillance of the locations and their surroundings. Partitioning is followed by a UAV-to-partitioned subspace matching algorithm so that each subregion of the partitioned surveillance space is assigned exactly one UAV. Because the size of the partition is minimized, the number of UAVs used is also minimized.

To my wife and my baby boy...

Acknowledgements

I would like to acknowledge Dr. James Chrissis, my advisor and thesis committee chair for all of the help and advice. In addition, Lieutenant Colonel Brian Lunday (US Army), Ph.D., and Dr. Darryl Ahner also deserve credit for great inputs and guidance along the way as committee members. Finally, my colleagues - fellow officers in the operations research program (both master's and Ph.D. students) - helped me get through some of the course work and provided an ear when I needed one. To all of those mentioned above, I say "thank you," and I hope I am afforded an opportunity to work with you again in the future.

Umar M. Khan

Table of Contents

Page

List of Figures

Figure Page

List of Tables

Table Page

OPTIMAL PARTITIONING OF A SURVEILLANCE SPACE
FOR PERSISTENT COVERAGE USING MULTIPLE
AUTONOMOUS UNMANNED AERIAL VEHICLES:
AN INTEGER PROGRAMMING APPROACH

I. Introduction

> Unarmed, unmanned aerial vehicles will be the tool of choice to monitor the activities of armed groups and the movement of civilians.
>
> – BBC News Africa, quoting Herve Ladsous, UN Peacekeeping chief in the Democratic Republic of the Congo [10]

1.1 Background

An unmanned aerial vehicle (UAV) carries a suite of sensors and sometimes armament, and it is usually controlled by personnel situated at a geographically separated location or perhaps near the range where the UAV is operating. While these vehicles have at times been referred to as Remotely Piloted Aircraft (RPA), Unmanned Aerial Systems (UAS), and more colloquially as "drones", they are referred to as UAVs in this research. Fixed-wing and rotary-wing UAVs are in production today, and several organizations make use of them. For example, the 2012 USAF Almanac lists three fixed-wing UAVs operated by the United States Air Force today in theater operations - The MQ-1 Predator, MQ-9 Reaper, and RQ-4 Global Hawk [6]. As another example, the United States Navy operates the rotary-wing RQ-8 Fire Scout to "provide reconnaissance, situational awareness, and precision targeting support for ground, air and sea forces" [12]. Government organizations not part of the Department of Defense (DoD), such as the Department of Homeland Security (DHS) and

law enforcement agencies, also use these aerial vehicles. In fact, the DHS not only makes use of UAVs, but is accelerating the integration of UAVs into law enforcement agencies for potential use over US airspace [40]. Finally, even some commercial entities are researching novel ways to conduct business using unmanned aircraft. In 2013, Jeff Bezos, CEO of online retailer Amazon, declared that within four to five years, his company would be able, on a limited basis, to deliver packages quickly to customers using a UAV delivery system [17].

Because of the many potential applications of UAVs, the industry that develops and markets these vehicles has responded by designing a wide variety of UAVs in terms of capability, size, takeoff and landing method, fuel, allowable payloads, and other factors. These various UAVs come in many forms. For example, considering exclusively the military applications of UAVs, the ScanEagle surveillance platform weighs 37.9 pounds, has a wingspan of just 10.2 feet and is fueled by gasoline. The much larger RQ-4A Global Hawk has a gross weight of 26,750 pounds, carries no weapons, has a wingspan of 116.2 feet, and runs on JP-8 fuel. Finally, the rotary-wing MQ-8B Fire Scout weighs about 2,070 pounds empty and can be modified to carry weapons. [3] The plethora of available UAVs is just one indication of their prominence in both domestic and international affairs dealing with security and commerce. Further importance of UAV surveillance capabilities is clear, given the DoD's position that the reconnaissance and surveillance mission remains the number one combatant command priority for unmanned systems [3].

The importance of UAVs to military intelligence gathering means that there may need to be many UAVs in the collective inventories of the U.S. armed forces. Because resources are limited, the DoD cannot simply acquire an unlimited number of UAVs to perform missions. That truth is underscored by the fact that the United States is now in an era of government sequestration in which the fastest growing occupation in the United States Air Force - war zone surveillance - is generating budget decisions that call for the produc-

tion of billions of dollars worth of UAVs [23]. However, not everyone is convinced that this rate of expenditure on UAVs is warranted. In an article for *National Defense*, former Secretary of the Air Force Michael Donley suggested that the parallel growth of manpower requirements warrants a re-look at UAV procurement activities. He expressed that spending on intelligence-surveillance-reconnaissance (ISR) capabilities might be excessive because such investments may be duplicating funding efforts by other military departments. In the same article, former Vice Chief of Staff of the Army General Peter Chiarelli stated, "With leaner times approaching and U.S. forces in Afghanistan drawing down, the Pentagon may no longer afford or need so much ISR support." Chiarelli noted that the military departments may have too much overlap in UAV capabilities and that these could be cut down, considering the redundancies now in place, in order to reduce unnecessary spending. [23]

This research considers exclusively a nonlethal military application of multiple UAVs. Specifically, the concern is with the problem of persistent surveillance, which is the use of a team of UAVs to cover an area of land while meeting time over target constraints. The term "persistent surveillance" is a source of confusion, but it is defined precisely in Section 1.1.1 in contrast to several other terms that are often taken as synonymous in the literature. Some key assumptions and restrictions will also apply and are described later, in Section 1.4.

1.1.1 Persistent Surveillance.

To understand precisely what "persistent surveillance" means, it is defined explicitly here because it is not a term that is used in the same sense across the literature. For example, Joint Publication 2-0 [9] uses the term, but fails to define it. Joint Publication 2-01 [7] defines persistent coverage as "near-continuous surveillance capability of the area of interest as opposed to periodic reconnaissance." Although that language is closer to how it is used here, it is still not precise enough to formulate the problem at hand. The DoD

Dictionary [8] defines persistent surveillance as "A collection strategy that emphasizes the ability of some collection systems to linger on demand in an area...." This definition is not sufficient for this research because it is too vague to provide a good foundation for a precise formulation. Finally, a report produced by the Army Science Board in 2008 [2] based on a study involving surveillance states, "Persistence is not well defined." The definition of persistent used in the Army study was: "If I have what I need, when I need it, for as long as I need it, it is persistent." Because of the confusion surrounding the term "persistent surveillance," the definitions that follow differentiate between that term and other terms that are sometimes taken as synonymous.

Definition I.1. *Persistent surveillance* is surveillance of an area of land by a collection of vehicles over a mission timeline such that none of a specified collection of pre-defined points of interest on the ground is left unobserved for longer than a defined, usually small (relative to mission timeline), amount of time.

Definition I.2. *Continuous surveillance* is surveillance of an area of land by a collection of vehicles over a mission timeline such that none of a specified collection of pre-defined points of interest on the ground is left unobserved at any time. Further, when the points of interest encompass every point on the area of land to be observed, then the program of surveillance is termed *total continuous surveillance*.

Definition I.3. *Standby surveillance* refers to the availability of a surveillance platform within the vicinity of points of interest over a surveillance space. The vicinity of those points is defined by a commander or other decision maker in the area of operations.

Definition I.4. *Periodic surveillance* is surveillance of an area of land based on a schedule. In this case, vehicles observe a location for a period of time, depart, return after a period of time, and continue this pattern on a regular schedule as determined by a decision maker.

This research uses the term "persistent surveillance" as it is defined in Definition I.1, which is essentially the definition used by Nigam and Kroo [34]. In practice, this persistent

surveillance is best executed by autonomous UAVs. The UAVs are considered autonomous in the sense that no significant human interaction is required from the time the vehicles are launched on a mission to the time they prepare to return to the base of operations. That is, the UAVs are preprogrammed to fly a particular pattern over their assigned regions.

1.2 Problem Statement

Given an area of land R and set P of interior locations of interest, the problem is to generate a persistent UAV surveillance program, using the minimum number of UAVs, that sweeps all of R continually over a mission timeline while revisiting locations in P within a specified time increment. To be clear, this is a two-fold problem. The first part of the problem is to decide how to minimize the number of UAVs that move over the space to provide persistent surveillance. The second part involves deciding which particular UAVs should be used to carry out the surveillance program such that the revisit time constraint is met for each of the points in P.

1.3 Research Objective and Scope

The objective of this research is to describe a way to determine an optimal assignment of UAVs to an area of land for automatic surveillance for a specified period of time. Here, optimal means utilizing the minimum number of UAVs to persistently cover a given surveillance space with minimum revisit times over specified locations within the space. Covered in this research are methods for partitioning areas into smaller mutually exclusive, collectively exhaustive areas and ways to assign UAVs to partitioned subregions of a surveillance space. Also covered is a brief discussion on the logistics of delivering UAVs to areas of operation as well as future work.

1.4 Assumptions

A few important assumptions apply to this research, and they are listed in this section.

1. The UAVs fly in uncontested airspace. This is possible if air supremacy is first achieved, which is also assumed.

2. Launch, recovery, and maintenance operations occur near enough to the area of land that is of interest to effectively carry out the program of surveillance.

3. Not all available UAVs have the same characteristics. Some UAVs are small and more capable of covering smaller areas through line of sight control while others can stay aloft on the order of days and sweep large areas.

4. All available UAVs are capable of being pre-programmed to fly with a measure of autonomy over the surveillance space. This is not a critical assumption, but rather it is a suggestion of how to implement the surveillance program effectively.

5. A UAV is considered to have covered a point over the surveillance space if it flies over that point. In other words, for simplicity, the precise physical characteristics of the UAV payload, *i.e.*, its sensors, are not taken into account. The cameras might be pointed to the side or in a forward direction, but the problem is simplified here by modeling the camera swath as transverse to the fuselage, extending horizontally along the craft's roll axis.

6. The UAVs fly at slightly different altitudes in order to avoid colliding with one another.

1.5 Summary

Using UAVs to observe a section of land has some clear advantages over relying on ground intelligence, solely on satellite imagery, or on manned aircraft alone. Ground in-

telligence carries the most risk to both U.S. military forces and local residents of the area of operations, and is therefore not desirable if less risky alternatives can provide equivalent intelligence (in cases where what we are interested in is images and movement of people in the area of interest). Satellites cannot be dedicated to a specific spot on the earth without extensive pre-planning, constellation design, and orbital analysis. This requires massive amounts of resources in terms of time and money, and such an undertaking is not normally used to survey *ad hoc* areas of interest, but rather long-term, strategic interests (for example, the nuclear launch sites of a foreign power). In contrast, UAVs are designed for just such missions where we need to collect information on the fluid movements of potential targets and on locations where suspicious activity may be taking place.

Pilots flying traditional aircraft can persistently survey an area just as autonomous UAVs can, but using manned aircraft to conduct persistent surveillance makes less sense than using UAVs to do the same. Persistent surveillance is a task best left to a mechanical device, not a human being who is naturally prone to error and even more likely to commit errors performing such a repetitive area sweep over long periods of time. Thus, for good reason, it makes sense to use UAVs that can operate in an autonomous fashion to conduct persistent surveillance in an area of operations.

II. Literature Review

2.1 Introduction

Covering or providing surveillance over an area of land using one or more UAVs has been studied from many different angles. There are as many variations on the problem as there are methods for formulating and solving them. This chapter presents some of those many varieties of the coverage problem and discusses how researchers have approached the task of formulating and solving associated models.

2.2 Previous Work

2.2.1 Path Planning.

Several researchers have addressed the problem of covering an area using UAVs. There are many different ways to define the problem and also many ways to solve the problems so defined. The specific case addressed in this research concerns persistent surveillance, and certainly, this is a topic that has been studied. To better understand the persistent coverage problem, we consider the many ways UAV coverage in general has been defined before considering persistent coverage specifically, because the methods of defining and solving all such problems are instructive.

Pohl [37] used evolutionary computation to satisfy multiple objectives related to UAV mission planning; in so doing, he extended the concept of the vehicle routing problem with time windows (VRPTW) to the swarm routing problem (SRP), involving a large set (or swarm) of UAVs. The basic problem, as Pohl points out, has not changed: to assign paths to multiple UAVs or a UAV swarm to cover all sites (*i.e.*, visit all targets) with an appropriate number of UAVs at each site at minimum cost and maximum safety.

In this context, an example helps to clarify the situation. Suppose ground vehicles depart from a depot carrying some packages up to each vehicle's capacity. These vehicles

must deliver their packages to a set of locations within some time window for each delivery. Further, each location is to be visited only once by a vehicle. The depot itself is also open during a specific time window only - it can be considered as just another site to visit. The task is to determine the shortest set of paths such that all packages are delivered within their time windows and all vehicles return to the depot before it closes. This model can be applied to UAVs delivering a camera package over sites defined to be ground space that needs to be observed by at least one UAV within specified time windows (say, within every five minutes). In that case, persistent coverage of the battlespace can be modeled as a VRPTW.

In a related approach, Toth (as cited in [37]) provides a graph-theoretic formulation of the VRPTW that can also be adapted to the persistent surveillance problem. In his formulation, the locations to visit are vertices of the graph and belong to the set $V = \{v_0, v_1, \cdots, v_n\}$, and the distances between any two sites i and j are captured by the set $A = \{(v_i, v_j) \in V \mid i \neq j\}$, which is the set of edges in the graph. The time windows arise by stipulating that each site must be visited no earlier than some earliest arrival time E, and no later than its latest arrival time L. The objective here is to find the assignment of UAVs to paths that minimize cost, which is defined by the total distance traversed by all vehicles traveling their assigned paths. Setting $E = L$ and assuming vehicles return to each site continuously while moving along their assigned paths, the maximum revisit time to each location can be found given the time of the first visit at each location.

Toth's formulation of the VRPTW can be regarded as the archetypal problem in its class, and it can be modified in a number of ways to suit various specific scenarios. Returning to the work of Pohl, his modification of the VRPTW for UAVs - an SRP - arises from his observation that the VRPTW assumes that one vehicle visits each customer, and it works well for ground-based delivery operations. However, when scaled up to a swarm of air-based UAVs for multiple targets, that is not the most efficient way to satisfy the ob-

jectives. Instead, Pohl argues that using a swarm of UAVs exploits the divisibility of the swarm and route subgroups of UAVs to different targets in parallel, having them regroup at other targets. This avoids the inefficiency of sending one vehicle to one target at a time.

The SRP formulation begins the same way as the VRPTW. In the SRP, there is a depot and a number of vehicles that must depart from the depot, service a number of customers within specified time windows, and return to the depot before it closes. Much of the VRPTW formulation carries over to the SRP; in particular, the same overall graph structure with the same nomenclature for the vertices and edges holds as in the VRPTW. Each customer in this case is a target having its own time window beginning at the earliest arrival time E, and ending at its latest arrival time L. Time L is the time by which a UAV must arrive at the target in order to complete service and still be able to return to the depot before it closes. Arriving early results in waiting time W. Where the SRP diverges from the VRPTW is that demand in the SRP is indicated by the number of UAVs that need to be at a target within its time window for the duration of the service time. Before, in the VRPTW, demand was satisfied by vehicle capacity. Also, in the VRPTW, service time is the time needed to make a delivery (*e.g.*, get an answer at the door, transfer the package, receive a signature, exchange pleasantries, etc.), but in the SRP service time is defined by the time UAVs need to spend over a target. To simplify problem complexity, Pohl stipulates that UAVs only split into or join sub-swarms at targets.

With these considerations in place, the objective of the SRP is to determine the set of paths for the UAVs such that the total distance is minimized, and the formulation is identical to that of the VRPTW, with a few exceptions. In the VRPTW, each vehicle has some capacity defined by what it can carry, but in the SRP, the capacity is defined by a UAV's travel capacity. In addition, the VRPTW calls for each location to be visited by only one vehicle. This constraint is removed in the SRP formulation. Demand at locations in

the SRP is also defined differently from demand in the VRPTW. In the SRP, the demand at a location is defined by the number of UAVs that must visit the location.

Suppose there are more objectives for the mission than just meeting demand at a set of targets, and there is a need to continuously revisit targets over a period of time. Maybe using a minimum number of UAVs to perform the mission is important. In those cases, one objective function is inefficient, and a multiobjective optimization problem may be indicated. Pohl's [37] model represents just such a multiobjective optimization problem. In fact, Pohl considers what happens if a vehicle exceeds its capacity to service a route, arrives early, or arrives late. In these cases, a swarm of UAVs can split into multiple subswarms, adding UAVs to the groups when necessary, to travel to multiple targets in parallel. Pohl's multiobjective formulation of the SRP then requires an adjustment to the objective function, namely, adding more functions to optimize. The main modification here is based on the fact that wait time is defined by the difference between a UAV's arrival time and the arrival time of the latest UAV, if the latest arrival time is past the earliest service time at a location. The reason for this is that all vehicles that are required to be on target to service it must be in place before service can begin. Pohl points out that a multiobjective formulation to this UAV routing problem is more effective because the problem has an irregular solution space, stating, "Time constraints introduce irregularities to the Pareto front such that non-dominated solutions become more isolated." Pohl's approach is to use evolutionary algorithms to solve his multiobjective problem.

Ha [27] looks at the task of continuously covering an area of land using the minimum number of UAVs. Sometimes, Ha argues, continuous coverage can net important results that would otherwise be out of reach. For example, during Operation Iraqi Freedom, it was 600 hours of continuous surveillance of an Al-Qaeda leader that led to his demise; moreover, a gap in the coverage could have given the targeted individual an opening to escape. Based on these considerations, Ha develops a cyclic scheduling approach to deter-

mine the minimum number of UAVs to cover an area of land continuously. To understand his approach, consider K UAVs comprising the set $F = \{(\Delta_1, T_1), (\Delta_2, T_2), \cdots, (\Delta_K, T_K)\}$. If $V_i = (\Delta_i, T_i)$, then, $F = \{V_1, V_2, \cdots, V_K\}$, where V_i is the attribute vector of UAV i. The variable Δ_i is the UAV's round trip time and T_i its loiter time. Further the variable Δ_i itself is an aggregation of three components for UAV i: ξ_1^i, the time from base of operations to target; ξ_2^i, the time from target back to the base of operations; and ξ_3^i, time spent in maintenance and repairs at the operating base. Thus, $\Delta_i = \xi_1^i + \xi_2^i + \xi_3^i$.

Having expressed the attribute vectors of the UAVs, Ha then sets about defining a cyclic schedule in this context. First, the expression $V_i \rightarrow V_j$ denotes that UAV i does a mission handoff to UAV j. If that mission handoff is successful, then, he writes $V_i \xrightarrow{s} V_j$. An ordered sequence of UAVs $E = (V_{i_1}, V_{i_2}, \cdots, V_{i_K})$, where $V_{i_j} = (\Delta_{i_j}, T_{i_j}), j = 1, 2, \cdots, K$ is called a cyclic schedule if $V_{i_1} \rightarrow V_{i_2} \rightarrow \cdots \rightarrow V_{i_{K-1}} \rightarrow V_{i_K} \rightarrow V_{i_1}$. This situation is illustrated in Figure 1, which depicts a cyclic schedule of size 6, corresponding to having six UAVs.

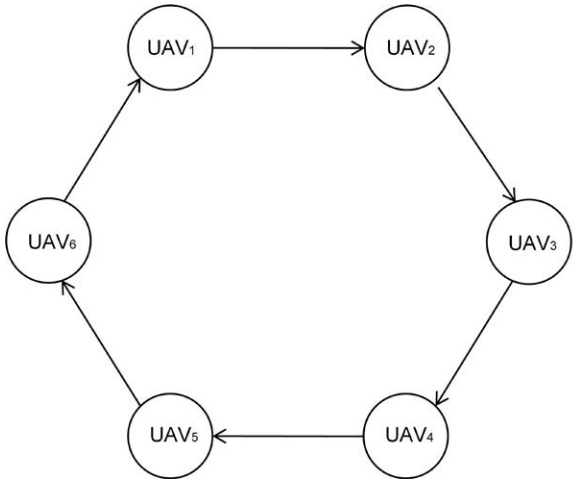

Figure 1. Cyclic Schedule ([27], p. 13)

Each directed arc in the figure depicts a mission handoff from the originating node to the terminal node. So, at a given target, UAV 2 arrives to receive a handoff from UAV 1 just as UAV 1 is ready to depart for base. When UAV 2 arrives, it loiters for time T_2 and hands off to UAV 3, and the process continues. A cycle is said to be completed when UAV

6 hands off to UAV 1. Any particular UAV is only used once in each cycle and when not in use, it is in "rest" at the base for refueling and maintenance. Critically, as Ha shows, continuous coverage is assured with $N \geq 2$ UAVs such that $(N-2)T < \Delta \leq (N-1)T$. Then, a schedule with N UAVs allows continuous coverage and one with $N-1$ or fewer UAVs introduces coverage gaps at a particular target. The problem then becomes one of minimizing N such that the schedule has no coverage gaps.

What Ha found was that continuous coverage is only possible in the deterministic case and that the number of UAVs required is increasing in round-trip time and decreasing in loiter time (assuming the other is held constant). Ha first considers this deterministic case with a homogeneous fleet of UAVs and then with a nonhomogeneous fleet, formulating both as scheduling problems. It is in this context that he introduces the concept of a *minimum cyclic schedule* that he uses to compute a schedule using the minimum number of UAVs to continuously cover a target area. In that case, the ratio T/Δ becomes a performance measure for a UAV; a large value for the ratio indicates that a UAV loiters longer with less support from other UAVs. Finally, he considers the stochastic case (both risk-neutral and risk-averse) in which UAVs have attributes that follow some probability distribution. The stochastic formulation introduces coverage gaps [27].

Ha provides s a linear programming formulation to find an optimal cyclic schedule that allows continuous coverage of the target area. The linear programming formulation begins with the definition of a binary decision variable, x_j as

$$x_j = \begin{cases} 1, & \text{if UAV } j \text{ is included in the schedule} \\ 0, & \text{otherwise.} \end{cases}$$

Thus, the objective is: $\min z = \sum_{i=1}^{K} x_i$. The feasible region of the linear program is the set of all feasible cyclic schedules. For convenience, Ha relabels T_i as a_i and Δ_i as b_i, where i

ranges over the set of UAVs. Then, he reasons, the feasibility conditions of a UAV cyclic schedule are given as

$$\sum_{\substack{j=1 \\ j\neq i}}^{N} a_j x_j \geq b_i,\ i = 1,2,\cdots,K,$$

which expresses the desire for each selected UAV's loiter time to exceed its round-trip time to a target. Putting all this together gives the binary integer programming formulation:

$$\min z = \sum_{i=1}^{K} x_i$$

subject to

$$\sum_{\substack{j=1 \\ j\neq i}}^{N} a_j x_j \geq b_i,\ i = 1,2,\cdots,K$$

$$x_i = \{0,1\},\ i \in \{1,2,\cdots,K\}.$$

As UAV fleet size increases, this model would take longer and longer to solve to optimality (if at all possible) using traditional methods. Realistically, as the fleet size goes up, a heuristic approach will be required.

If the continuous coverage requirement is relaxed, allowing for small coverage gaps not to exceed some specified amount of time ε, then the continuous coverage problem can be generalized. Because the optimal schedule is determined by the ratio Δ/T, $\Delta/(T+\varepsilon) < \Delta/T$ for some small $\varepsilon > 0$. This implies that fewer UAVs are needed under the relaxed assumption, and what results is a model of persistent rather than continuous surveillance. Note that the original formulation with perfect handoffs is the same as the new model that admits coverage gaps with $\varepsilon = 0$.

If the target area is dynamic and if contact with the ground station and between UAVs is desired, then a trade space arises between achieving good coverage and maintaining connectivity. This problem of coverage in wireless sensor networks is important and has been investigated by many. Along these lines, Yanmaz [41] considers using autonomous UAVs to survey an area of land with such constraints. The UAVs must maintain connectivity with a ground station and with each other at all times. He presents a probabilistic connectivity-based mobility model for a network of autonomous UAVs. In [41], UAV autonomy means that each UAV decides its own path taking into account only its communication requirement. The trade space arises because of UAV transmission ranges. A given area can be sensed faster if UAV coverage overlap is minimized, but the UAVs may need to fly closer to each other in order to stay connected and to be able to deliver the sensed data to the ground station.

Traditionally, mobility models for sensor networks have been coverage-based; an example is found in Yanmaz and Guclu (as cited in [41]). In the example, there is an assumed repulsive force between UAVs; at any given navigation decision point, a UAV, say UAV 1 in a network of (suppose) four UAVs, would experience a collection of repulsive forces that act on it by the other UAVs. The resultant force vector $\vec{R}_1$ is the vector sum of the forces incident on UAV 1, and the net force on UAV 1 is given by $\vec{R}_1 = \sum_j \vec{F}_{j1}$. This forces UAV 1 to travel in the direction of vector $\vec{R}_1$. Further, the forces acting on UAV 1 are inversely proportional to the distances from UAV 1 to the other UAVs - the closer UAVs come to each other, the harder they push on each other. In addition, UAV 1 experiences a force inversely proportional to its sensing range in the direction of its motion, which ensures that the UAV avoids retracing already covered areas.

Whereas in the coverage-based model each UAV computes a resultant force and moves accordingly, in a connectivity-based model, UAVs take communication into account. The algorithm Yanmaz proposes has the UAVs using only their current location and direction to

maintain contact with each other and the ground station. The algorithm is general enough to allow for a heterogeneous network of UAVs that can enter and leave the system as they surveil an area of land that may not be fixed. Because the algorithm is probabilistic, momentary loss of contact between a UAV and the ground station can occur, but it is highly unlikely that a UAV will become isolated, and if so, highly unlikely it would be isolated for very long.

Yanmaz compares the coverage-based and connectivity-based UAV motion models when the ground station is in the corner of the surveillance space and also when it is in the center. What he finds is that a critical spatial density is required for the connectivity-based model to be an efficient coverage plan. Further, the location of the ground station affects the connectivity-based mobility model by a scaling factor only. As for transmission range, as that increases, spatial coverage gets better in the connectivity-based model because as sensing range increases, the UAVs can spread out more and the system tends desirably toward less sensing overlap. Yanmaz also investigates how the system behaves under a single-hop assumption versus a multi-hop assumption. In a single-hop scenario, coverage-based mobility performs better as the number of UAVs increases, but performance is not significantly improved in the connectivity-based model as the number of UAVs increases. Moving to the multi-hop scheme, however, the performance gap shrinks; then, the important factor in coverage and communication becomes spatial density, or, the number of UAVs over the surveillance space [41].

Ahmadzadeh, Buchman, Cheng, Jadbabaie, Keller, Kumar, and Pappas [14] use a different approach to the UAV coverage problem. They consider planning the trajectories of multiple autonomous UAVs to maximize spatio-temporal coverage such that the UAVs avoid collisions and satisfy initial and final position requirements. They developed algorithms with the needs of two programs in mind: DARPA HURT (Defense Advanced Research Projects Agency Heterogeneous Urban RSTA (reconnaissance, surveillance and

target acquisition) Team) and the Office of Naval Research (ONR) Intelligent Autonomy program. The Intelligent Autonomy program focuses on developing software to coordinate autonomous UAVs, USVs (unmanned surface vehicles), and UUVs (unmanned undersea vehicles).

In [14], Ahmadzadeh, *et al.* design the Time Critical Coverage (TIC^3) planning tool as part of the Integrated Cognitive-Neuroscience Architectures for Understanding Sense-making (ICARUS) project, which is one of several projects under the Intelligent Autonomy program of the ONR. The TIC^3 planning tool starts when it receives a request for a motion plan for each of several vehicles under its control, along with the entry and exit state for each vehicle - information such as three-dimensional location, velocity vector, and arrival time. The planning tool then requests information on obstacles, threat zones, and sensor availability, which then allows it to determine the largest area that can be covered. It outputs not way-points but secondary objective points complementing the primary mission set in paths between entry and exit. If needed, the planning tool can be invoked more than once during a mission as required. The authors note that the problem has been addressed using cellular decomposition, where a cell is considered covered when traversed by a UAV (or when it scans the entire cell, usually using a boustrophedon or lawnmower, back-and-forth motion), but they also note that this has been used mainly in the single-robot situation. Also, most prior work in area coverage has focused on sensor networks. Instead, Ahmadzadeh, *et al.* use a sampling-based technique to cover an area.

Because TIC^3 is a variation of the motion planning problem (with optimality considerations), it is normally an NP-hard problem. However, the TIC^3 problem is constrained by a time budget. As such, they needed an efficient way to get good solutions. To that end, they formulate a sampling-based technique for area coverage. The variables used in the formulation are given in Table 1.

Table 1. Variable definitions for TIC^3 planner

Variable	Definition
N	Number of heterogeneous autonomous vehicles
v_i	Constant forward velocity of vehicle i
$w_i \in W_i$	Controllable turning rate of vehicle i
$x_i = (p_i^x, p_i^y, \theta_i) \in X_i$	State of vehicle i: position (p_i^x, p_i^y), orientation θ_i
$\{p_i^{\text{entry(exit)}}, t_i^{\text{entry(exit)}}\}$	Boundary position and time conditions
$\Omega \subset \mathcal{R}^2$	Coverage area, union of polygonal regions
$O \subset \mathcal{R}^2$	No-travel zones, union of polygonal regions
Ψ	Sensor footprint mapping; $\Psi_i : X_i \to 2^{\mathcal{R}^2}$
T_{budget}	Time given to compute the solution

Using these variable definitions, the dynamics of vehicle i are represented by

$$\dot{p}_i^x = v_i \cos(\theta_i);\ \dot{p}_i^y = v_i \sin(\theta_i);\ \dot{\theta}_i = w_i. \tag{1}$$

Equation 1 can also be written in shorthand as the function $\dot{x}_i = f_i(x_i, w_i)$.

An exact solution to the problem is the set of trajectories for N vehicles $\{x_1^*(t), x_2^*(t), \cdots, x_N^*(t)\}$ such that

$$\{x_1^*(t), x_2^*(t), \cdots, x_N^*(t)\} = \underset{\{x_1(t), \cdots, x_N(t)\}}{\text{argmax}} \bigcup_t (\Psi_i(x_i(t)) \cap \Omega),$$

the maximum coverage for the union of intersections of sensor footprints within the coverage area. As vehicles cover the area, no-fly and no-sail zones must be respected, expressed by $O \cap \{x_1^*(t), x_2^*(t), \cdots, x_N^*(t)\} = \emptyset$. In addition, the boundary conditions, $p_i^*(t_i^{\text{entry}}) = p_i^{\text{entry}}$, $p_i^*(t_i^{\text{exit}}) = p_i^{\text{exit}}$, and system dynamics, $\dot{x}_i^*(t) = f_i(x_i^*(t), w_i(t))$, where $w_i(t) \in W_i, 1 \leq i \leq N$, must also be satisfied. Ahmadzadeh, *et al.* provide a graphical representation in [14] of the scenario involving two vehicles, reproduced in Figure 2.

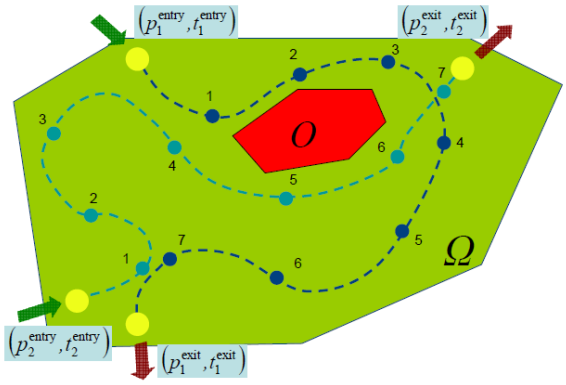

Figure 2. TIC^3 **problem with two UAVs, ([14], p. 5)**

As Figure 2 suggests, to apply trajectory solutions to vehicles, the trajectories must be converted into way-points for each vehicle. Connecting the dots along way-points gives us trajectories of maximal coverage that also avoid no-fly and no-sail zones.

The TIC^3 problem is an infinite-dimensional non-convex optimization problem because the search space is the infinite set of all feasible trajectories, and the combination of the coverage area and no-fly/no-sail zones could produce non-convex constraints. Because of this, Ahmadzadeh, *et al.* discretize the problem (discretizing trajectories and time), giving an approximate discrete representation. Trajectory discretization means that the allowable turning rates for vehicle i are a subset W_i^s of W_i, $W_i^s = \{w_i^1, w_i^2, \cdots, w_i^{m_i}\}$, where m_i is the number of discrete turning rates allowed for vehicle i. Time discretization means that vehicle i turns at some rate in W_i^s for an increment of time δt_i. Each vehicle can only adjust its turning rate every δt_i time units, implying that during a mission, vehicle i will conduct at most $K_i = \left\lceil \frac{T_i}{\delta t_i} \right\rceil$ turns. The discretized version is still high-dimensional and exhaustive search of such a space may yield an optimal solution, but it is likely that it would also violate the time budget to produce a solution. Instead, Ahmadzadeh, *et al.* use heuristics to find suboptimal solutions.

The remainder of [14] compares receding horizon control (RHC) methods with sampling-based methods, which are the two broad categories of heuristics the authors consider for

computing solutions for the TIC^3 problem. The RHC approach, in an iterative fashion, implements a dynamic programming type of algorithm to optimize a cost function over a period of time called the *planning horizon*. A generated trajectory is implemented over a shorter execution horizon and the optimization is repeated for the state into which the system will transition; usually a terminal cost is added to the objective function to guarantee convergence of the RHC method. An RHC optimization problem generally estimates the cost-to-go function from a selected terminal state to the goal. If no-travel zones are represented as the union of regions $A_k x > B_k$, the coverage problem can be expressed as an IP [14]

$$\underset{\{W_1^S,\cdots,W_N^S\}}{\operatorname{argmin}} \; [area(\Omega - \bigcup_{i,t} \Psi_i(x_i(t)))]$$

subject to

$$x_i(t_i^{entry}) = x_i^{entry}$$

$$x_i(t_i^{exit}) = x_i^{exit}$$

$$\|x_i(t) - x_j(t)\| > d_{safe}$$

$$A_k x_i(t) > B_k.$$

The size of this problem is quite large, so Ahmadzadeh, *et al.* break it down into a set of smaller IPs. If a planning horizon is $[i\tau,(i+1)\tau], i = m, m+1, \cdots, n$, where $m\tau = t^{\text{entry}}$ and $n\tau = t^{\text{exit}}$, then the RHC for the time period $[k\tau,(k+1)\tau]$ is the IP [14]

$$\arg\min[area(\Omega(k-1) - \bigcup_i \psi_i(x_i(t)))] + \sum_i C(x_i((k+1)\tau), x_i^{exit}, t_i^{exit})$$

subject to

$$x_i(k\tau) = x_i^{exit}((k-1)\tau)$$

$$\|x_i(t) - x_j(t)\| > d_{safe}$$

$$A_k x_i(t) > B_k.$$

Here, $\Omega(k-1)$ is the area remaining to be covered and the function C is the terminal cost for vehicle i.

In computed results, Ahmadzadeh, *et al.* found that in order to get 90% coverage using the RHC method, the time required was about one hour, which is far more than T_{budget}. However, reducing the planning horizon can cut the computation time at the expense of coverage. For example, they achieved 80% coverage in 83 seconds of computation time using the RHC method under a shortened planning horizon. In contrast, the sampling-based method was very fast, computing solutions between 17 and 36 seconds, resulting in coverage rates between 60 and 68 percent. This may be acceptable for some circumstances, and if it is, then the fast, sampling-based method might be the best method to use. Instead, if a greater amount of coverage is critical, then the RHC method is the better choice.

In another study, Ahmadzadeh, Keller, Jadbabaie, and Kumar [15] use an integer programming formulation to present a path planning algorithm for multiple fixed-wing UAVs with body-fixed cameras. To get a sense of how the field of view (FOV) of a UAV camera is related to its flight path, consider Figures 3 and 4, depicting front and left camera FOVs, respectively. The work in [15] specifically addresses the cooperative motion planning problem for heterogeneous UAVs used in surveillance. Each vehicle is modeled as a non-holonomic point-mass moving at constant speed with minimum turning radius (also known as *Dubin's car* in the literature, as cited in [15]). In the paper, they note that much research has been conducted concerning multi-UAV task scheduling and planning, but those studies

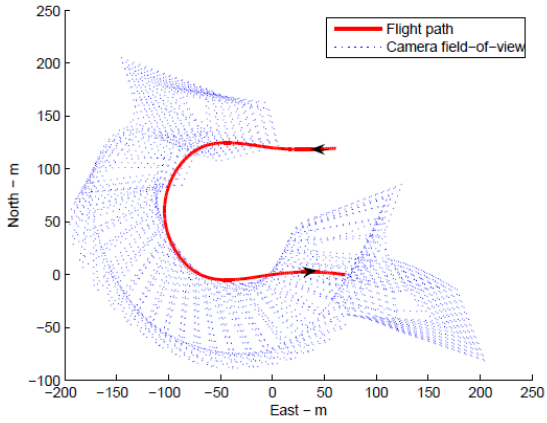

Figure 3. Front camera FOV ([15], p. 1)

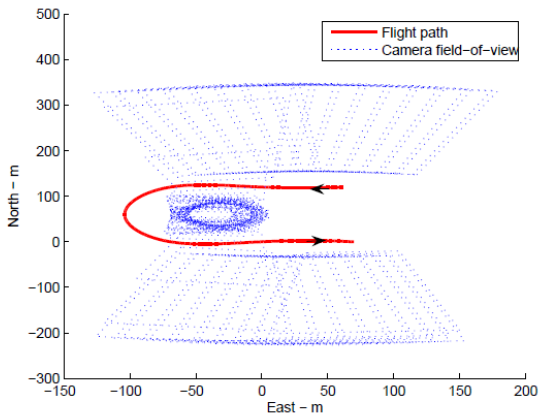

Figure 4. Left camera FOV ([15], p. 2)

do not address coverage. Further, some work on the coverage problem uses cellular decomposition techniques, where each cell is considered covered when a vehicle crosses it or when the vehicle performs some motion over the cell (such as boustrophedon, or back-and-forth motion). However, those methods focus on single-robot coverage.

The problem in [15] is described by a closed, bounded region $\Omega \subset \mathscr{R}^2$ over which N heterogeneous UAVs $\{u_1, u_2, \cdots, u_N\}$ operate while carrying fixed cameras with refresh time τ. The objective is to find feasible trajectories $\{\gamma_1(t), \gamma_2(t), \cdots, \gamma_N(t)\}$ for UAVs $\{u_1, u_2, \cdots, u_N\}$ in order to maximally cover the region Ω in each time interval $[n\tau, (n+1)\tau], n = 0, 1, \cdots$. An arbitrary point p is covered in time interval $[k\tau, (k+1)\tau]$ if there exists time $t \in [k\tau, (k+1)\tau]$ such that p is visible to at least one UAV. It is assumed that UAVs travel at fixed and distinct altitudes at constant speeds $\{v_1, v_2, \cdots, v_N\}$ along paths of bounded curvature.

Ahmadzadeh, Keller, Jadbabaie, and Kumar use mathematical conventions which should be explained before proceeding. First, if $\alpha = (\alpha_1, \cdots, \alpha_n)$ is an n-tuple of nonnegative integers, then consider the sum defined by $[\alpha] = \sum \alpha_i$ and the partial derivative defined by $\dfrac{\partial^\alpha}{\partial x^\alpha} = \dfrac{\partial^{[\alpha]}}{\partial x_1^{\alpha_1} \cdots \partial x_n^{\alpha_n}}$. Then, if $f : \mathscr{R}^n \to \mathscr{R}$, we say that f is of class C^k if it is at most k times continuously differentiable (up to k partial derivatives exist and are continuous). If $f : \mathscr{R}^n \to \mathscr{R}^m$, then f is class C^k if each function f_i is class C^k. Finally, let $\|\cdot\|$ be the usual

Euclidean norm. These concepts are defined in order to later define feasible trajectories and the like.

Now, given a subset $V \subseteq \mathscr{R}^2$, the measure $\mu(V)$ is defined by

$$\mu(V) = \int_V \chi_V(x)dx, \tag{2}$$

where

$$\chi_V(x) = \begin{cases} 1, \ x \in V \\ 0, \ x \notin V. \end{cases}$$

The center of mass of the inertia is given by the integral

$$M(V) = \int_V xdx. \tag{3}$$

Next, Ahmadzadeh, Keller, Jadbabaie, and Kumar define a UAV trajectory by the function $\gamma : [t_0, t_1] \to \mathscr{R}^2$ as $\gamma_i(t) = (x_i(t), y_i(t))$; then, the curvature (signed) $\kappa(t)$ of a path $\gamma(t)$ is given by

$$\kappa(t) = \frac{1}{\|\gamma'(t)\|^3}(x(t)'y(t)'' - x(t)''y(t)').$$

Given these mathematical expressions, a trajectory is feasible for UAV u_i if it is class C^2, or twice continuously differentiable and $|\kappa(t)| < 1/\rho_i$ for all t where ρ_i is the minimum turning radius of a circle that is flyable by u_i. Adapting the work of Do (as cited in [15]), if $\kappa : [t_0, t_0 + \tau] \to [-1/\rho, 1/\rho]$ is a piecewise continuous curvature function for the planar trajectory $\gamma(t)$ with initial conditions $\gamma(t_0) = (x(t_0), y(t_0)), \theta(t_0)$, and constant speed

$\|\gamma'(t)\| = v_i$, then the parameterized curve $\gamma : [t_0, t_1] \to \mathscr{R}^2$ can be expressed by

$$\gamma(t) = (x(t), y(t)),$$

Thus, the elements needed to completely specify a trajectory $\gamma_i(t)$ are the curvature $\kappa_i(t)$ and initial conditions $\gamma_i(t_0)$ and $\theta_i(t_0)$. Using the terminology of calculus, $\gamma(t)$ is of class C^2 and a flyable trajectory for a UAV with constant velocity v having initial conditions $\gamma(t_0)$ and $\theta(t_0)$ with minimum turning radius ρ. Using Do's work, Ahmadzadeh, Keller, Jadbabaie, and Kumar were able to change the search space from flyable trajectories $\gamma_i(t)$ to bounded scalar functions $\kappa_i(t)$, allowing them to restate their objective as generating curvature functions $\{\kappa_i(t) : |\kappa_i(t)| \leq 1/\rho_i, i = 1, 2, \cdots, N\}$ to achieve maximum coverage for all time intervals $[n\tau, (n+1)\tau], n = 0, 1, \cdots$.

Finally, Ahmadzadeh, *et al.* field tested their algorithm on four actual UAVs. They solved the IP using mixed randomized and heuristic search algorithms. Generating 300-second trajectories for the UAVs took 7 seconds on a 2 GHz computer with 768 MB of RAM (solving the IP 20 times). Figure 5 displays two different 15-second coverages of an area using pictures snapped by the UAVs that were then stitched together using Autostitch tools.

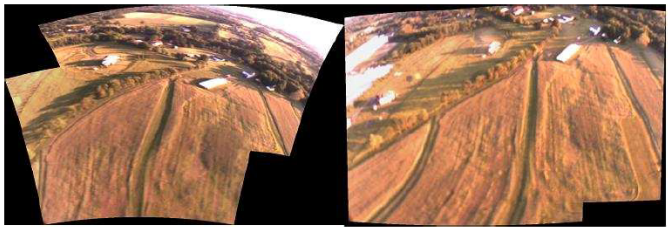

Figure 5. Two samples of tesselated coverage area ([15], p. 6)

The path planning algorithm presented in [15] generates feasible trajectories while coupling camera FOVs and flight paths. By running simulations and field tests using UAVs at different altitudes, Ahmadzadeh, *et al.* did not have to deal with collision avoidance in their

study. It should also be noted that in their formulation, each part of the area to be covered had equal priority.

Ousingsawat [36] conducts path planning for a single UAV over a prioritized surveillance space to maximize coverage. The priority of a region of the surveillance space is modeled using the concept of *entropy*. Roughly speaking, the more entropy in a region, the higher its priority. The objective of the planning tool Ousingsawat introduces is to maximize area coverage in the shortest time while meeting the physical constraints of the UAV in motion (turning radius, speed, etc.). In terms of entropy, the objective is to plan paths to reduce entropy as much as possible in minimum time. The paper first describes UAV dynamics as a hybrid system, then moves on to area and camera footprint parameters, and finally discusses path generation and simulation results [36].

In hybrid modeling, the system under observation exhibits both continuous and discrete characteristics. In [36], UAV movements are considered to take place over $\mathbb{R}^2$, or, the (x,y) plane. The UAVs can occupy three possible discrete states $x_D \in \{0,1,2\}$; respectively, the values 0, 1, and 2 indicate going straight, turning left, and turning right. The continuous states, represented by $s = \{x,y,V,\psi\}$, consist of four variables; (x,y) is location, V is total velocity, and ψ is UAV heading.

The area under consideration is rectangular. Different regions of the area will be of differing priorities. Ousingsawat imposes the constraint that the entire area must be explored. Further, no discontinuities can be admitted as they would result in a non-convex problem, making it much more difficult to solve. The priorities are assigned using a measure of entropy, which indicates the uncertainty of a region. In the paper, a boustrophedon search pattern is assumed and the rectangular area is broken into a grid of cells; as such, each column of cells has the same entropy (*i.e.*, same priority). Coverage of the area is then defined by the summation of the entropy in all of the cells. If the grid is $N \times M$, having N rows and

M columns, then coverage is defined mathematically by

$$COV = 1 - \frac{\sum_{i=1}^{N} \sum_{j=1}^{M} NE_{ij}}{E_0},$$

where the entropy of cell (i, j) is given by E_{ij}. The variable i iterates over the rows (y axis) while j iterates over the columns (x axis); the initial entropy is E_0.

The planning tool in [36] is a two-part mechanism. In the first part, the tool finds the number of revisits that is required on each path. The second part seeks the optimal order of paths that satisfy the UAV constraints. The path is constructed using information from both parts of the planning tool; simulations showed more than 97% coverage. Figure 6 shows a path developed using the planning tool and the resulting reduction in entropy over the surveillance space.

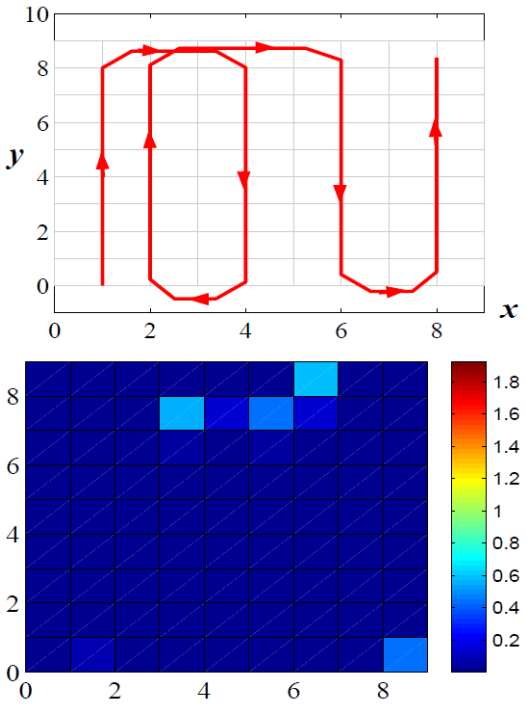

Figure 6. Path and final entropy ([36], p. 6)

2.2.2 Area Decomposition.

This section covers the ways in which area decomposition problems can be defined and discuss the methods researchers have used to solve them. Although such problems can be defined in a multitude of ways, the general methods available for solving partitioning problems can be placed into two broad categories: exact methods and heuristic methods. Exact methods include enumeration of solutions and integer programs. Heuristic methods are further categorized into constructive and iterative methods. Constructive methods include random mapping and hierarchical clustering. In contrast, iterative methods include greedy algorithms, the Kernighan-Lin algorithm, simulated annealing, and evolutionary algorithms [30].

A minimum Manhattan network, so named because it makes use of the ℓ_1 or Manhattan (sometimes called taxicab) norm, consists of a set T of n points called terminals in the plane. A network $N(T) = (V,E)$ is called a Manhattan network on T if the set of edges E consists of rectilinear segments connecting points in the set of vertices $V \supseteq T$ such that for any two terminals in T, $N(T)$ contains the minimum-length ℓ_1 path between them. A minimum Manhattan network on T, then, is a Manhattan network of minimum length; Figure 7 illustrates such a network.

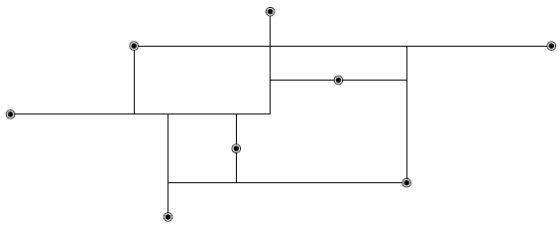

Figure 7. Example minimum Manhattan network ([20], p. 3)

Under certain restrictions on the allowable edges and given an enclosing rectangle for the set T, this problem can be modified to solve for the minimum Manhattan network that partitions the rectangle into smaller rectangles.

Chepoi, Nouioua, and Vaxès [20] describe a *minimum Manhattan network* (MMN), which was introduced by Gudmundsson, Levcopoulos, and Narasimhan [26]. In [20], a rounding algorithm is proposed based on a linear programming formulation to solve it. Specifically, they propose and prove correctness of a rounding 2-approximation algorithm based on an LP-formulation of the MMN. Kato, Imai, and Asano (as cited in [20]) previously gave such an algorithm, but did not prove correctness.

Choset [21] surveys results in coverage path planning, and in so doing, discusses different possible cellular decompositions of a space for efficient robot exploration. He considers three types of cellular decomposition: approximate, semi-approximate, and exact. In approximate cellular decomposition, the cells used to decompose an area are the same size and shape, but the collective area of the cells does not encompass the entire space. Semi-approximate methods use partial space discretization where the cells have fixed width, but the tops and bottoms are of arbitrary shape; in a semi-approximate scheme, robots move along the generated, equal-width columns, recursively exploring the space. Finally, an exact cellular decomposition partitions a search space in the mathematical sense - any two cells are disjoint and the collection of all cells completely covers the entire space and no more. Typically, an area that is decomposed exactly is searched using simple back-and-forth motion by multiple robots.

An example exact cellular decomposition procedure, developed by Choset and Pignon [22], is boustrophedon cellular decomposition (BCD). In the BCD, a line sweeps an area generating cells; if any obstacles are present, a cell is divided above and below the obstacle and recombined to form a single cell after passing the obstacle. Traditionally, exact cellular decompositions have been used for two purposes. Those purposes are either to deal with obstacles in an environment or to divide a target space over multiple vehicles [33].

Carlsson [18] presents a type of equitable partition that decomposes an area where vehicles are routed through a collection of depots such that each vehicle receives a fair

share of the workload. Carlsson gives an algorithm that takes as input a planar, simply-connected region R that has defined on it a probability density function f. The region R contains n depot points $P = \{p_1, p_2, \cdots, p_n\}$ that represent starting locations of n vehicles. It is assumed that the points each correspond to exactly one vehicle. Though client locations are unknown, they are assumed to be independent and identically distributed according to the probability density function f. The goal is to partition R into n subregions with one vehicle assigned to each member of the partition. If large samples are drawn, the workload in each subregion is asymptotically equal. Carlsson shows that the problem is solved by treating each subregion R_i as a traveling salesman problem (TSP) with a set of points that includes the depot and all points in R_i. The problem is easily visualized in Figure 8.

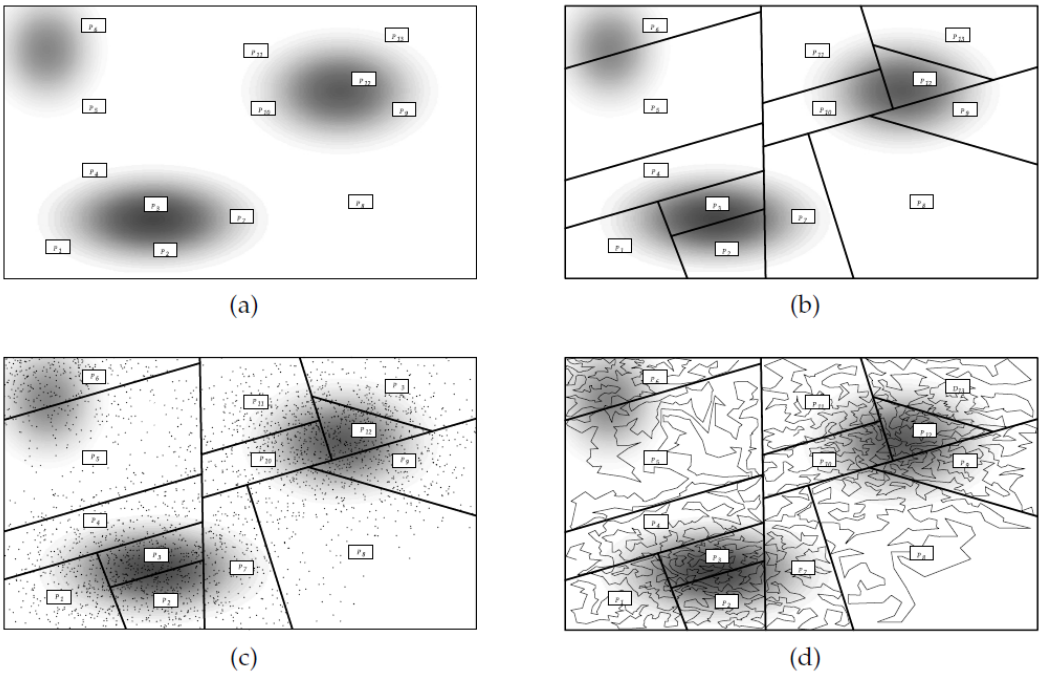

Figure 8. (a) Depot set and density function f; (b) Area partitioned; (c) Points sampled independently of f; (d) TSP tours of each subregion asymptotically equal ([18], p. 2)

As Carlsson shows, the situation here is a special case of the equitable partitioning problem. In that class of problems, a pair of densities f_1 and f_2 is defined on a region R. The partitioning of R must be such that $\iint_{R_i} f_1 \; dA = \frac{1}{n} \iint_R f_1 \; dA$ and $\iint_{R_i} f_2 \; dA = \frac{1}{n} \iint_R f_2 \; dA$

for all i, where one density represents the set of depots and the other the TSP workload over a subregion when points are sampled from f. Now, it is possible to simply induce a partition by using vertical lines across an area, but that might not give the best solution in the end. Further constraints are imposed; a natural constraint to consider is that each subregion R_i should include the depot assigned to it (and only that one depot). Another important factor is the shape of the region to be divided. If R is convex, each region R_i may be required to also be convex. However, in the case where R is nonconvex, relative convexity is desired among all subregions. That is, the shortest path between two points u and v in R_i for the i^{th} subregion must be contained in R_i. An interesting visual example of the algorithm applied to a real-world map is presented in Figure 9.

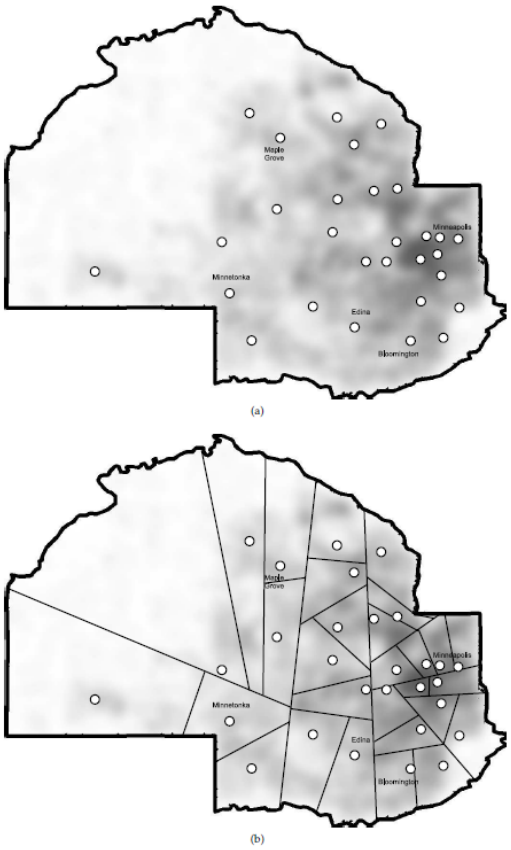

Figure 9. (a) Hennepin County, MN with locations of 29 largest post offices; (b) Equitable partition: same population ([18], p. 17)

Maza and Ollero [31] apply polygon area decomposition to a convex area R with no holes or obstacles that must be searched. In their work, a team of heterogeneous UAVs is to search an area of land for objects of interest such as fires, cars, property damage, etc. Initially, each UAV being used is situated on an edge of the polygon search area as shown in Figure 10.

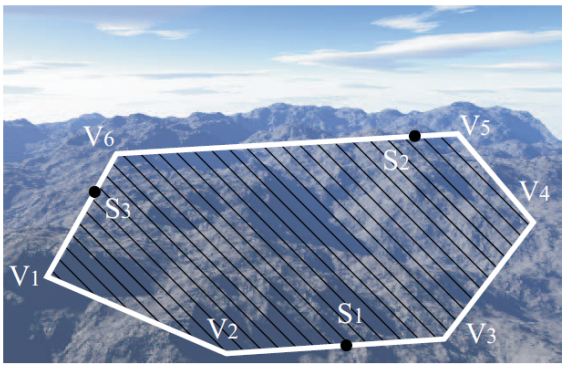

Figure 10. Polygon with vertices V_i and UAVs at starting positions S_i ([31], p. 3)

Beginning this way, Maza and Ollero build on the anchored area partition problem presented by Hert and Lumelsky [28], who employ a semi-approximate cellular decomposition. Now, if $\{S_1, S_2, \cdots, S_n\}$ is a set of starting positions for n UAVs and if $\mathcal{P}$ is the area of the entire region (and $\mathcal{P}_i$ the area of each partitioned subregion), then each UAV has an area requirement, denoted $AreaRequired(S_i)$, specifying the desired area of each subregion $\mathcal{P}_i$. Then, a polygon $\mathcal{P}$ containing q sites (called a *q-site polygon*) is termed *area-complete* if $AreaRequired(S(\mathcal{P})) = Area(\mathcal{P})$. The expression $AreaRequired(S(\mathcal{P}))$ represents the sum of the areas required by all sites in $\mathcal{P}$. Citing [28], Maza and Ollero explain that the desired area partition can be accomplished using $n-1$ line segments. Each line divides a q-site area-complete polygon into two convex polygons, one of which is q_1-site area-complete and the other q_2-site area-complete. The area partition algorithm can be repeated $n-1$ times to yield n convex 1-site area-complete polygons.

The UAVs are considered to operate on a base coordinate system (BCS) with respect to the environment (x-axis north, y-axis west, and z-axis up); however, cameras are assumed to not have orientation devices. The UAVs themselves are associated with another coordinate system based on their own positions - a UAV coordinate system, or, UCS - in which the axes are x-axis forward, y-axis left, and z-axis up. The camera of each UAV is fixed in the x-z plane. Figure 11 describes the imaging scenario of a single UAV.

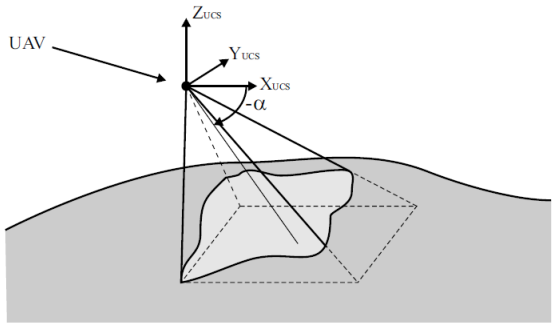

Figure 11. Imaged area is intersection of image pyramid and terrain ([31], p. 4)

According to Maza and Ollero, the sensing width of a UAV moving in the UCS x-z plane is given by

$$w = 2z_{BCS} \tan\gamma \left[\sin\alpha + \cos\alpha \tan\left(\frac{\pi}{2} - \alpha - \beta\right)\right], \tag{4}$$

where z_{BCS} is UAV altitude with respect to the base coordinate system of the environment and angles β and γ are parameters of the camera FOV. Huang [29] shows that a lawnmower UAV search pattern in each partitioned subregion is an efficient coverage method where the spacing of the parallel search lines is the sensing width of a camera, given in Equation 4. Because it takes time to turn, it makes sense to chose a boustrophedon path that minimizes the number of turns. Given the q-site polygon as shown in Figure 12 (with optimal sweep directions indicated by arrows), the algorithm produces a path as shown in Figure 13. The optimal sweep directions in Figure 12 are optimal in the sense that those directions min-

imize the assigned polygon's diameter along the sweep direction. Note, only directions perpendicular to edges need to be tested.

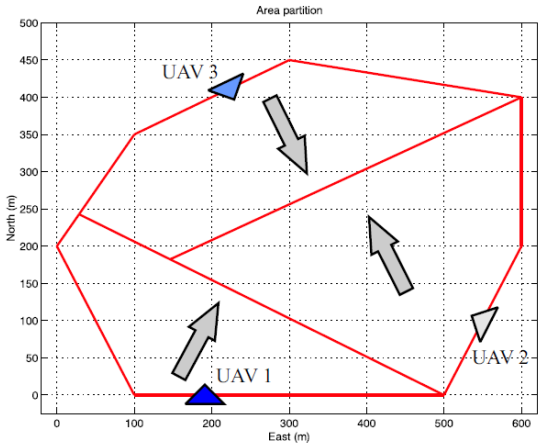

Figure 12. Area partition ([31], p. 8)

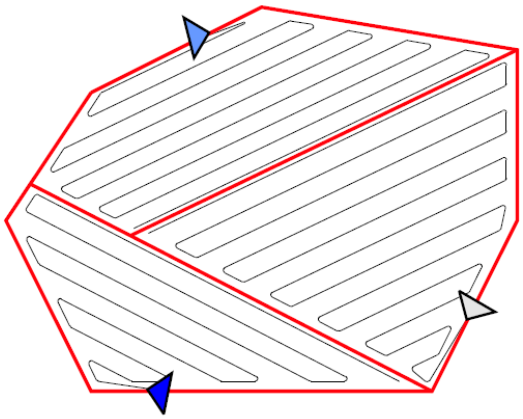

Figure 13. lawnmower pattern search ([31], p. 8)

Another way to break down a space for exploration by machines is to use grid decomposition, or an occupancy grid map (OGM) representation of the space. Quijano and Garrido [38] explore two possible grid decompositions. One decomposition uses a hexagonal grid and the other a quadrangular grid. Figure 14 illustrates the difference.

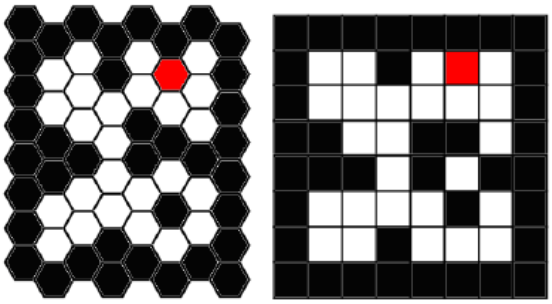

Figure 14. Hexagonal and Quadrangular Grid Decomposition over same map ([38], p. 2)

Quijano and Garrido note that because the diagonal and vertical (or horizontal) distances between square centers in a quadrangular decomposition are different (diagonal of a square is larger than any side by a factor of $\sqrt{2}$), managing different distances and scales for the purpose of robot exploration can add complexity to the problem. In that case, in order to

simplify the process of exploring the space, one can restrict robot movement to only vertical and horizontal movements. In the case of a hexagonal decomposition, this is not a problem because the vertical, horizontal, and diagonal distances between centers of hexagons are the same.

Quijano and Garrido [38] find that though a map may be represented by both the hexagonal and quadrangular grid decompositions, the space can be better represented using hexagons rather than squares even if the resolution is enhanced in both cases. If the space is small, then the choice of decomposition is superfluous. Four different algorithms are developed in [38] to search a space once it has been decomposed into both hexagons and squares. The exploration algorithms are versions of well-known graph search algorithm types: breadth-first, breadth-first random, depth-first, and best-first. When they applied their algorithms to each decomposition of the same map, what they found was that the variance in the number of movements required by robots searching the map was lower in the hexagonal case than in the quadrangular case. The overall number of movements required in the hexagonal cases was also lower than in the quadrangular setup. Similar results applied when the space contained obstacles, except in that situation, the initial starting position of robots was key to the number of movements needed for robots to explore the space.

Nigam and Kroo [34] conducted work specifically on the persistent surveillance problem using decomposition techniques. In their study, they look at the coverage of an area of land using multiple UAVs. The authors start with a semi-heuristic control policy for a single UAV and extend that approach to the case of multiple UAVs. They perform this extension in two ways. The first is to extend a reactive policy for a single UAV (each UAV reacts to the environment and other UAVs on its own) to multiple UAVs and the second is to partition the surveillance space and then allocate a UAV to each member of the partition for parallel surveillance. The assignment of UAVs to subregions of the surveillance

space is based on auction algorithms. Nigam and Kroo compare the two ways to extend the single-UAV policy, noting interesting results.

In the case of an area divided into two cells that must be continuously monitored by a single UAV, suppose that the UAV can only choose to do one of two actions: go left or go right. Then, the optimal policy is decided by its first action, as after the UAV has decided initially to go left or right, in order to have continuous coverage of the area, it must alternatively go left and right, shuttling between the two cells. This simplified single-UAV persistent coverage scenario in [34] is depicted in Figure 15.

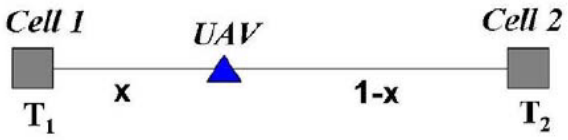

Figure 15. Simplified two-cell persistent coverage problem ([34], p. 2)

The figure requires some explanation.

Each cell has an associated age, given by T_1 and T_2; these times represent the time elapsed since cell 1 and cell 2 were last observed, respectively. The UAV is initially located a distance x from the left cell and is traveling at velocity V_{survey}. If the distance between cells 1 and 2 is 1 unit (x and V_{survey} scaled accordingly), then initially, the UAV is $1-x$ units from cell 2. Nigam and Kroo seek a UAV policy to minimize the maximum age over both cells. In this case, that policy simplifies to determining which way to go first, left or right. If T_1 is taken to be less then T_2 (without loss of generality), then age graphs can be constructed for both the case where the UAV goes left first and for when the UAV goes right first; these graphs comprise Figures 16 and 17, respectively. In these figures, the optimal policy is the one that minimizes the peak of the maximum age curve (in black in both figures). Because the optimal policy is determined after the first move, the planning horizon is finite for the total possible distance traveled to visit both cells of $2/V_{survey}$.

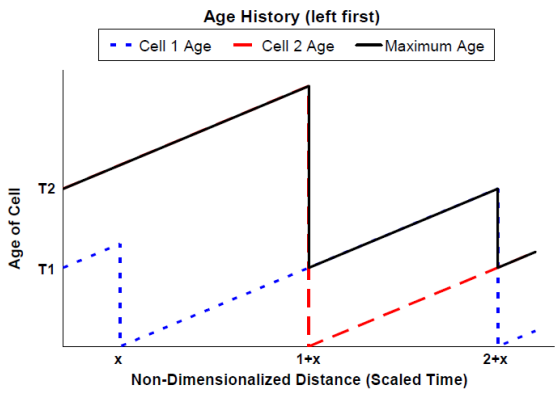

Figure 16. Age of cells, left first ([34], p. 3)

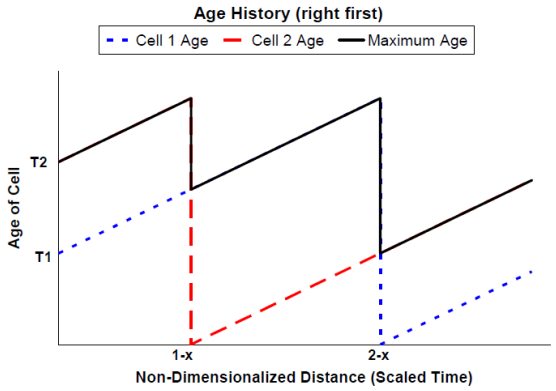

Figure 17. Age of cells, right first ([34], p. 3)

Nigam and Kroo show that the cell with the greatest value is the critical cell because the concern here is only with the maximum age recorded, thus, when extending the 1-D single-UAV example to a 1-D example with five cells, the optimal policy is to choose the cell of maximum value - the target cell - and take the maximum step toward it. This method, a target-based approach, is in contrast to a sum-of-values approach in which the UAV moves toward the area with the highest sum of values of cells (by linearly combining cell ages and distances from the UAV). If two cells are of equal value, then the cell that requires the least heading change becomes the target cell. The researchers use the weight parameter $-1/V_{survey}$ five-cell setup as in the two-cell situation, but they caution that such a weight may not be optimal for the multiple cell case in general. The weight parameter is derived using an iterative sampling (ISIS) based optimizer. The optimal policy results in a spiral search pattern for a square surveillance space.

After comparing various approaches to the single-UAV case (different direction-finding methods), Nigam and Kroo move on to the multiple UAV case. The two methods researchers use to treat the multiple-UAV problem are a multi-agent reactive policy (extension of the single-UAV policy) and space decomposition (optimally partitioning, and searching the space in parallel using one UAV per partitioned subregion). Here, only the SD approach is considered. It should be noted, however, that for a large enough num-

ber of UAVs, the two approaches tend to converge on the same maximum age over all cells. In SD, the space is partitioned so that it can be optimally, persistently covered. If the UAVs are homogeneous, then an equipartition would suffice, but no such assumption is made in [34]. Because the UAVs can be of different capabilities, partitioning requires more thought. Nigam and Kroo point out that optimal partitioning is generally hard to do, and several others have taken up the problem. But many approaches suffer from issues of scalability, require *a priori* knowledge of the domain, or are difficult to extend to the persistent coverage problem. In [34], the authors generate the optimal partition using recursive partitioning, as shown in Figure 18.

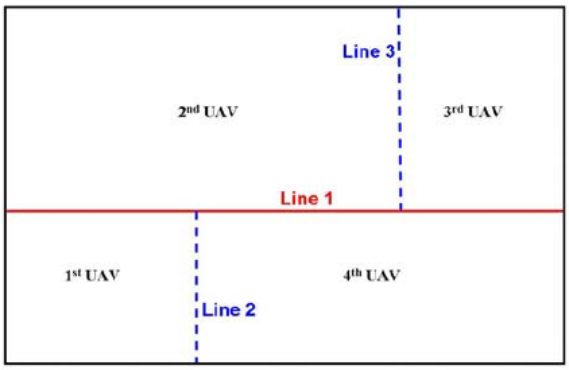

Figure 18. Recursive partition of a rectangular space ([34], p. 7)

In the figure, the space is first divided such that half of all UAVs fall into each half of the partitioned space. This process runs recursively until each UAV is assigned to exactly one partition and each partition contains exactly one UAV.

After partitioning the space, the next task is to optimally assign UAVs to subregions of the space; the goal is to find an assignment that minimizes the maximum age over all cells in any subregion of the surveillance space (a minimax or bottleneck assignment problem). Garfinkel [24] uses a threshold algorithm to solve this problem; specifically, he uses a Ford-Fulkerson algorithm in each iteration. Instead of using Ford-Fulkerson methods, Nigam and Kroo apply an auction algorithm. What Nigam and Kroo found was that as the number

of UAVs increased, the MRP and SD methods resulted in increasingly similar performance in terms of maximum age over all cells in the space. However, the performance of both methods with respect to the lower bound on the optimal maximum age decreased, due possibly to more congestion in the area or restriction to rectangular partitions.

Nigam and Kroo also consider what effect UAV dynamics have on performance. Assuming UAVs travel at constant velocity and constant altitude, they find that a simulation ignoring turn rates and moments is suitable. Instead, minimum turning radius is instrumental in defining the minimum distance between one cell of the space and another. When a UAV has to travel from a point A to another point B, to find the minimum length trajectory, the lengths of four paths between the points - as illustrated in Figure 19 - are calculated, and the minimum-length path is chosen.

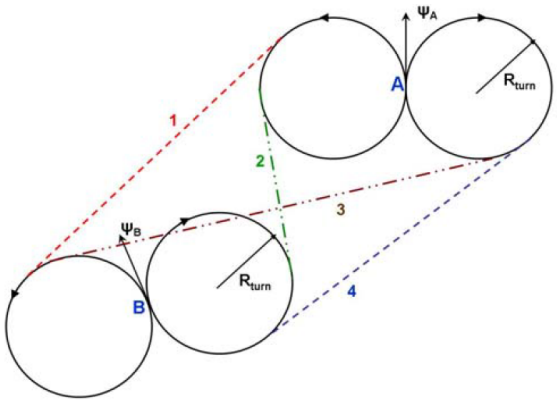

Figure 19. Possible optimal paths from A to B ([34], p. 11)

Two types of distance could be used to define a policy for UAV trajectories, a Euclidean distance policy (EDP) or an actual distance policy (ADP). The Euclidean distance is the straight line distance from A to B, whereas the actual distance accounts for the total distance traveled by a UAV as it executes turns and flies in its characteristic fashion from one point to another. What Nigam and Kroo discovered is that the ADP policy will result in better performance than an EDP policy. Table 2 summarizes the average (of fifty trials) maximum ages recorded using actual and Euclidean distance policies.

Table 2. Average maximum age, comparing EDP and ADP

	$C_{Lmax} = 1.03$		$C_{Lmax} = 1.18$		$C_{Lmax} = 1.67$	
Num UAVs	EDP	ADP	EDP	ADP	EDP	ADP
1	261.7	255.8	198.5	196.1	108.4	107.1
3	235.9	209.2	194.7	179.0	145.9	144.4
5	226.3	196.9	188.2	174.7	145.7	141.8
10	124.6	106.6	101.3	94.5	80.3	79.0

In Table 2, the value C_{Lmax} refers to the *maximum lift coefficient* of a UAV, which relates the lift generated by an object to the fluid around the body, it's velocity and some reference area, such as the surface area of the fixed-wing UAV. Corresponding to each lift coefficient is a distinct turning radius of 5, 3.125, and 1.67 m, respectively. In the case of multiple UAVs, Nigam and Kroo used the MRP rather than the SD approach for multiple UAV coordination. The UAVs themselves are not large, each having a mass of 1 kg, and in the case of one UAV, the surveillance space size is 50×50 m^2 and in the multiple UAV case, the space is 75×75 m^2. In all cases, the sensor footprint is equal to the size of a cell. The data in Table 2 show that having more UAVs results in better average age over the cells of the surveillance space, but as the number of UAVs gets larger, the difference between the EDP and ADP methods becomes smaller. In other words, the performance benefits saturate when the number of UAVs becomes large.

The partitioning procedure in [34], recursive partitioning, is one way to divide a rectangle into smaller rectangles. In [32], de Meneses and de Souza offer another approach to solving the partitioning problem using integer programming. In their work, they consider a rectangle R in the plane and a finite set P of n points in the interior of R. A feasible partition divides R into smaller rectangles such that no points in P lie inside of any partitioned subregion of R. The objective of the partitioning algorithm in de Meneses and de Souza is to find a feasible rectangular partition of minimal length, where the length of a partition is the total length of the cuts used to create the partition. This is an NP-complete problem with

applications in very large-scale integration design. Figure 20 shows a rectangle with points inside, a non-guillotine partition, and a guillotine partition. The RGP term used to describe Figure 20(a) refers to the class of problems defined by rectangles with interior points or "holes."

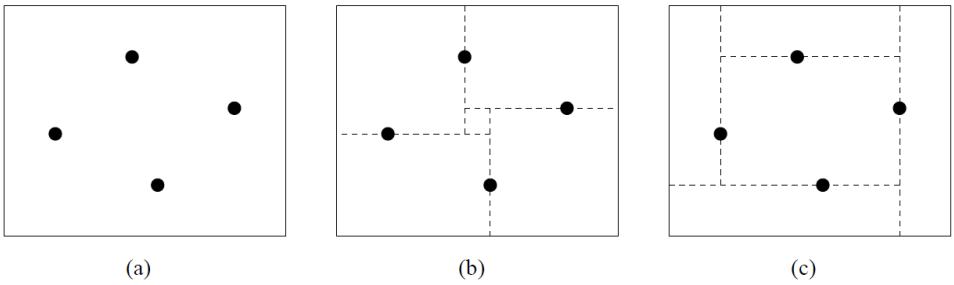

Figure 20. (a) Instance of RGP (b) Non-guillotine partition (c) Guillotine partition ([32], p. 6)

Note that in Figure 20, the optimal partition is not the guillotine partition. In computational experiments, de Meneses and de Souza found that a guillotine partition never solved the problem exactly. When the points are completely *noncorectilinear* (no two points belong to the same horizontal or vertical line), as is the case with the RGP in Figure 20, the complexity of the problem increases.

De Meneses and de Souza discuss the many approximate algorithms in the literature that have been used to solve this problem; they range in complexity from $O(n \log n)$ to $O(n^5)$. A rectangle with points inside is called an RGP, and an instance of the RGP is $I = (R, P)$, where R and P are a rectangle and a set of points, respectively. A grid is defined in [32] by the set of straight vertical and horizontal lines intersecting at the points inside R (belonging to P). Such a grid is called the *grid induced by P*, and is denoted $GI(P)$. Points in P are called *terminal points*, or more simply, *terminals*. Those points at intersections of horizontal and vertical lines of $GI(P)$ that are not in P are called *Steiner points*. Figure 21 shows both grid points and Steiner points. De Meneses and de Souza reason that an optimal solution S^* to $I = (R, P)$ consists of straight lines that lie on the grid $GI(P)$.

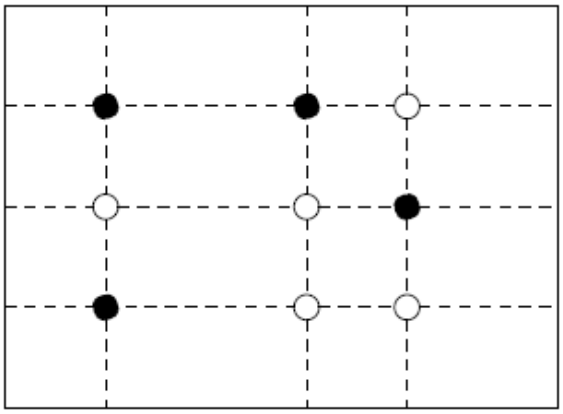

Figure 21. Terminal points (black), Steiner points (white), and GI(P) (dotted lines) ([32], p. 7)

To solve the problem, de Meneses and de Souza set up an IP in two ways. The first is the *segment model* and the second is the *set partitioning model*. The first step in making this a $0-1$ integer programming problem using the segment model is deciding whether each grid segment is part of an optimal solution. Any resulting optimal solution cannot include *knees* or *islands*. A knee is defined as a terminal or Steiner point where exactly two grid segments meet at a right angle, and an island exists when only one segment is incident on a terminal or Steiner point. Figure 22 illustrates a knee and an island.

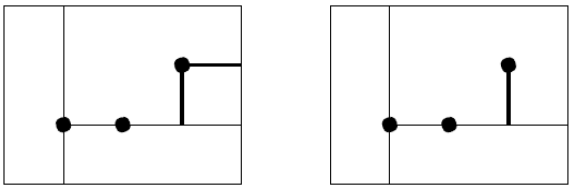

Figure 22. (a) a knee and (b) an island at a terminal point ([32], p. 7)

If knees or islands are admitted, then it is not possible to produce a partition of the space where each subregion is a rectangle. In fact, the absence of knees and islands serves as a necessary condition for a subset $C \subseteq GI(P)$ of grid segments to form a feasible rectangular partition of R with respect to P. What de Meneses and de Souza show is that given an in-

stance $I = (R, P)$ of the RGP, only when every terminal point in P has at least two segments of C incident to it does C induce a feasible rectangular partition of R with respect to P.

Proceeding from these observations, de Meneses and de Souza construct a $0-1$ IP as follows. For each grid segment $e \in GI(P)$,

$$x_e = \begin{cases} 1, & \text{if } e \text{ belongs to a solution } S \\ 0, & \text{otherwise.} \end{cases}$$

Letting $|GI(P)| = m$, an m-dimensional binary vector x characterizes a solution. Because the objective is to find a minimum-length partition, the length of each segment is needed. If the length of every segment of $GI(P)$ is captured in the vector $d \in \mathbb{R}^m$, where the e^{th} component of d is the length of segment e in $GI(P)$, then the objective is to minimize $d_e^T x_e$. Expressed another way, the objective is to minimize $\sum_{e=1}^{m} d_e x_e$.

Each grid point i may connect up to four grid segments. If those segments are denoted $i(1), i(2), i(3)$, and $i(4)$, then, in order to achieve a feasible solution, there must be certain constraints on the terminal and Steiner points. Combining these constraints with the objective function, the IP formulation follows (for each point in $GI(P)$).

$$\text{Minimize} \quad \sum_{e=1}^{m} d_e x_e$$

subject to

$$x_{i(1)} + x_{i(2)} \geq 1$$

$$x_{i(1)} + x_{i(4)} \geq 1$$

$$x_{i(3)} + x_{i(2)} \geq 1$$

$$x_{i(3)} + x_{i(4)} \geq 1$$

$$x_{i(1)} + x_{i(2)} - x_{i(3)} \geq 0$$

$$x_{i(1)} + x_{i(2)} - x_{i(4)} \geq 0$$

$$x_{i(1)} + x_{i(4)} - x_{i(2)} \geq 0$$

$$x_{i(1)} + x_{i(4)} - x_{i(3)} \geq 0$$

$$x_{i(3)} + x_{i(2)} - x_{i(1)} \geq 0$$

$$x_{i(3)} + x_{i(2)} - x_{i(4)} \geq 0$$

$$x_{i(3)} + x_{i(4)} - x_{i(1)} \geq 0$$

$$x_{i(3)} + x_{i(4)} - x_{i(2)} \geq 0$$

$$0 \leq x \leq 1$$

$$x \text{ integer}$$

The first four constraints avoid knees and islands at terminal points and the next four avoid them at Steiner points. Clearly, if $|P|$ is large, then the IP formulation will be very large as well, as this formulation above would essentially be multiplied in size by the number of points. The authors prove that a vector $x^S \in \mathbb{R}^m$ is part of a feasible rectangular partition S if and only if x^S satisfies all terminal and Steiner point constraints.

In the set partitioning model, to solve the problem of finding the minimum-length partition of a rectangle R, de Meneses and de Souza start with the standard set partitioning problem. That is, given a set $H = \{1, \cdots, m\}$ and the set $K = \{K_1, \cdots, K_n\}$ of subsets of H (the power set of H), if $J = \{1, \cdots, n\}$, then the set $J^* \subseteq J$ is called a partition of H if $\cup_{j \in J^*} K_j = H$ and for all $j, l \in J^*$ where $j \neq l$, we have $K_j \cap K_l = \varnothing$ (dividing H into mutually exclusive and collectively exhaustive subsets of H). To each subset $K_j \in K$, a cost c_j is associated, and the goal of the integer program here, to find the minimum-length partition of R, is then given by the IP formulation

$$\text{Minimize} \quad \sum_{j=1}^{n} c_j y_j$$

subject to

$$\sum_{j=1}^{n} a_{ij} y_j = 1, \qquad i = 1, \cdots, m;$$

$$y_j \in \{0,1\}, \qquad j = 1, \cdots, n.$$

To find proper values for the coefficients a_{ij} and c_j, de Meneses and de Souza first define the units of feasible rectangles that form an allowable partition of R.

Definition II.1. If $GI(P)$ is the induced grid corresponding to an instance $I = (R,P)$ of the RGP, represented by a rectangle R with a set P of interior points, then a canonical rectangle is one whose sides lie on two consecutive vertical and horizontal segments of $GI(P)$ (including the borders of R). [32]

An instance $I = (R,P)$ of the RGP and its induced grid $GI(P)$ is displayed in Figure 23 along with a few examples of canonical rectangles. In essence, canonical rectangles are demarcated by the grid lines induced by the terminal points in the interior of a rectangle, and the borders of that rectangle. As it turns out, the number of canonical rectangles that result from an instance of the RGP is $O(|P|^2)$. De Meneses and de Souza reason that any feasible rectangular partitioned subregion of the entire rectangle R must be composed of one or more canonical rectangles. Figure 24, taken from [32], illustrates this composition of feasible rectangles using canonical rectangles. Given a set P of terminal points in R, the number of feasible rectangles is $O(|P|^4)$

Thus, a rectangular partition of R with respect to P is the division of R into feasible rectangles, which are themselves composed of unions of canonical rectangles. Here, de Meneses and de Souza define the cost of any feasible rectangle R_j in K as the sum of the perimeter of R_j and the sum of the lengths of the sides of R_j that lie on the boundary of R. Finally, de Meneses and de Souza define the variables a_{ij} and y_j given their characterization

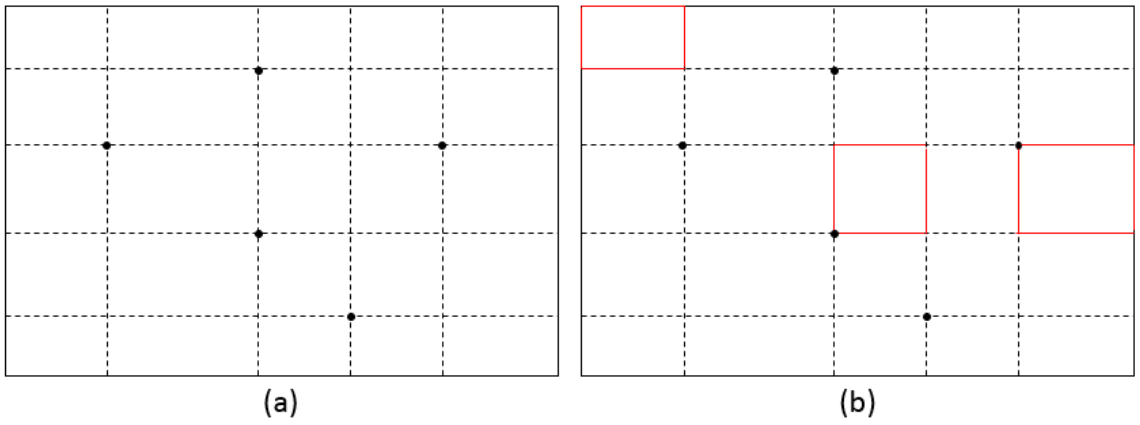

Figure 23. (a) Instance $I = (R, P)$ of the RGP and induced grid $GI(P)$ (b) example canonical rectangles of I

of canonical and feasible rectangles as

$$y_j = \begin{cases} 1 & \text{if feasible rectangle } R_j \text{ is in the partition,} \\ 0 & \text{otherwise.} \end{cases}$$

and

$$a_{ij} = \begin{cases} 1 & \text{if feasible rectangle } j \text{ contains canonical rectangle } i, \\ 0 & \text{otherwise.} \end{cases}$$

De Meneses and de Souza looked at the segment model from the point of view of the polytope produced by the inequalities. Inequalities associated with terminal points (what they call Class I constraints) and inequalities associated with Steiner points (Class II), when included in the segment model, generate what is called the "basic" model. But other classes of constraints exist, and when all of them (Classes I-VI) are included in the segment model, it is termed the "full" segment model. The full model makes for a stronger formulation than the basic model. A Class III constraint is depicted in the point configuration shown in Figure 25. The constraint matching the point configuration of Figure 25 is given by

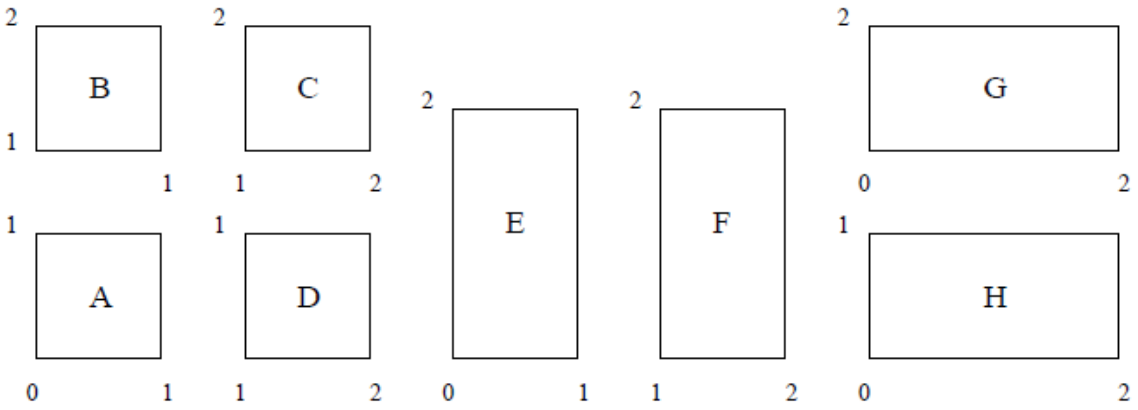

Figure 24. RGP is 2×2 square with P consisting of centroid of square. Four canonical rectangles result. Canonical rectangles A and B comprise feasible rectangle E and canonical B and C make up feasible G. ([32], p. 23)

$x_1 + x_2 + x_3 + x_4 \geq 2$, and there are $O(n)$ such constraints, where n is the number of points in the interior of R (terminal plus Steiner points).

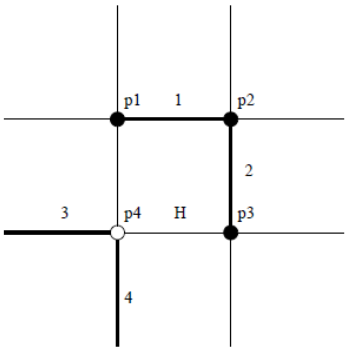

Figure 25. Point configuration of a Class III constraint ([32], p. 17)

These Class III inequalities define facets of $\mathcal{P}_R$, the polytope given by the convex hull of the integer solutions of the formulation given for the segment model. De Meneses and de Souza further show that $\mathcal{P}_R = \text{conv}\{x^s \in \mathbb{R}^m \ : \ S \text{ is a rectangular partition of } R \text{ with respect to } P\}$, where $m = |GI(P)| = \dim(\mathcal{P}_R)$. That is, the polytope $\mathcal{P}_R$ is full-dimensional. The other classes of inequalities, Classes IV-VI, correspond to point configurations shown in Figure 26, taken from [32]. With the exception of Class IV inequalities, they all define facets of

$\mathcal{P}_R$ without qualification. A Class IV inequality, however, defines a facet of $\mathcal{P}_R$ if and only if in the point configuration for the inequality - shown in Figure 26(a) - both pairs of points (p_2, p_3) and (p_4, p_5) contain at least one Steiner point.

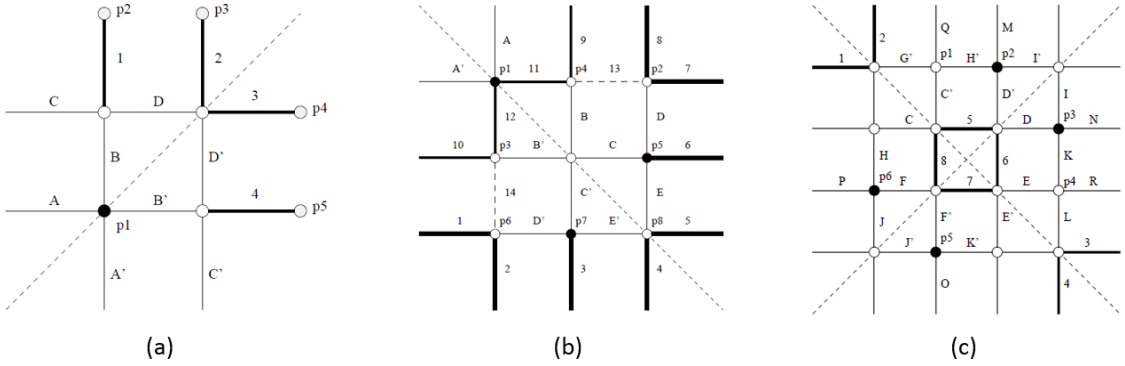

Figure 26. Point configuration: (a) Class IV Inequality, $x_1 + x_2 + x_3 + x_4 \geq 1$; (b) Class V Inequality, $2\sum_{i=1}^{8} x_i + \sum_{i=9}^{12} x_i - \sum_{i=13}^{14} x_i \geq 6$; (c) Class VI Inequality, $\sum_{i=1}^{8} x_i \geq 2$ ([32], pp. 18-21)

Denoting the segment model formulation in [32] by F_S and the set partition model by F_R, what de Meneses and de Souza found was that the second formulation is stronger. They determined this by comparing the bounds obtained by solving the linear relaxation of F_R with those of F_S and proving that if W^* represents the optimal value of the linear relaxation of F_R and Z^* that of F_S for a given instance of the RGP, then $W^* \geq 2Z^* + 2\text{Per}(R)$, where $\text{Per}(R)$ is the perimeter of R. Moreover the inequality is not necessarily satisfied at equality.

Based on computational experiments, de Meneses and de Souza found that in the segment model, the branch-and-bound algorithm performed better than the branch-and-cut algorithm. In the set partitioning model, the researchers implemented a branch-and-price algorithm; they found that the better quality of the set partitioning bounds makes the branch-and-price algorithm more efficient than the branch-and-bound segment model. When the best known approximate algorithm is applied to each instance of the RGP tested, on average, the approximate solution was 10% off the optimum; worse, it never converged on

the optimal value. With high noncorectilinearity, the difficulty of using these algorithms increases.

2.3 Summary

There are a number of ways to define the coverage problem for a region given a set of UAVs. Certainly, there are coverage problems involving single-UAV scenarios, multiple homogeneous UAVs, multiple heterogeneous UAVs, continuous coverage, persistent coverage, coverage for the sake of searching a space once with minimal overlap, and more. Further, the methods used to solve these types of problems are just as numerous. Some techniques that have been used involve integer programming, using scheduling theory, applying the concept of entropy to define percentage of area covered, genetic algorithms, heuristics, dynamic programming, and others. A common overarching approach to the coverage problem in general - although it is not absolutely necessary - is to first decompose the area to be surveyed into subregions or cells and then to assign UAVs to surveil each cell separately. Decomposition of a space is often a hard problem, and most researchers make some simplifying assumptions to make the problem either tractable or at least solvable in a reasonable amount of time given the application.

Of the models discussed in this chapter, the one that was selected for the methodology of this research is the model provided by de Meneses and de Souza. In the next chapter, surveillance spaces that contain points of interest are modeled as rectangles with holes, or instances of the RGP. The RGPs are then divided into smaller, non-overlapping rectangles using a set partitioning model that is solved by a 0-1 integer program. Furthermore, the algorithm used to assign UAVs from a set of available vehicles to the partitioned subregions of the surveillance space is also described. The assignment algorithm seeks to minimize the revisit times over each member of the partition of the space by assigning the appropriate UAV to each subregion.

III. Methodology

3.1 Introduction

This chapter describes the methodology used to set up and solve the persistent surveillance problem given the assumptions set out in Chapter I. The chapter is divided into several sections. In the first two sections, the surveillance space partitioning and UAV assignment processes are explained in detail. The third section uses a flow chart to give a high-level summary of the process of randomly generating operational scenarios and solving them, and the final section presents the operational scenarios that are actually solved, the results and analysis of which appear in Chapter IV.

3.2 Surveillance Space Partitioning

The general approach taken in this research to solve the persistent surveillance problem is to divide or partition an area into subregions and then to assign exactly one UAV per region (to conduct surveillance on the whole area). Consider terrain where there exist a number of locations that must be monitored from a military intelligence point of view. For example, one might be the house where a suspected enemy combatant lives. Another location could be a suspected meeting place, where high-level members of a terrorist organization have been known to congregate. There are many possibilities. Sometimes, it is necessary to collect intelligence on not only these locations but the areas surrounding them. For instance, being able to track the individuals traveling to and from a meeting place can provide a source of valuable intelligence that can help military analysts understand human relationships, movements and actions, and other information that can be used to determine what is happening on the ground. Through this kind of intelligence gathering, it is possible to catch individuals planting explosive devices. It also becomes easier in this case to dis-

cover what associations individuals have with other individuals, possibly known criminals or terrorist suspects.

A persistent surveillance program executed over the area can help uncover what is happening on the ground and what human relationships exist between actors of interest to military intelligence. Regard the area of interest as a two-dimensional map and suppose there are "interesting " locations on that map. Around the set of locations, a rectangle is drawn. Then, identify with each location a point so as to maximize corectilinearity. These points are terminal points. Next, construct the grid induced by these terminal points over the map, which produces some Steiner points. For partitioning the rectangle, two main goals have been explored in the context of partitioning rectilinear polygons (such as rectangles): (1) minimizing the number of rectangles, and (2) minimizing the total length of the cut segments required to produce the rectangles. Because the rectangle has interior points that need to be considered (called "holes" in the literature), the problem is NP-complete [35]. The goal here is the first - to minimize the number of rectangles that result from partitioning R. It is necessary to mathematically express this desire as the objective of the IP. A feasible partition must have all cuts forming the partition pass through at least one terminal point, and each terminal point must lie on a cut. After partitioning the space, the resulting number of subregions must be minimal because exactly one UAV will be assigned to each region. If the number of regions produced by the partitioning algorithm is minimal, then the number of UAVs needed to carry out the persistent surveillance program is also minimal. Figure 27 describes the process of generating a grid from a set of locations and what an optimal partition might look like if the objective is to minimize partition length. In this case, the partition also minimizes the number of rectangles.

Let Figure 27(b) represent an instance, I of the RGP, where the outside rectangle is R and the set of three terminal points is P. That is, $I = (R, P)$ is an instance of the RGP, a rectangle R with a set P of interior terminal points. Figure 27(c) also shows $GI(P)$, the

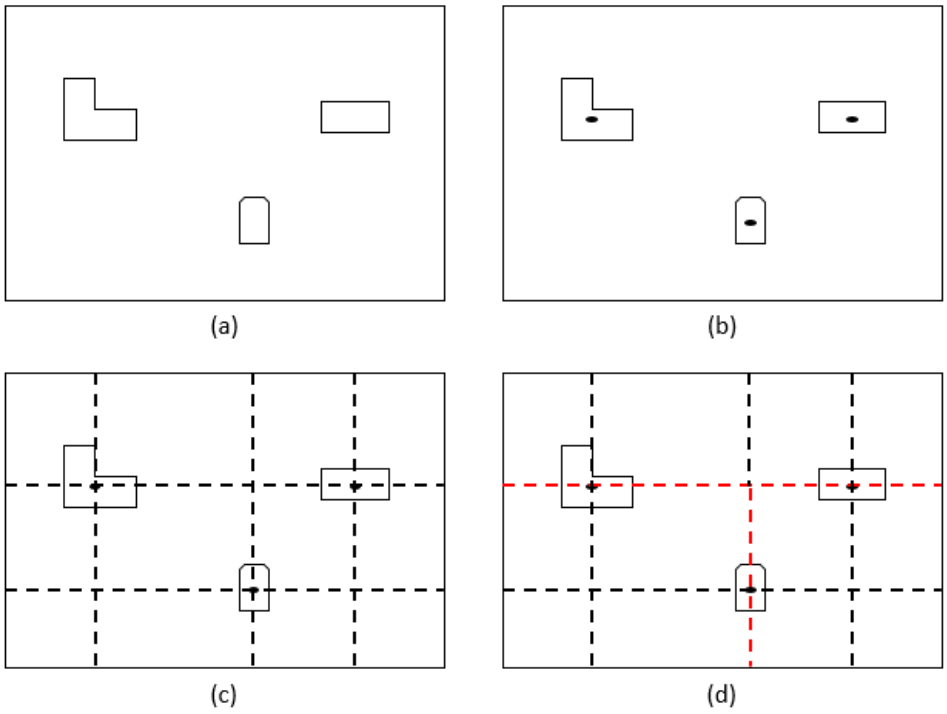

Figure 27. (a) Locations of interest (b) Introducing terminal points (c) Induced grid with 3 terminal points and 3 Steiner points (d) Notional minimal partition

grid induced by the set P, which reveals three Steiner points. To minimize the partition length, segment model in [32] can be used. In that case, to formulate an IP for this problem, the segments and points of the RGP need to be indexed. Then, a vector $\vec{d} \in \mathbb{R}^{17}$ defines the length of each segment in $GI(P)$. Suppose that the dimensions of R are 20 units by 14 units, and further, that each segment of $GI(P)$ is indexed left to right, then top to bottom (horizontal segments, then vertical). The terminal and Steiner points are indexed together going left to right from the top row to the bottom. Using such an indexing, let $\vec{d} = (5,6,5,4,5,6,5,4,5,5,4,5,5,4,5,5,4)$, where the i^{th} component of $\vec{d}$ is the length of the i^{th} segment of $GI(P)$. A solution to this problem is another vector of decision variable values (0 or 1), $\vec{x} \in \mathbb{R}^{17}$. The objective is to minimize $\langle \vec{d}, \vec{x} \rangle$, and the constraints on grid points are exactly as given in [32], multiplied over three terminal and three Steiner points.

Note that the solution exhibited in Figure 27(d) is expressed by the vector of decision variables, $\vec{x} = (1,1,1,1,0,0,0,0,0,0,0,0,1,1,0,0,0)$.

In a real-world case, represent an area can be represented as a rectangle and a set of interesting locations inside of the rectangle using points that maximize corectilinearity. But there may be more than one way to place points on structures (one per structure) such that the points maximize being in horizontal and vertical lines. Figure 28 depicts a set of buildings and some possible configurations for the set of terminal points P.

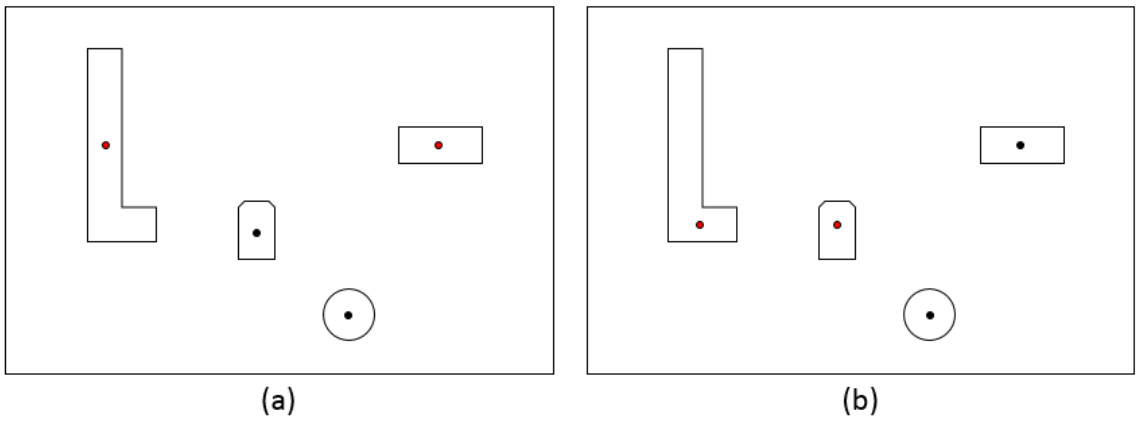

Figure 28. (a) Maximum corectilinearity of P (b) Alternative with maximum corectilinearity of P

Thus, consider an instance of the RGP wherein the set P might not be fixed. Suppose, that is, that we have a set of locations - buildings, perhaps - in an area we wish to survey using UAVs. Then, we can model each location as a point. But where on each building do we place the point? The centroid of the building outline on a 2-D map seems like a natural candidate for a terminal point. However, doing that might not maximize corectilinearity among the terminal points. Thus, we can consider different configurations for the set P and then find the minimum-length partition of each configuration, take the minimum overall and make that partition the output of the process.

However, the objective is the partition that results in the smallest number of rectangles. To that end, a conjecture is stated about the minimum-rectangle partition of the RGP, given

that the set P can vary in some sense. When the set P is not fixed, we call P variable and denote it as P_v, and consider the RGP a variable RGP (VRGP); this is really a set of RGPs, one instance per set P_v. Let L_{R,P_v} be the length of any partition of R given the set of terminal points P_v. Then, the conjecture is stated as follows.

Conjecture 1 Given an instance of the VRGP, $I = (R, P_v)$, a minimum-length partition divides R into the minimum number of rectangles. Furthermore, the absolute minimum-length partition is of length $\min\left\{\min_{P_v} L_{R,P_v}\right\}$.

Now, if the surveillance space is quite large, say, on the order of tens of square kilometers, then the VRGP could essentially be modeled as an ordinary RGP by choosing the terminal points to coincide with centers of mass relative to surrounding structures of interest from an intelligence perspective. To motivate Conjecture 1, it holds true in the case of Figure 27(d). Consider another example in Figure 29, where there are five areas of interest, to each of which is assigned a point such that corectilinearity is maximized. There can be at most two pairs of corectilinear points in this case; note that in each of the scenarios in Figure 27(b)-(f), there are two pairs of corectilinear points (Corectilinearity is maximized in every case.). Figure 27(f) shows the minimum length partition, which yields the smallest number of rectangles. It is important to observe here that where the terminal point is placed on each location can vary, and that choice results in a different set of possible cuts.

If the interior points are completely noncorectilinear, as in Figure 30, then there is little concern about the placement of points within locations as no vertical or horizontal line passes through any two locations simultaneously. As a result, the point on each location can be chosen to be the centroid of the location. Now, observe a necessary (but not sufficient) condition to ensure the cuts generate the minimum-length partition: for any pair of points on a vertical or horizontal grid line, a single cut must pass through them in order to achieve the minimum-length partition of the rectangle, which, by conjecture, results in the smallest

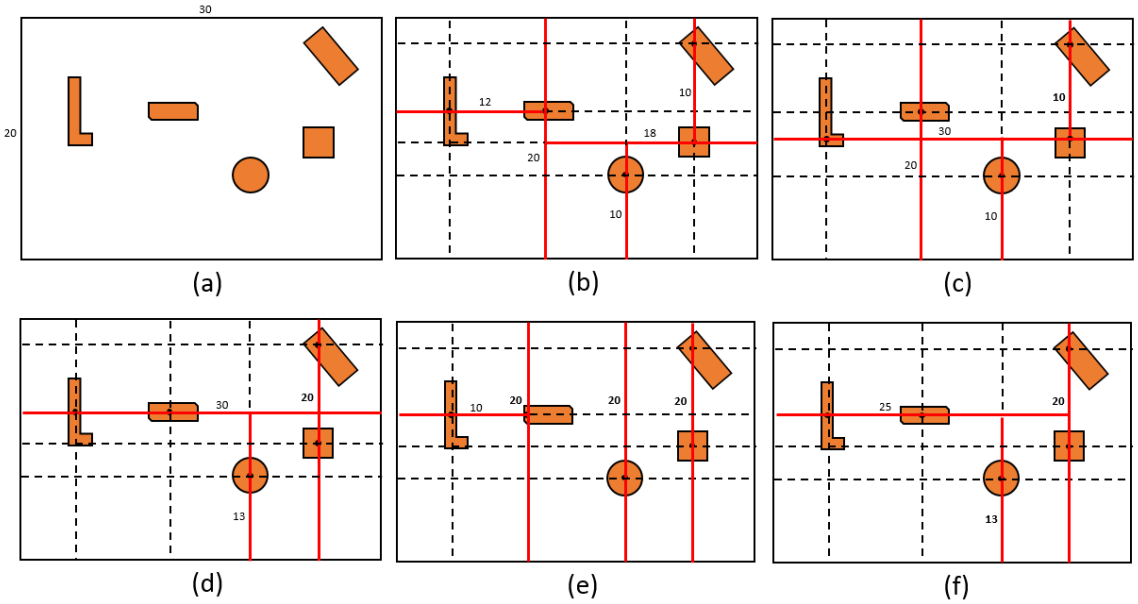

Figure 29. (a) Locations of interest (b) 6/70 (rectangles/length) (c) 6/70 (d) 5/63 (e) 5/70 (f) 4/58

number of rectangles. If collinearity is ignored when making cuts, more cuts than necessary will be generated, increasing partition length and introducing more rectangles.

Again, the conjecture holds; in Figure 30(f), the smallest number of rectangles result from the minimum-length partition. To be clear, this is not saying that the minimum-length partition is the only way to achieve the smallest number of rectangles in the partition. Conjecture 1 only states that the minimum-length partition guarantees the smallest number of rectangles are generated. Looking for the minimum-length partition is critical to solving the partitioning problem using integer programming techniques.

3.2.1 Integer Programming Partitioning Formulation.

In [32], de Meneses and de Souza showed that the set partitioning model of the RGP problem produces generally better results than the segment model. In light of their research, a set partitioning model is pursued here to generate the minimum-length partition of the RGP. Based on Conjecture 1, this minimum-length partition is necessarily composed of the

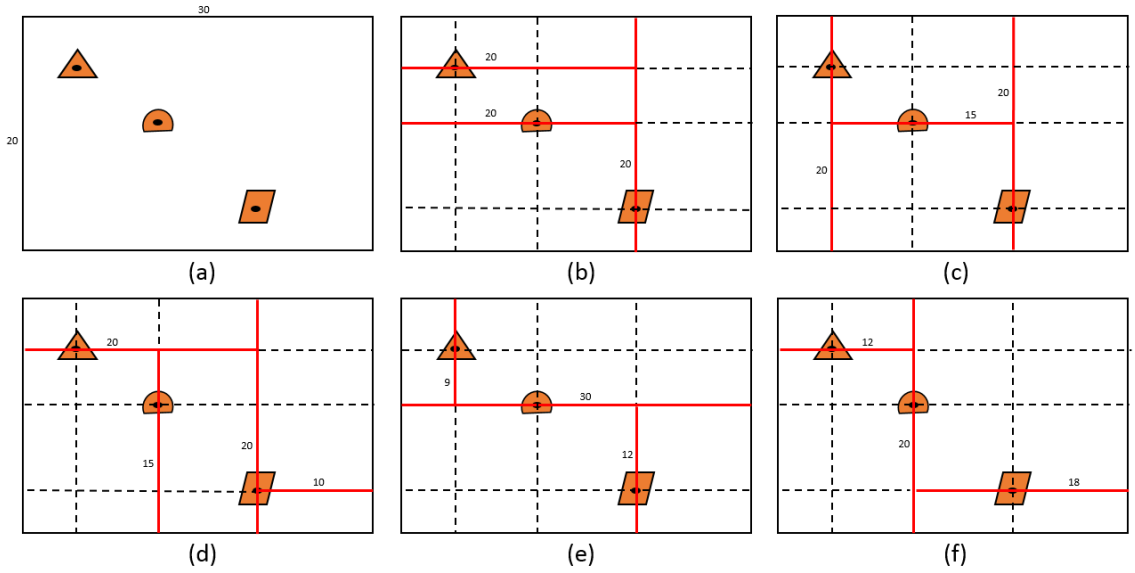

Figure 30. (a) Locations of interest (b) 4/60 (rectangles/length) (c) 4/55 (d) 5/65 (e) 4/51 (f) 4/50

minimum number of rectangles. Because a set partitioning model is used, the length of the partition is related to the perimeters of the rectangles included in the partition.

Consider the four operational scenarios in Figure 31, modeled as instances of the RGP. In each part of Figure 31, the ordered pair associated with each terminal point in the RGP is each point's coordinates, given that $(0,0)$ corresponds to the lower left corner of rectangle R. All rectangles in Figure 31 are of size 40 km $\times$ 50 km. Next, for each rectangle R_i, we draw $GI(P_i)$ in Figure 32.

The standard set partitioning problem presented in Chapter 2 was:

$$\text{Minimize} \quad \sum_{j=1}^{n} c_j y_j$$

subject to

$$\sum_{j=1}^{n} a_{ij} y_j = 1, \qquad i = 1, \cdots, m;$$

$$y_j \in \{0,1\}, \qquad j = 1, \cdots, n.$$

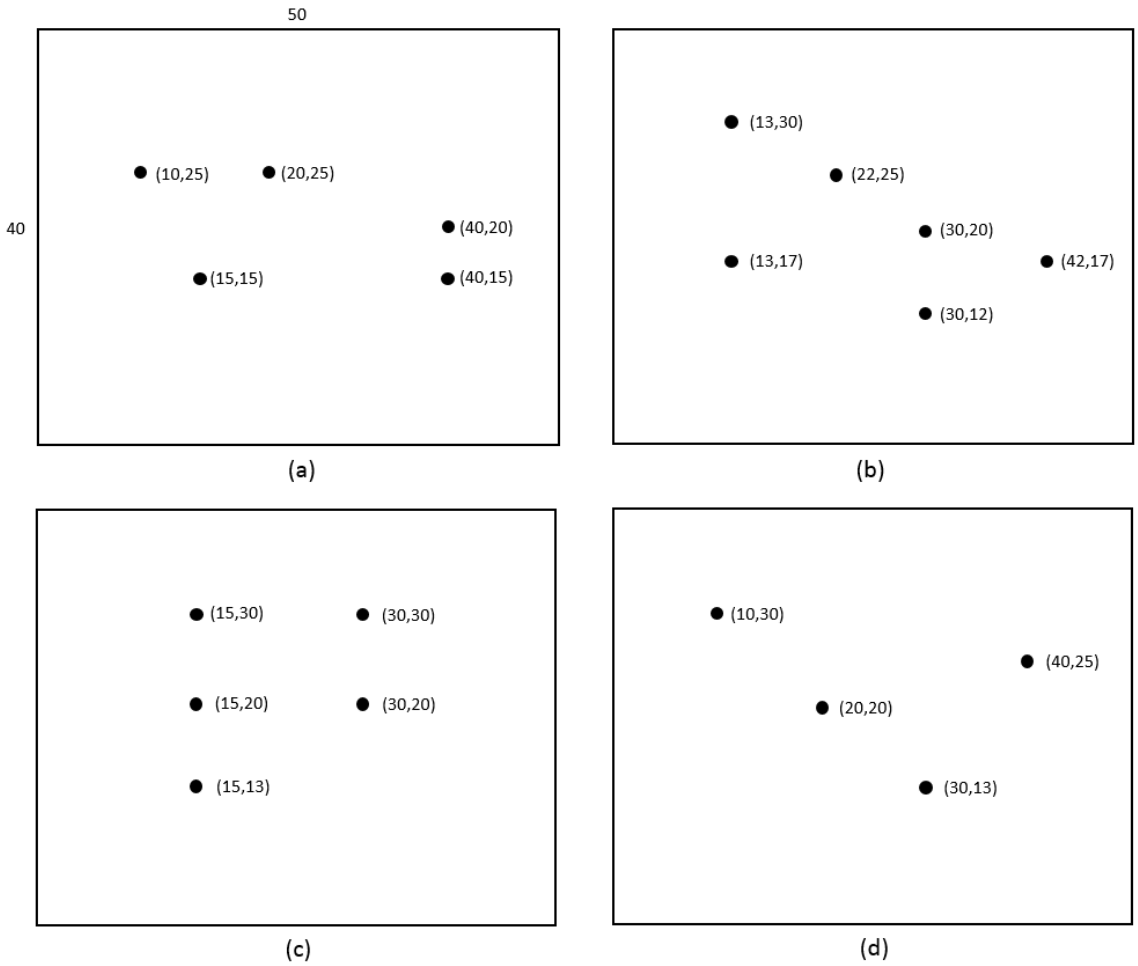

Figure 31. (a) $I_1 = (R_1, P_1)$ **; (b)** $I_2 = (R_2, P_2)$ **; (c)** $I_3 = (R_3, P_3)$ **; (d)** $I_4 = (R_4, P_4)$

In [32], the cost of each feasible rectangle was its perimeter plus the lengths of the sides coincident with the sides of R. However, when implementing the set partitioning model, a simpler cost structure resulted in the same optimal solution as the cost structure presented by de Meneses and de Souza. In fact, setting the cost of each rectangle to its perimeter resulted in the same minimal cost as that achieved using the cost function described by de Meneses and de Souza.

Each instance of the RGP is encoded as a list of points (x and y coordinates) corresponding to the intersections of segments of $GI(P)$ (terminal and Steiner points) and those points on the borders of R that intersect segments of $GI(P)$. These points are entered into a

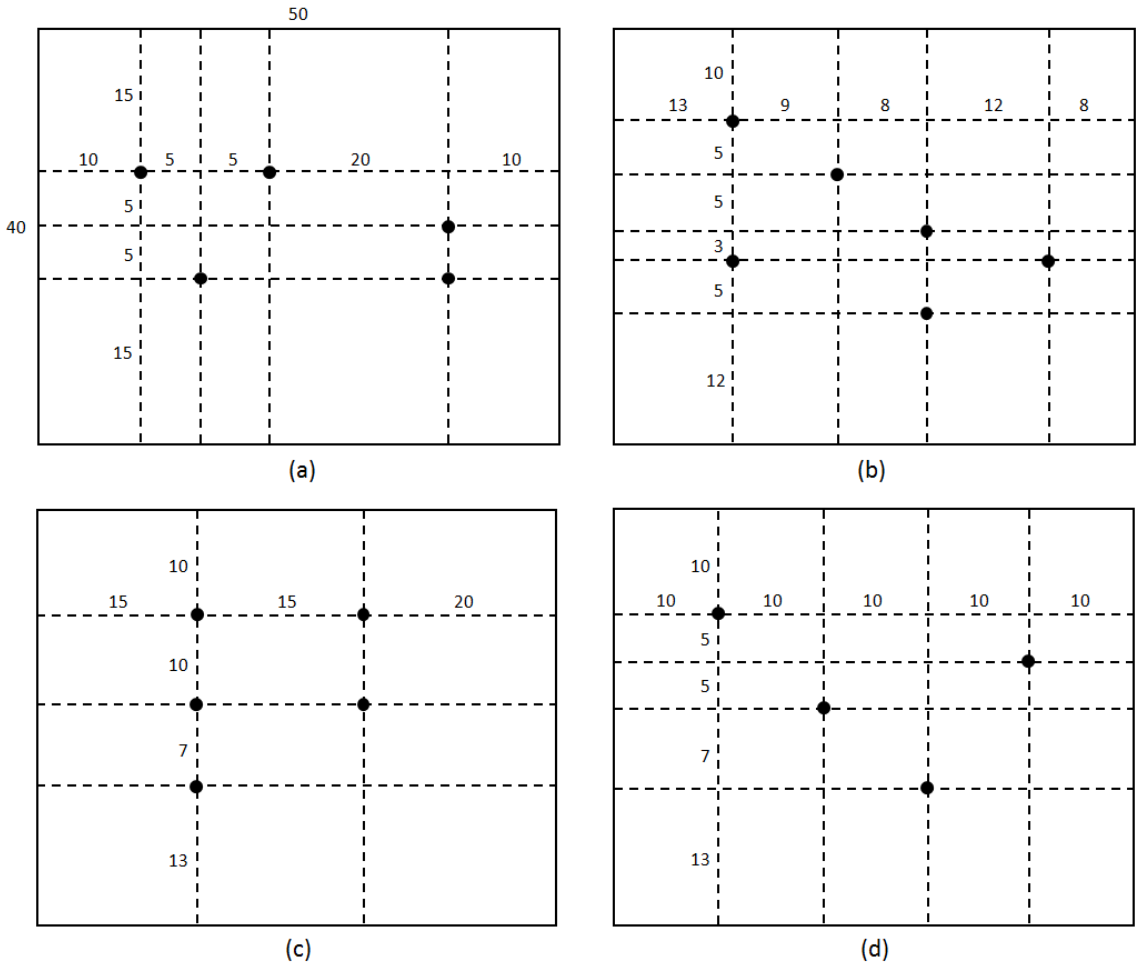

Figure 32. **(a)** $GI(P_1)$ **; (b)** $GI(P_2)$ **; (c)** $GI(P_3)$ **; (d)** $GI(P_4)$

Microsoft® Excel® spreadsheet to be read into a MATLAB® program, developed to solve any given instance of the RGP. First, the code uses the matrix input from Excel® to generate objects including points and rectangles. All feasible rectangles are identified, defining the search space of the IP algorithm. The output of the code is a set of feasible rectangles (each defined by two points - the top left and bottom right) that partition the surveillance space R. Instrumental to this task is the *bintprog* function of MATLAB®, which executes a branch-and-bound algorithm to solve the binary IP formulation of the set partitioning problem. Applying this process to the scenarios of Figure 32 produces the partitions given in Figure 33.

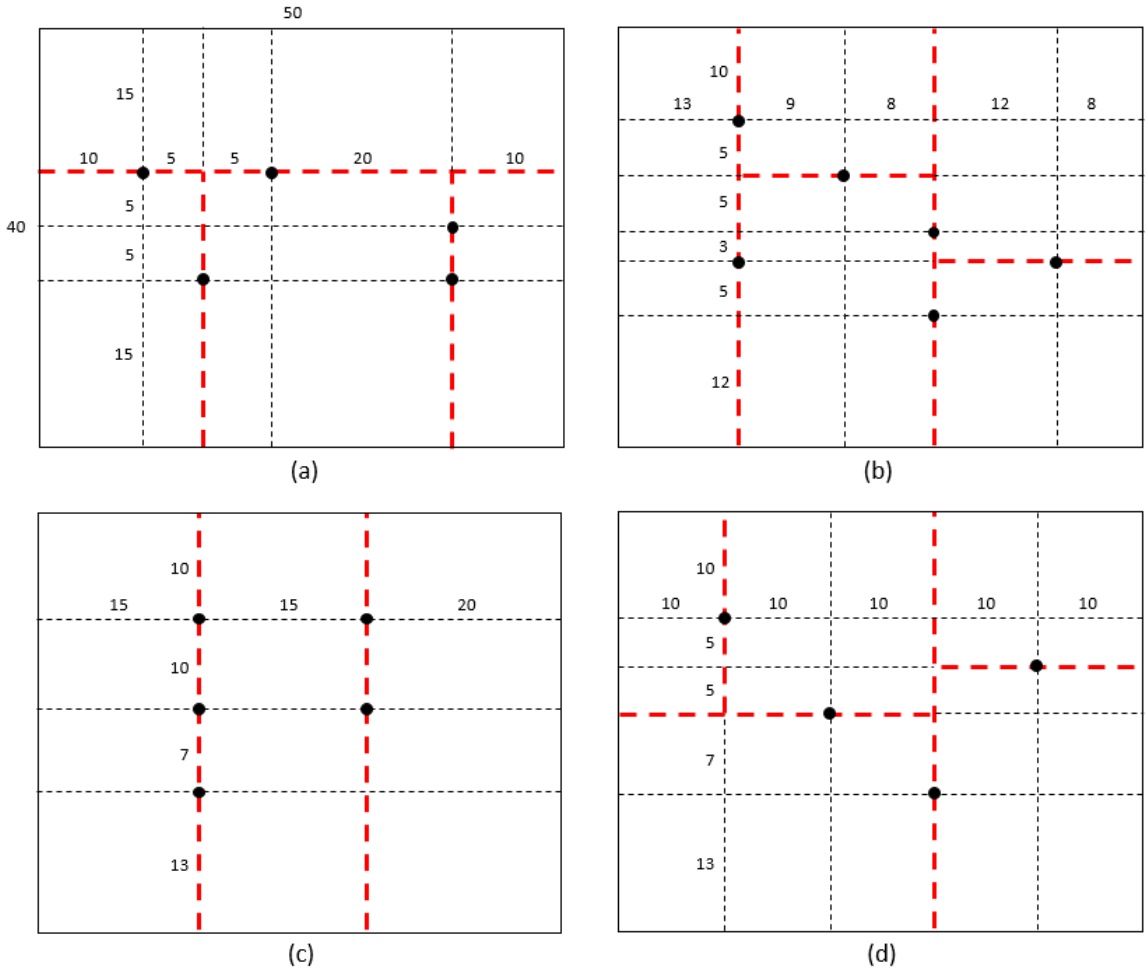

Figure 33. (a) I_1 **solved ; (b)** I_2 **; (c)** I_3 **; (d)** I_4

3.3 UAV Assignment

Once the surveillance space is partitioned, consider the task of assigning exactly one UAV to each member of the partition, $Part(R)$. The objective is to assign the appropriate UAV to each member $Part(R)$. In order to do that, the flight pattern of the UAVs needs to be considered. It takes a significant amount of time for an aircraft to execute a coordinated turn. In fact, Huang [29] points out that the number of turns a UAV needs to make while conducting a survey is the main factor in the cost difference between different sweep directions. As a consequence, if minimal revisit time is desired, a reasonable expectation

for a persistent surveillance program, UAV paths that minimize the number of turns are required. Moreover, Maza and Ollero [31] explain that simulations show back-and-forth, or boustrophedon motion, to be more efficient than a spiral pattern. All this amounts to stating that it is more efficient for a UAV to sweep a rectangle by moving back and forth parallel to the longest side of that rectangle.

Also consider the size of each member of $Part(R)$. For a small region, it makes more sense to assign a smaller UAV to it, capable of making tight turns, rather than, say, a larger aircraft with a greater maximum speed, which is better suited for larger members of $Part(R)$. As such, the partitioning algorithm is progressive in the sense that the minimally-capable UAV is assigned to a given region such that the maximum revisit time desired by a decision maker is respected. This also ensures parsimony in terms of the types of UAVs delivered to an area of operations. For example, if an RQ-11 Raven can meet a decision maker's needs, then it makes sense to order that UAV to the field rather than the more expensive RQ-7 Shadow to do the same job. Other considerations that are important when considering how to assign UAVs to regions of the space include the time it takes to deliver a system to the theater, how many of a particular airframe are in the inventory, UAV fuel type, means of takeoff, ceiling, payload capacity, etc. All of these concerns are important factors in determining which type of UAV should be assigned to each member of $Part(R)$. For example, if JP-8 fuel is scarce in a particular area of operations but gasoline is plentiful, then it might make sense to assign a gasoline-powered UAV instead of one that uses JP-8, if both systems are otherwise comparable and could appropriately be assigned to the same member of $Part(R)$.

Still other considerations important to the assignment process include personnel issues such as deployment tempo of UAV operators, the type and amount of equipment that needs to be delivered along with UAVs to an area of operations, UAV susceptibility to jamming or attack, vehicle reliability and maintainability, and the logistics of returning UAVs to the

United States from a theater after operations have been completed. If a UAV is delivered to theater because it can cover an area in a manner consistent with a decision maker's surveillance plans, but it is not very maintainable given the circumstances, then perhaps a different UAV would have been a better choice. Thinking about these issues before deciding on a particular UAV for a given region can reduce waste in terms of time and money by delivering the right system at the right time.

Although the number of UAVs operated by the departments of the United States Government, including the military services, the NSA, CIA, and others is large, here the UAV assignment problem is simplified by restricting the available UAVs to a subset of all UAVs available for military (surveillance only) use. To better understand the class of vehicles from which a set may be selected to perform persistent surveillance, the general classes of UAVs are presented in Figure 34.

Category	Mini	Tactical	Strategic
Altitude	Low	Low to medium	Medium to high
Endurance	Short (about an hour)	Medium (up to several hours)	Long (ranges from hours to days)
Range	Close-range	Limited to line-of-sight (approximately 300 kilometers or less) (about 186 miles)	Long range
Example	Raven 	Shadow 	Global Hawk 

Figure 34. UAV categories ([5], p. 9)

Thus, given a partitioned surveillance space, UAVs are chosen generally from one of these categories. If, for example, the partitioned space includes both a 5 $km \times 2$ km rectangle and a 50 $km \times 15$ km rectangle, and the mission timeline is on the order of a few hours, then it makes sense to include both a mini UAV and a tactical UAV in any air package sent

to surveil the space persistently. On the other hand, if a member of the partition of R is 150 $km \times 75$ km and the mission timeline is on the order of days, then a strategic UAV such as the RQ-4 Global Hawk should perhaps be included in the UAV package.

This research assumes that the UAVs that are available to use in a persistent surveillance program are those identified in Figure 34, namely, the RQ-11 Raven, RQ-7 Shadow, and the RQ-4 Global Hawk. To decide which one to use for a given member of $Part(R)$, the flight and camera swath characteristics of each vehicle are needed. These are estimated in Table 3.

Table 3. UAV characteristics: Global Hawk, Shadow, and Raven

UAV	Cruise Speed (km/h)	Camera Swath (km)
RQ-4 Global Hawk	640	10
RQ-7 Shadow	185	3
RQ-11 Raven	48	1

Given this information, along with the dimensions of $Part(R)$, and a decision maker's desired maximum revisit time for the locations identified by the intelligence community, the output produced is the best UAV of the three options for each subregion of R - the one that optimizes (minimizes) revisit times to terminal points along the path of a UAVs sweep within each subregion. The system diagram shown in Figure 35 depicts the inputs and output of this assignment process.

The assignment process requires some explanation. Suppose $E \subset Part(R)$ is of height h and width w. Figure 36 helps to develop the formula for the estimated maximum revisit time t_{est} to a terminal point associated with a UAV sweeping the region in a lawnmower pattern. Part (a) of Figure 36 is a case where E has a width that is less than or equal to the width of the camera swath s of one of the UAVs that could be selected to sweep that region (such as an RQ-11 Raven). If a Raven is chosen to sweep this area, then it can sweep the entire area and visit point $p = (x, y)$ in one pass. Depending on where p is along the height of E, the maximum revisit time will vary.

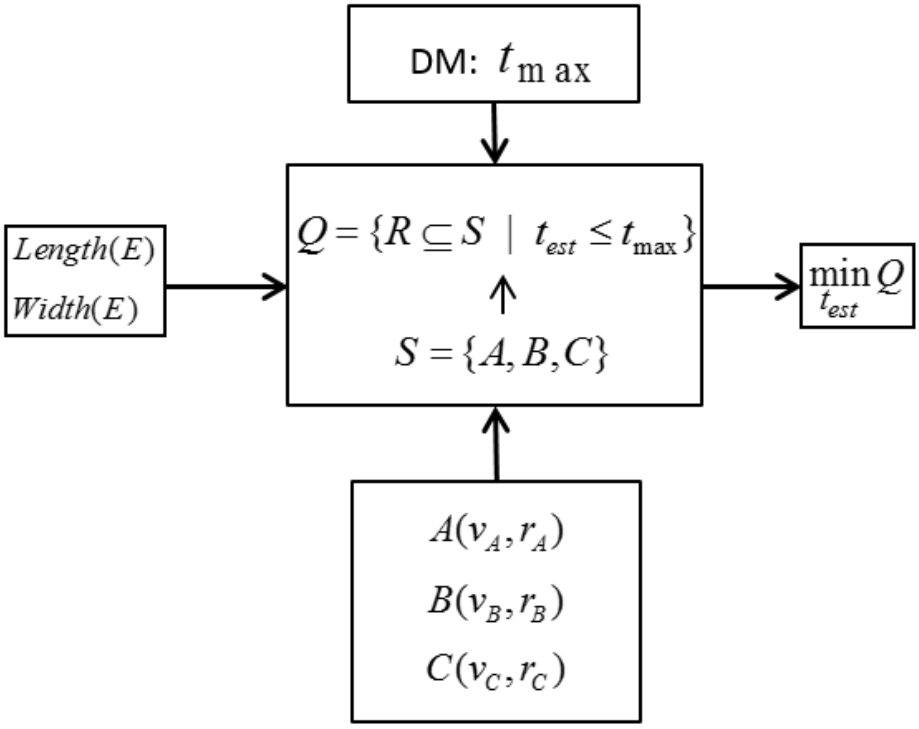

Figure 35. UAV assignment process for any $E \subset Part(R)$ given UAVs A (RQ-4), B (RQ-7), and C (RQ-11).

Assume for the moment that $y > h - y$. In that case, if the UAV is traveling from the bottom of the rectangle to the top, then first observes point p in $t_1 = y/v_C$ hours. It then revisits point p on the return sweep toward the bottom of E in $t_2 = 1/60 + 2(h-y)/v_C$ hours, assuming that a 180° turn takes one minute to execute. Then the vehicle revisits p once more in $t_3 = 1/60 + 2y/v_C$ hours as it passes the point while moving toward the bottom and returns to the point, traversing a distance of $2y$ km while traveling at the cruising speed, v_C km/h. The estimated maximum revisit time to point p, if a Raven is chosen to conduct the surveillance, is then given by $t_{est} = \max\{t_2, t_3\}$. Following this calculation of t_{est}, the subset of the available UAVs that satisfy $t_{est} \leq t_{max}$ (where t_{max} is a decision maker's desired maximum revisit time) is identified, and the element of this subset with the minimum value (the best UAV) is assigned to survey E.

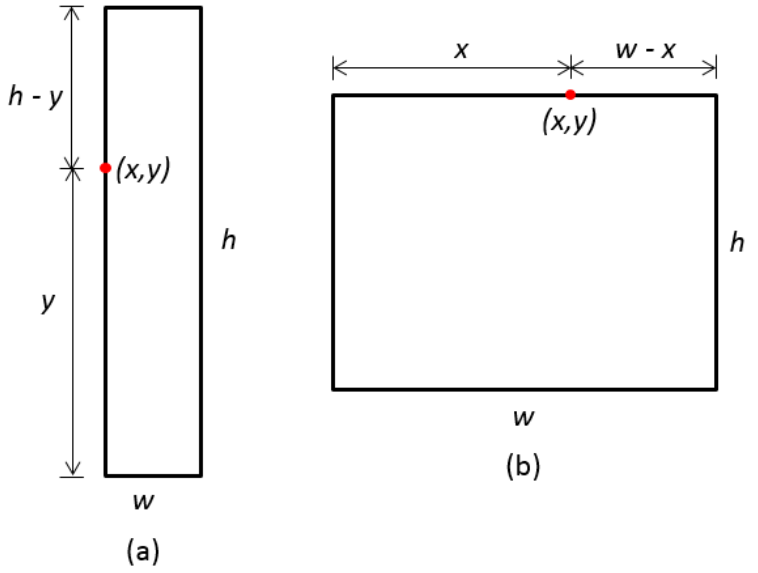

Figure 36. (a) Case: $w \leq s$**; (b) Case:** $w > s$

If E looks more like the rectangle in Figure 36(b), where the UAV sensor swath may have less size than the height of E, then the time it takes for some UAV initially traveling in a left-to-right direction from top to bottom, say UAV A, to revisit point p after its initial visit in $t_1 = x/v_A$ hours is

$$t_2^{LR} = [2(w-x) + 2wh/s]/v_A + 2h/s + 1/60.$$

Returning to p at this point takes the UAV $t_3 = 1/60 + 2x/v_A$ hours, which is relatively small. On the fourth visit, $t_4 = t_2$. The UAV repeats this process until the end of the mission timeline. The maximum revisit time in this scenario becomes $t_{est}^{LR} = t_2^{LR}$, where LR indicates the left-to-right initial direction of the UAV's motion. The situation changes if the UAV initially sweeps in a right-to-left pattern instead of moving left-to-right at the outset. When this happens, the maximum revisit time occurs on the second pass as well, and

$$t_{est}^{RL} = [2x + 2wh/s]/v_A + 2h/s + 1/60$$

hours. Because UAV operators have control over the initial direction of flight (right-to-left or left-to-right) the initial direction can be chosen to be that which minimizes the estimated revisit time, $t_{est} = \min\{t_{est}^{LR}, t_{est}^{RL}\}$. These calculations depend on the UAV continuously retracing its path going from the top to bottom of R; that is, whatever path it follows as it sweeps to the bottom of the rectangle, it retraces on the return trip. Thus, the overall path of a UAV is determined by its initial sweep of the surveillance space.

3.4 Partitioning and Assignment Flowchart

Figure 37 summarizes in a flowchart the high-level process of randomly generating a surveillance space (an instance of the RGP), dividing the space into smaller rectangles, and then assigning the appropriate UAV to each smaller rectangle. The details of this implementation, that is, the pseudocode used to produce the output, are located in Appendices B and C.

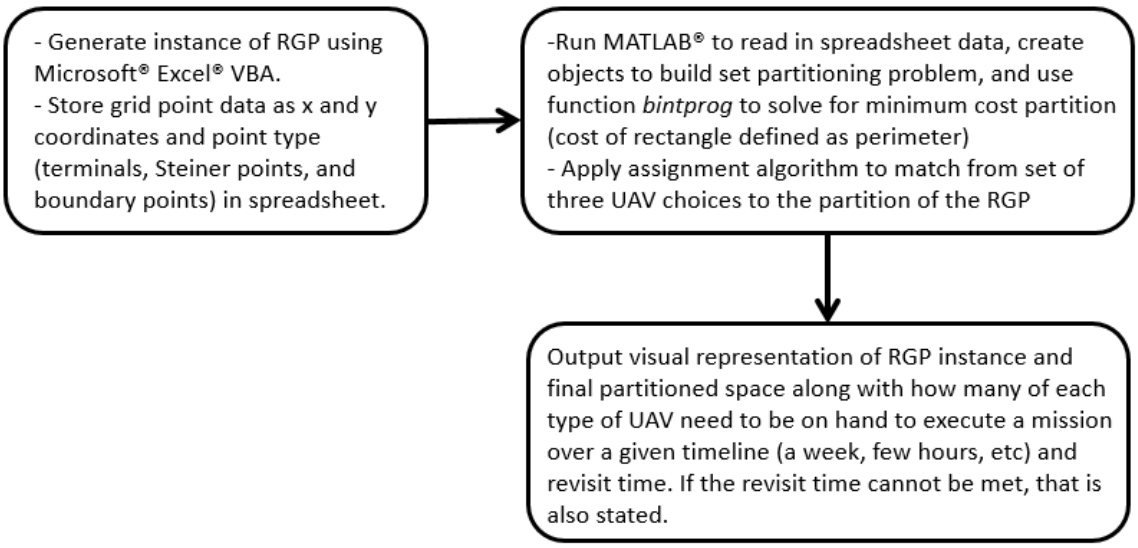

Figure 37. High-level depiction of partitioning and assignment process

3.5 Operational Scenarios

Having developed the code to solve instances of the RGP using MATLAB®, the next step was to write code using Microsoft® Excel® Visual Basic for Applications (VBA) to generate scenarios as random instances of the RGP. The inputs to that process are the number of desired terminal points and the dimensions of the surveillance space. Without loss of generality, the terminal points are spaced apart from the edges of the rectangular surveillance area. Each scenario is detailed in Figures 38-39; for these cases, they are presented as pure instances of the RGP. However, they could just as easily have come from a map with Global Positioning Satellite coordinates. In the next chapter, the process of partitioning a space and assigning UAVs to the partition is implemented by applying that process to each operational scenario in Figures 38-39.

3.6 Summary

In this chapter, the process used to partition a space based on an IP formulation methodology provided in [32] is outlined. Further, the algorithms used to decide which UAV to assign to each member of the partitioned space from a pool of available UAVs is also described as a way to assign the minimally-capable UAV to each subregion of a partitioned space, reducing waste in spending. Finally, the entire process is summarized in a single flowchart to better understand the end-to-end method for creating a persistent surveillance program over a rectangular surveillance space, which is modeled as an instance of the RGP.

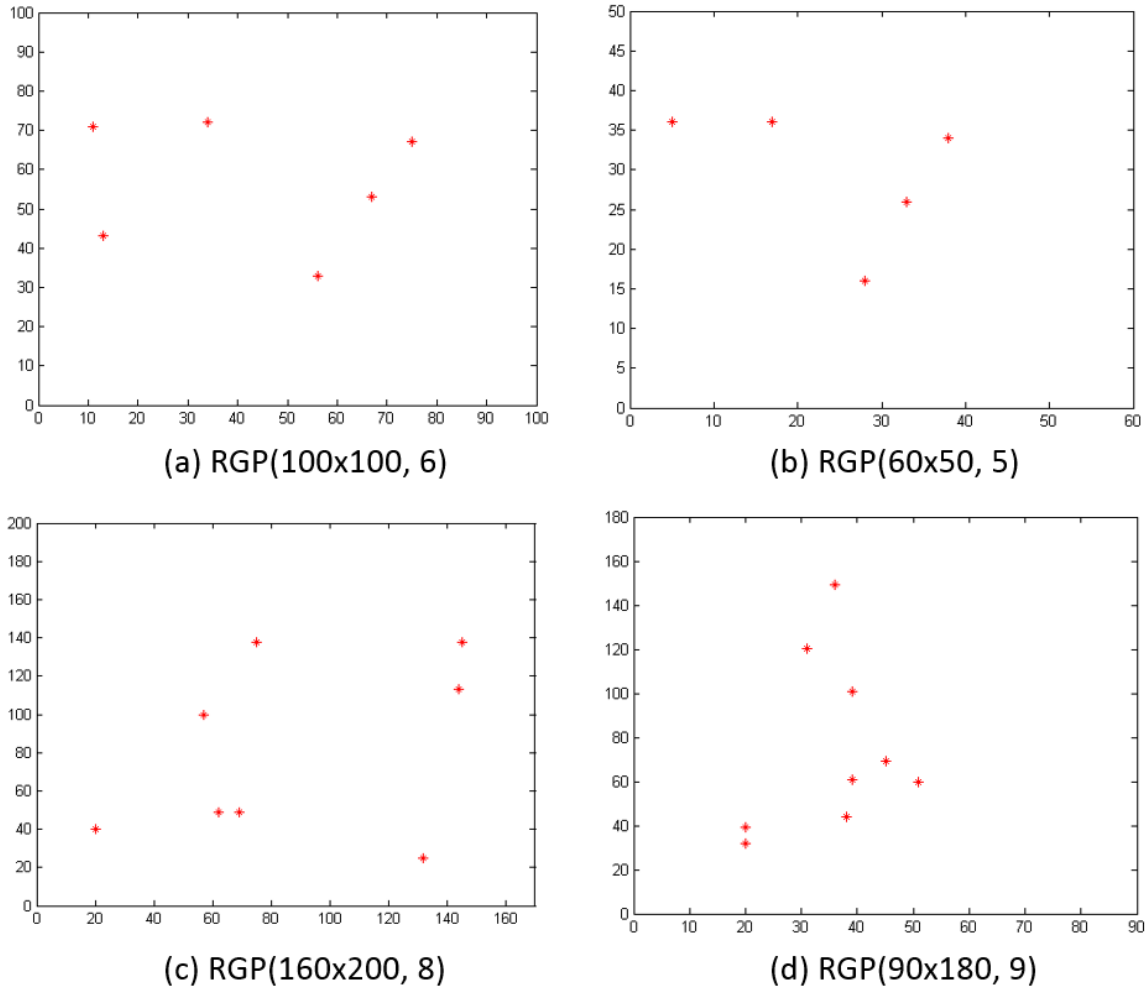

Figure 38. Scenarios: Set I

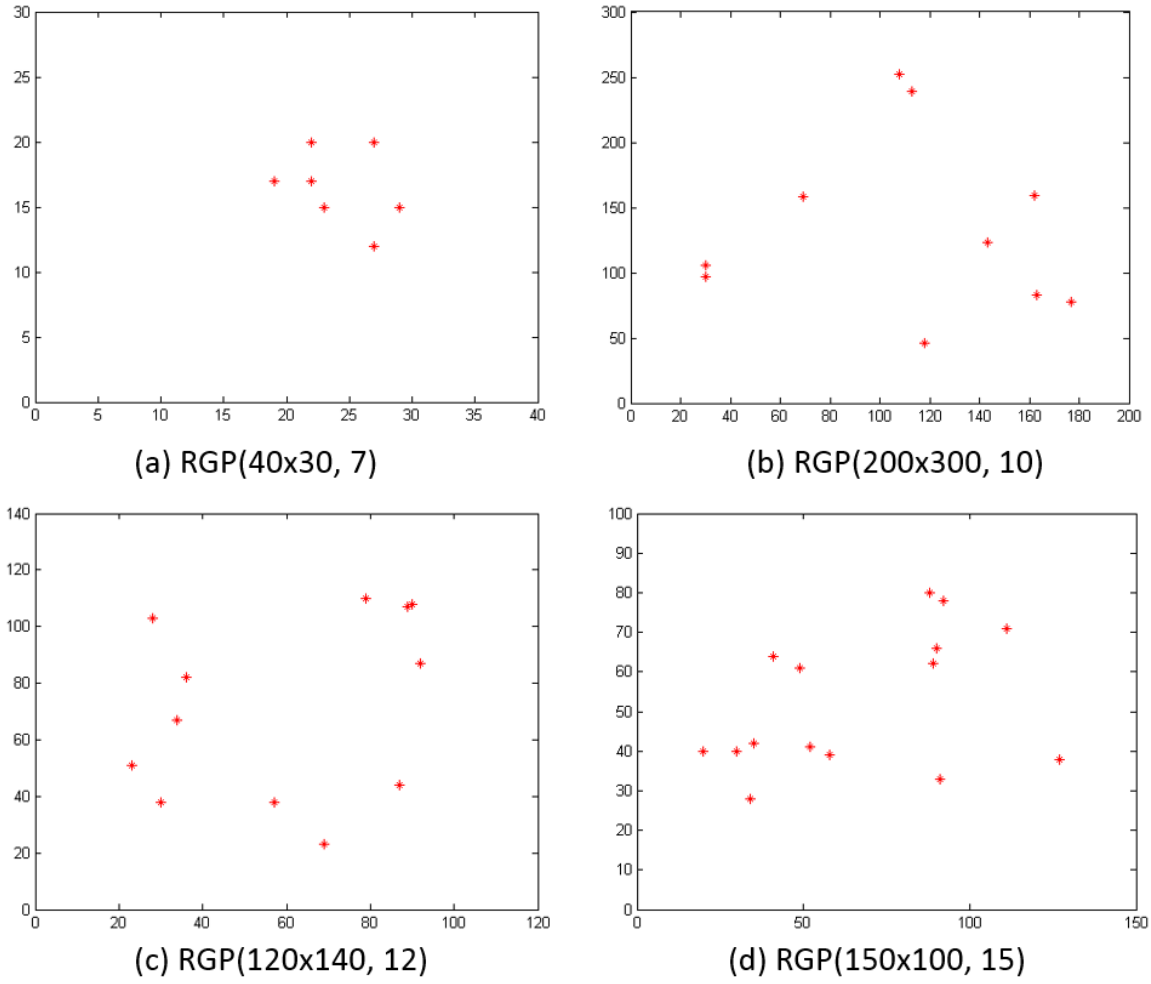

Figure 39. Scenarios: Set II

IV. Implementation and Analysis

4.1 Introduction

In this chapter, the algorithms developed in Chapter 3 for partitioning a surveillance space based on the work of [32] and assigning exactly one UAV to each member of the partition are implemented to solve operational persistent surveillance scenarios. This is followed by an analysis of the results and a discussion on the insights and limitations associated with the approach used here. Finally, this chapter concludes with a brief description of the logistics of moving UAVs into an area of operations.

4.2 Implementation

The solutions to the scenarios of Set I are presented as partitions of the associated RGP instances in Figure 40. Within each member of the partition of each surveillance space, the appropriately assigned UAV is indicated. Figure 41 presents the solutions to the scenarios in Set II.

Each solution is accompanied by the RGP parameters and the maximum revisit time in hours over all subregions based on their assigned UAVs. For example, in Figure 40(b), the dimensions of the surveillance space are 60×50 *km* and the number of terminal points is 5. In addition, the maximum revisit time over any partitioned subregion is 5 hours.

One quantity not displayed in Figures 40 and 41 is the mission timeline. The reason for this omission is that the mission timeline only dictates how often UAVs over a partitioned subregion must be swapped based on UAV endurance. For example, if the scenario depicted in Figure 40(b) has a mission timeline of 48 hours, then in region 1 (top left rectangle), UAV operators would need to swap the operating RQ-7 Shadow, which has an endurance of six hours, for a fresh vehicle a total of eight times over the course of 48 hours. This is precisely why a minimum of two and UAVs are required for each region. It is better,

however, to have a minimum of three UAVs on hand (if available) for each region. In that case, one is in operation, one is in maintenance mode, and the third is a spare. Thus, for the 300 km^2 rectangle in Figure 40(b), having 12 RQ-7 Shadow UAVs and three RQ-11 UAVs on hand would ensure continuous execution of the persistent surveillance program on that space.

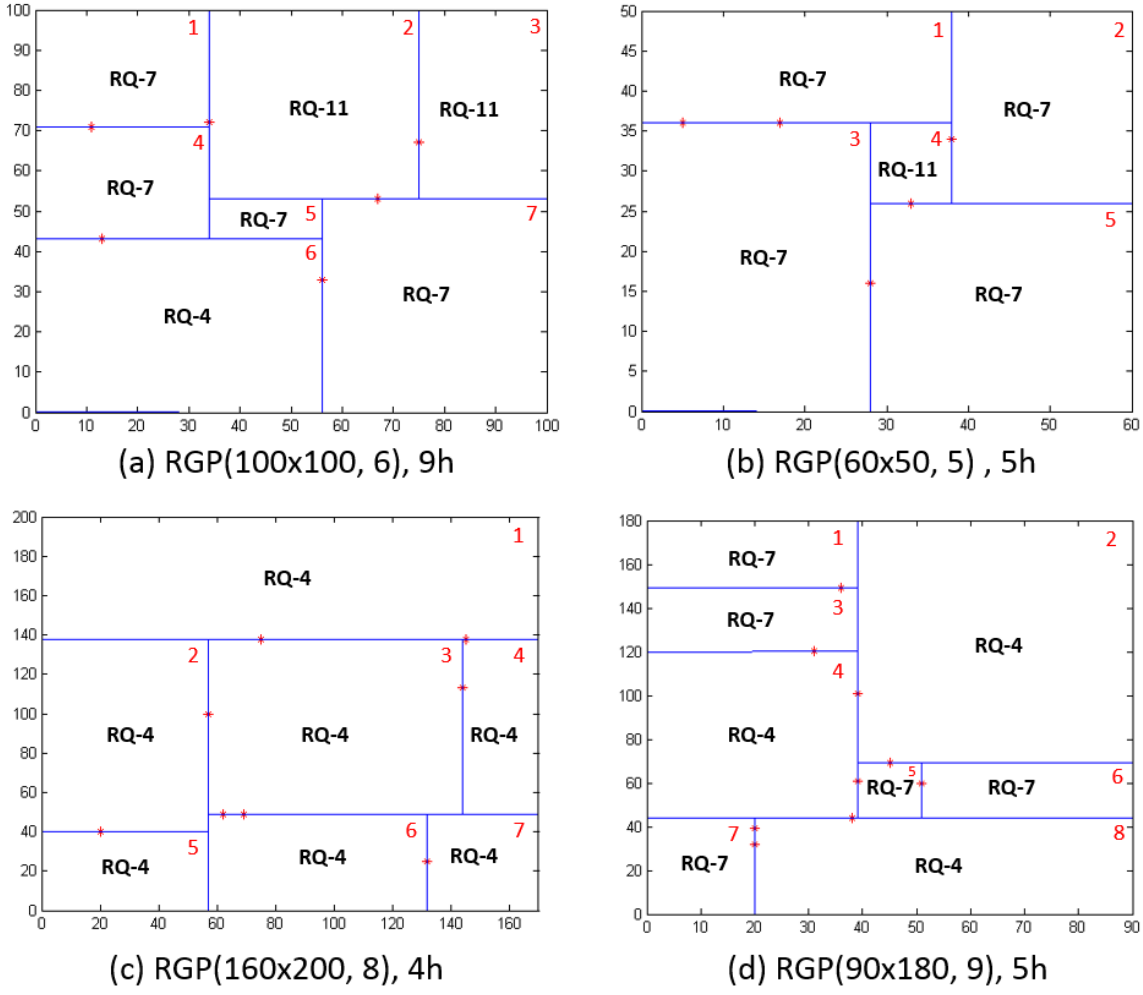

(a) RGP(100x100, 6), 9h

(b) RGP(60x50, 5) , 5h

(c) RGP(160x200, 8), 4h

(d) RGP(90x180, 9), 5h

Figure 40. Solutions to scenarios in Set I

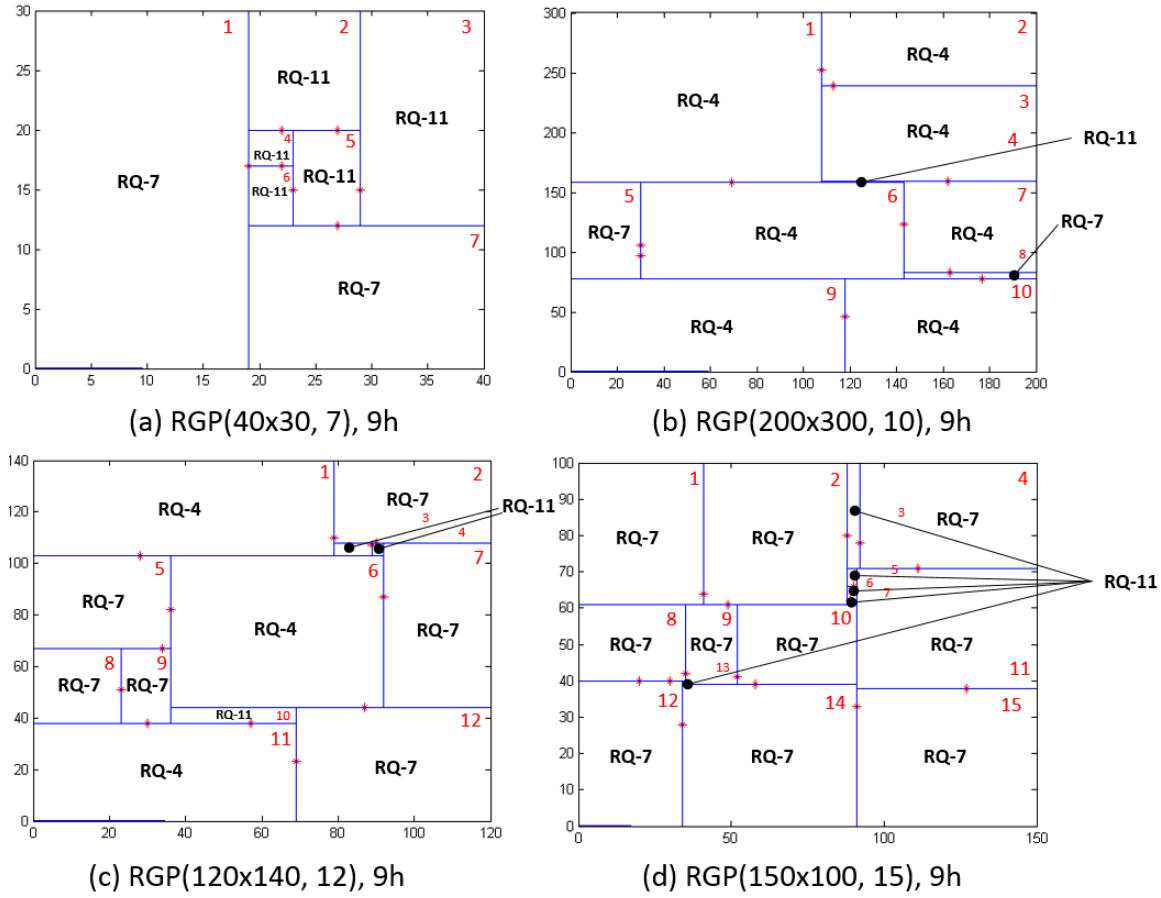

Figure 41. Solutions to scenarios in Set II

4.3 Analysis

4.3.1 Partitioning and Assignment.

Knowing the maximum revisit time of each cell gives more information about the decomposed surveillance space to a decision maker. With this level of detail, a decision maker can manage expectations of a surveillance program. The decision maker can effectively communicate to authorities and imagery customers the level of surveillance that can be obtained using a parsimonious number of UAVs of the correct types for the surveillance mission. Beyond simply being able to communicate what can be achieved by a surveillance program of this type, the decision maker can reduce waste in spending by ordering only the

correct types of UAVs in the correct numbers. It makes little sense to request an RQ-4 Global Hawk, a very expensive UAV with extensive support equipment, when two or three RQ-7 Shadow UAVs might suffice for a particular surveillance mission.

Although it makes good sense to have on hand three UAVs for each subregion under surveillance, the actual number that need to be on hand is a matter of UAV reliability and maintainability, which is outside the scope of this research. Furthermore, on the battlefield, a decision maker such as a military commander is afforded flexibility in making decisions about how to execute the surveillance program to include how many UAVs need to be requested for a given surveillance program. Modifications to the solution presented by the algorithm in this research are expected, making the output of the process implemented here a good starting point for a persistent surveillance program that can be adapted to any specific need in theater.

In particular, ordering more or less than the minimum number of UAVs (as projected by the algorithm presented in this research) of a given type for a particular subregion is an option for a commander. If the commander decides that current intelligence is more accurate than previous estimates, and that a region may not be important enough to surveil, the commander can opt to apply resources elsewhere. On the other hand, if a commander is not satisfied with the revisit time (desiring a shorter revisit time interval) that can be expected from the mapping of UAVs to subregions as described in this research, then the commander can order more of that particular type of UAV, or even replace that type with a more capable UAV; switch an RQ-11 for an RQ-7, for example. Without a starting point, however, the task of deciding how to partition the surveillance space and deciding which UAV should be assigned to each subregion to meet revisit time expectations is more difficult. With the algorithm given in this research, the task becomes simpler and can be finished more quickly.

The partitioning algorithm presented in this research works well for medium-sized problems, measured in terms of the number of feasible rectangles generated by the RGP. For scenarios involving up to 15 terminal points (which generate a number of feasible rectangles), the algorithm quickly provides an optimal solution, but including more terminal points generates increasingly many feasible rectangles, and the output tends to become unreliable. In some cases, when the number of terminal points approaches or exceeds 20, no feasible solution is produced by the algorithm. Thus, a limitation of the process to solve the persistent surveillance problem is that it does not work well for larger problems.

The reason for this limitation is that unlike a linear program (LP), which is a continuous optimization problem, an IP (a discrete optimization problem) has no general optimality conditions. Thus, even though the solution space of a general IP may be quite small in comparison to the solution space of an LP, solving the IP can take a long time and require great effort, whereas very large LPs can be solved often much more simply using general techniques with little difficulty using modern software [39]. Thus, various methods have evolved over time to solve IPs. These methods fall into three categories, namely, enumeration techniques (a class that includes branch-and-bound, the method used by the *bintprog* function in MATLAB®), cutting-plane techniques, and group-theoretic techniques [25]. The focus here is on branch-and-bound, as it was used to solve the problems posed in this research.

When the *bintprog* function is called in MATLAB® to solve a problem formulated as an IP, the function uses an LP-based branch-and-bound algorithm to produce a solution. The algorithm employed in MATLAB® relaxes the binary constraint on the decision variables x, allowing $0 \leq x \leq 1$. This procedure works by searching for a binary integer feasible solution, updating the best integer point found by the current iteration, and verifying that no better integer feasible solution is possible by solving a series of LPs [11]. Typically, using the default options of *bintprog*, the algorithm terminates, finding no feasible solution

for larger problems. However, an operational scenario of the type studied in this research is not likely to include large numbers of points that need to be observed for a long period of time. If that does become the case, then grouping points in clusters and identifying each cluster as a single terminal point (at the cluster centroid) can help reduce the dimensionality of the problem.

The most time-consuming part of solving an IP is verification of optimality. Once a solution is reached, it must be verified as being optimal, and to do that, the algorithm must check the solution against a number of other candidate solutions. For integer programs, even small problems can result in a large space in which to search during optimality verification. This is sometimes referred to as "combinatorial explosion." In those cases, solving an IP to optimality becomes very difficult, if not impossible, and one is forced to resort to heuristic methods that do not guarantee optimality [39]. The fact that *bintprog* implements a branch-and-bound algorithm, an exact solution method, means that it is limited in the size of problem it is capable of solving given any particular hardware on which a solution is attempted.

In their research, de Meneses and de Souza used a branch-and-price algorithm to solve their IP-formulated partitioning problem, comparing its performance to the best known approximate method of solution. A branch-and-price algorithm is a variation on the branch-and-bound algorithm (branch-and-bound implemented by MATLAB® in *bintprog* function) in which column generation is allowed. This means that at each node of the search tree generated by a branch-and-bound algorithm, columns may be generated to tighten the bounds on the LP-relaxation at that stage. Branch-and-price is used to solve large-scale IPs, and it is complementary to cutting in the branch-and-cut algorithm, which involves row generation [16]. It is possible that larger partitioning problems - larger than those represented by the operational scenarios in this research - could be solved more readily using a branch-and-price algorithm.

As for the assignment algorithm implemented in this research, it is executed after the space is partitioned. It would be better to couple the partitioning and assignment processes, but that would make the problem intractable for even a small number of UAVs [34]. Instead, Nigam and Kroo first use auction algorithms in [34] to optimally assign UAVs to partitioned subregions of a surveillance space. However, they admit that using such algorithms, the optimal allocation is not always achieved. Thus, they turn to a process of iteratively improving the bounds on the cost matrix of their formulation; this slows down the procedure, but it does result in the optimal allocation of UAVs to partitioned subregions. Here, the simple algorithm of assigning a UAV to a partition if it can meet the maximum revisit time requested by a decision maker, suffices and can be executed in minimal time. This assumes that the UAV flies a lawnmower pattern along rows of width equal to the UAV's camera swath. The algorithm works for the application of this research because the goal is not to minimize the maximum age over all cells of the space, but to simply meet a maximum revisit time for all of a set of identified points within the space.

4.3.2 Special Cases.

If operational scenarios are such that the locations within a surveillance space (the terminal points) are aligned in certain ways, then problems could arise when attempting to impose an optimal partition on the space. For example, consider a scenario modeled by the RGP in Figure 42.

The fact that all of the points are on a diagonal line means that no two points are corectilinear, which would induce a partition of $n+1$ subrectangles given n terminal points.

One way to reduce the number of partitions is to reorient the viewing plane so that the points all line up in a horizontal or vertical line. If the viewing plane is rotated to accomplish this, say, so that the points are horizontal, then the surveillance space is divided exactly in two. In that case, if the UAV assigned to each partition begins its surveillance

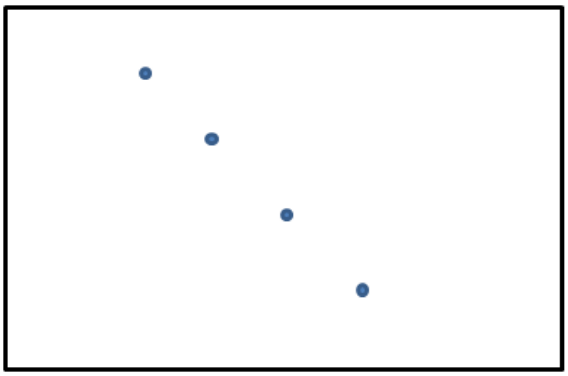

Figure 42. All points diagonally collinear

sweep on the bottom edge of its assigned region, then the revisit time for the line of points is equal to the time needed for a UAV to sweep its rectangle once because by the time the top region is swept, the UAV in the bottom region will have reached the line of points. On the return trips, the top UAV will have revisited the line of points. This pattern continues over the mission timeline.

The action of orienting a space so as to maximize corectilinearity can be considered as a preprocessing step. This preprocessing entails keeping a record of all collections of points that are collinear in any direction whether that is horizontal, vertical, or at some diagonal angle. The largest such collection can, without loss of generality, be considered to be parallel to the horizontal edge of the final orientation of the surveillance space. Aligning the points along a rectilinear path can help reduce the size of the partition.

4.3.3 Postprocessing.

After a surveillance space is partitioned using the minimum number of rectangles (given a set of terminal points), the number of UAVs used should be minimized because exactly one UAV is assigned to each member of the partition. However, the number of required UAVs may not be minimized, and for that reason, some postprocessing may be required. For example, consider Figure 41(b), where subregion 8 is a sliver that could be subsumed

into region 7, all of which could then be surveyed using one RQ-4, eliminating the need for the extra RQ-7 for subregion 8. As another example, consider Figure 41(c), where two RQ-7 aircraft are used to survey subregions 8 and 9, and at the same time, one RQ-7 is used to survey subregion 5, which is slightly larger than subregions 8 and 9 combined. It stands to reason that if subregions 8 and 9 were combined, then one RQ-7 could be used to survey that area. These pathological situations are not addressed in Nigam and Kroo [34] nor are they addressed in de Meneses and de Souza [32].

In both the case of Figure 41(b) and of Figure 41(c), this type of reconfiguration of the partition would require some terminal points to fall inside a rectangle making them infeasible rectangles. However, if the revisit time at that point does not change significantly or if the reconfiguration has no negative operational consequence, than the subregions 8 and 9 should be combined to eliminate the need for one RQ-7, further minimizing the number of UAVs required. Thus, during postprocessing, it makes sense to neglect the feasibility condition used during the original partitioning process, and instead, consider cases where the number of UAVs used can possibly be further minimized.

Another problematic consequence of the partitioning algorithm that requires postprocessing is exhibited in Figure 41(d). There, several RQ-11 Raven UAVs are used to survey very small regions. One in particular, subregion 13, is $1\ km \times 1\ km$. The reason for this is that some of the terminal points are so close together that they are almost corectilinear, but not quite. This type minor misalignment causes these pathological cases to arise. One way to deal with them is to align points that are slightly out of line. These minor adjustments are not likely to have profound operational effects, but they will help generate a more reasonable partition and further minimize the number of UAVs required.

4.3.4 Logistics.

Shipping UAVs into an area of operations is a supply chain management problem in the study of logistics. Most of the considerations along these lines are outside the scope of this research. For the sake of completeness, however, how UAVs are usually delivered into areas of operation is discussed in this section. The usual methods include shipment by cargo aircraft such as the U.S. Air Force's C-17 Globemaster III, which has a payload capacity of 170,900 lbs, or, about 85.5 short tons [1]. Further, the C-17 has a maximum loading width of 18 ft, a floor length of 68.2 ft, and a maximum loading height between 12 and 14 feet depending on location within the cargo hold [1]. That means that it can easily accommodate many RQ-11 Ravens and RQ-7 Shadows, but fewer RQ-4 Global Hawks due to its proportions. The C-17 is a versatile aircraft that can carry a number of other UAVs into theater as well. For example, in Figure 43, military personnel prepare to load the U.S. Navy's rotary-wing RQ-8B Fire Scout onto a C-17 aircraft.

Figure 43. MQ-8B Fire Scout Prepared for Loading onto C-17 Globemaster III ([19])

Larger aircraft are also used to carry some UAVs and their support equipment. For example, in Figure 44, U.S. Air Force personnel associated with Goodfellow Air Force Base unload an RQ-4 Global Hawk from a C-5 Galaxy cargo aircraft.

The C-5 can hold not only the Global Hawk, but its Mission Control Element and Launch Recovery Element in one load. It takes more than one but less than two full loads of a

Figure 44. Global Hawk Emerging from C-5 Galaxy ([4])

C-17 to carry all of these items [13]. Also, the C-5 is an excellent transport vehicle for the control elements of other UAVs, including High Mobility Multipurpose Wheeled Vehicles (HMMWVs, sometimes called "humvees") with trailers, vehicle-mounted shelters, etc. Using C-17 and C-5 aircraft, most common UAVs and their support equipment can be transported to theater effectively. This is also true in the case of RQ-11, RQ-7, and RQ-4 UAVs.

4.4 Summary

In this chapter, the results of having applied the partitioning and assignment algorithm described in Chapter 3 were presented along with a discussion of how for each partitioned subregion of the space, three of the type of UAV assigned to the subregion should be ordered to pursue persistent surveillance over a surveillance space. A brief description of the means of transporting select UAVs, namely the RQ-11 Raven, RQ-7 Shadow, and RQ-4 Global Hawk (and their support equipment), into an area of operations followed. The C-5 Galaxy and the C-17 Globemaster are effective vehicles for that purpose.

Also considered in this chapter was a limitation of the binary integer programming solver in MATLAB®. This limitation is based on the fact that integer programming problems become harder to solve and sometimes cannot be solved to optimality using exact

techniques such as the branch-and-bound algorithm implemented in *bintprog*. Therefore, using *bintprog* is an effective method for solving medium-sized IP problems in terms of the number of feasible rectangles that are generated by a given instance of the RGP. Larger problems are more difficult to solve to optimality using the procedure described in this work. However, modifying some of the default options used by *bintprog* or using different solver packages in MATLAB® may allow one to solve larger instances of the RGP. In the next chapter, this research in its entirety is summarized by way of a review followed by insights, impact, and potential future research.

V. Conclusions and Recommendations

5.1 Introduction

This chapter provides a summary of the work presented in this thesis. The insights and impact of this research, topics for future research efforts, and conclusions are also presented.

5.2 Review

The problem of persistently surveying an area of land admits many approaches and solution methodologies. To begin, this research explicitly defined persistent surveillance in contrast to the many other terms in the literature which sometimes conflict or are taken as synonymous. In fact, persistent surveillance is defined to mean surveillance over an area such that certain points in the area and their surroundings are continually revisited within some increment of time, for example, every five hours. The UAVs are assumed to be able to fly without much interference from kinetic or energy-based weapons (including jamming). It is also assumed that UAVs can be programmed to autonomously fly predesignated patterns at different altitudes (so as to avoid collision). To conduct persistent surveillance, the space is partitioned into the minimum number of rectangles using a $0-1$ integer program, and the appropriate, minimally-capable UAV is assigned to each member of the partition using a simple algorithm. Because exactly one UAV is assigned to each region, this is equivalent to minimizing the number of UAVs needed to carry out the surveillance program.

Using a modern, commercially-available desktop computer, instances of the RGP were solved using the software package MATLAB®. The scenarios themselves were generated randomly using Excel® VBA, but they could just as easily have come from real-world data, for example, map data including Global Positioning Satellite coordinates. The UAV

assignment problem considers what maximum revisit time a decision maker requests over the subregion. Revisit time is calculated assuming that the UAVs sweep their areas using a lawnmower pattern, retracing their paths on return trips to their points of origin. The surveillance space is defined by x and y coordinates, which are generated randomly using Excel® VBA; the points defined by this method are then transferred to and processed using MATLAB® code that generates a partition on the space.

Also discussed in this work was the type of IP solution technique implemented by the MATLAB® solver, *bintprog*. The function *bintprog* implements a branch-and-bound algorithm, which is an exact solution technique. Branch-and-bound is useful for solving small to medium-sized instances of the RGP in terms of the number of feasible rectangles generated by the set of terminal points. Larger instances are more effectively solved using heuristic techniques, but those cannot generally guarantee optimality. The simply-stated reason for this issue is "combinatorial explosion," which refers to the rapidly increasing difficulty in verifying optimality for IP solutions as the solution space increases in size.

Finally, this thesis concluded with some brief remarks on the logistics of moving UAVs from their home bases to areas of operation around the world. The C-17 Globemaster III and the C-5 Galaxy are both cargo aircraft operated by the United States Air Force that are capable of transporting most UAVs and their support equipment to where they are needed in theater. Support equipment include large items such as the mission control element and the launch recovery element of the RQ-4 Global Hawk, which are easily transported aboard a C-5 aircraft. Having a smaller capacity than the C-5, the C-17 can still carry much of the equipment needed in theater to operate UAVs, but more flights would be needed to complete some deliveries using only C-17s.

5.3 Insights

Solving medium-sized instances of the RGP (up to 15 terminal points) takes very little time. In the cases where the number of terminal points is less than 15, the software was able to solve the problem very quickly. When the number of terminals was less than 10, the amount of time it took to solve the IP was about 3 seconds. At 12-15 terminals, the time needed was still under 30 seconds. These timings were achieved running MATLAB® version 2013b on a machine that has 16 GB of dual data rate 3 synchronous dynamic random access memory (DDR3 SDRAM) having peak transfer rate of 12,800 MB/s. The processor of the computer is a 3.9 GHz quad-core desktop Intel® chip, and the hard drive is a Samsung® solid-state drive with a 6 Gbit/s serial advanced technology attachment III (SATA III) interface. As of this writing, these specifications are fairly good, but not the latest available hardware. Thus, using a commercially available computer, quick solutions can be found for medium-sized persistent surveillance problems of the type described in this research, namely, instances of the RGP.

Another insight into this problem and the solution methodology is that sometimes interesting locations within a surveillance space may be very close together. In those instances, the partitioning algorithm could create very small subregions to survey. These pathological cases can be avoided if the locations identified by the intelligence community are first identified with each other in clusters. Then, each cluster's centroid could take the place of an individual terminal point. This avoids having to form many, very small subrectangles and still obtain a useful surveillance program.

5.4 Potential Future Research

A number of extensions and improvements over the work presented here are possible. Some of them are detailed next.

5.4.1 Expand Pool of UAVs.

Including a larger set of available UAVs in the model would provide more flexibility and more realism. There are many different platforms and UAVs available on the market, and making more of them available to the algorithm might produce options of lower operational cost.

5.4.2 Probabilistic Models.

This research did not consider chance occurrences during surveillance. If the terminal points are not fixed or if the UAVs are characterized by known failure rates, then UAV paths would become more complicated. Generalizing the model to include these possibilities would extend the work in this research.

5.4.3 Model Camera Footprint.

Finally, a great deal of refinement is possible if the camera swath for each vehicle is modeled precisely. With a precise consideration of how the cameras are angled on any given UAV, more realism can be injected into the model presented here.

5.5 Conclusion

To conclude, IP techniques can be used to divide a space for parallel search using a number of autonomous UAVs flying at different altitudes, exactly one assigned to each subregion of the divided space in the persistent surveillance problem. Here, the term "persistent surveillance" is defined in contrast to the many ways it has been defined in the past. A common desktop computer running commercially available software can be used to set up and solve both the associated IP and the assignment problem for each partitioned subregion created by the IP. The quick solution generated by the software will ensure that a parsimonious number of minimally-capable UAVs is used to cover the space and achieve revisit

time constraints. However, the output of the process presented here should not be taken as the absolute perfect answer to a persistent surveillance problem. A decision maker should interpret such a solution as a good starting point from which (possibly) a better solution could be built. In particular, a better solution could arise from conditioning the terminal points inside of the surveillance space before processing them to find the solution. Conditioning in this context means finding centroids of clusters of terminal points inside of the space and associating each cluster with its centroid - in a sense, collapsing clusters to points to avoid extremely small partitions. This conditioning could be improved if it is preceded by preprocessing of the space itself to orient the terminal points such that the maximum number of collinear points are horizontally situated.

This research presents an original approach to the problem of continually (in fact, persistently) surveying an area of land during for the duration of a mission timeline, given some desired maximum revisit time for a number of defined locations within that area. This is the first work to consider the application of integer programming to divide a space into subregions for efficient persistent surveillance by multiple autonomous UAVs. Moreover, this work, for the first time, defines explicitly the terms "persistent," "continuous," and "periodic" surveillance whereas these terms are currently considered synonymous in much of the literature.

The impact of this research is that it is possible, using the techniques described here, to derive a persistent surveillance program from locations on a map that are provided by the intelligence community. With these techniques, personnel with access to a modern desktop computer and some relatively inexpensive software can quickly generate a partition of the space and assign appropriate UAVs to each partition for efficient search of the entire space to include areas surrounding the points of interest identified by intelligence personnel. The procedure used here is flexible in that a commander can use the output of the algorithms as a starting point and make different decisions based on factors not considered in this model

(but could be considered in future refinements). In fact, some amount of postprocessing is expected. That is, the model is a good tool to obtain a fairly decent solution, but a decision maker (or other competent authority) needs to review any such solution to ensure optimality has actually been achieved. Using this procedure represents a chance to save money and other resources (fuel, operating costs, etc.) during defined military surveillance missions.

This research could go in a number of directions including the introduction of more UAV choices, modeling camera characteristics, and considering what happens when UAV reliability and maintainability are factored into the model. Whatever direction it is taken, the basic problem of persistent surveillance is an important one, and it makes sense to use the minimum amount of resources to accomplish the task.

Appendix A. Excel® VBA Code

```
'Author: Umar M. Khan, Maj, USAF
'Student, Dept of Operational Sciences
'Air Force Institute of Technology
'Wright-Patterson Air Force Base, OH
'
'Date: February 20, 2014

Option Explicit

Const width = 150
Const height = 100
Const numTerminals = 15
Const minXCoordVal = 20
Const maxXCoordVal = 130
Const minYCoordVal = 20
Const maxYCoordVal = 80
Const terminalPoint = 1
Const boundaryPoint = 2
Const steinerPoint = 3

' Generate Scnerio 8...code exactly the same for every scenario
Const GridOutputSheet = ''Scenario8''
Dim prepOutput As Range
Dim gridOutput As Range
Dim rngLastCell As Integer
Dim nextRow As Range
Dim terminalXcoords(1 To numTerminals) As Integer
Dim terminalYcoords(1 To numTerminals) As Integer
Dim xDimMax As Integer
Dim yDimMax As Integer

Sub GenerateGridTangle()
    Sheets(''PrepSheet'').Cells.ClearContents
    Sheets(GridOutputSheet).Cells.ClearContents
    Set prepOutput = Sheets(''PrepSheet'').Range(''entryField'')
    Set gridOutput = Sheets(GridOutputSheet).Range(''GridTangle'')
    'exercise rng
    Dim h As Integer
    Dim b As Double
```

```
    For h = 1 To 20000
        b = Rnd
    Next h
    Call GenerateTerminalPoints
    Call GenerateBoundaryPoints
    Call GenerateSteinerPoints
    Call SortGridTangle
End Sub

Function findLastUnusedRow(G As Integer) As Integer
    Dim lastRow As Range
    'What is the last (used or unused) cell in ''R5''!A:A ?
    Set lastRow = Sheets(GridOutputSheet).Cells(Sheets(GridOutputSheet).Rows.Count, ''A'')
    If G = 1 Then
        'What is the last used row in GridOutputSheet!A:A ?
        findLastUnusedRow = lastRow.End(xlUp).Row + 1
    ElseIf G = 2 Then
        findLastUnusedRow = lastRow.End(xlUp).Row - 1
    Else
        findLastUnusedRow = -1 ' error
    End If
End Function

Sub DeleteDuplicateRows()
    Dim x As Long
    Dim LstRow As Long
    Application.ScreenUpdating = False
    Sheets(GridOutputSheet).Select
    Cells.Select
    Selection.Sort Key1:=Range(''A1:B1''), Order1:=xlAscending, Key2:=Range(''B1'') _
        , Order2:=xlAscending, Header:=xlGuess, OrderCustom:=1, MatchCase:= _
        False, Orientation:=xlTopToBottom, DataOption1:=xlSortNormal, DataOption2 _
        :=xlSortNormal
    LstRow = ActiveCell.SpecialCells(xlCellTypeLastCell).Row
    For x = LstRow To 2 Step -1
        If (Cells(x, 1).Value = Cells(x - 1, 1).Value And _
            Cells(x, 2).Value = Cells(x - 1, 2).Value) Then
            Cells(x, 1).EntireRow.Delete
        End If
    Next
```

```
    Application.ScreenUpdating = True
End Sub

Sub GenerateTerminalPoints()
    ' Generate Terminal Points (x, y values between minCoordVal & maxCoordVal)
    Dim i As Integer
    Dim xCoord As Integer
    Dim yCoord As Integer

    For i = 1 To numTerminals
        xCoord = Int((maxXCoordVal - minXCoordVal + 1) * Rnd + minXCoordVal)
        yCoord = Int((maxYCoordVal - minYCoordVal + 1) * Rnd + minYCoordVal)
        prepOutput(xCoord, yCoord).Value = 1
        gridOutput(i, 1) = xCoord
        gridOutput(i, 2) = yCoord
        gridOutput(i, 3) = terminalPoint
        terminalXcoords(i) = xCoord
        terminalYcoords(i) = yCoord
    Next i
End Sub

Sub GenerateBoundaryPoints()
 ' Generate boundary points (includes repeats for collinear terminal points)

    Dim j As Integer

    For j = 1 To numTerminals
        rngLastCell = findLastUnusedRow(1)
        Set nextRow = Sheets(GridOutputSheet).Cells(rngLastCell, 1)
        nextRow.Cells(j, 1).Value = terminalXcoords(j)
        nextRow.Cells(j, 2).Value = 0
        nextRow.Cells(j, 3).Value = boundaryPoint
        prepOutput.Cells(terminalXcoords(j), 1).Value = boundaryPoint
        nextRow.Cells(j + 1, 1).Value = terminalXcoords(j)
        nextRow.Cells(j + 1, 2).Value = height
        nextRow.Cells(j + 1, 3).Value = boundaryPoint
        prepOutput.Cells(terminalXcoords(j), height).Value = boundaryPoint
        nextRow.Cells(j + 2, 1).Value = width
        nextRow.Cells(j + 2, 2).Value = terminalYcoords(j)
        nextRow.Cells(j + 2, 3).Value = boundaryPoint
```

```
        prepOutput.Cells(width, terminalYcoords(j)).Value = boundaryPoint
        nextRow.Cells(j + 3, 1).Value = 0
        nextRow.Cells(j + 3, 2).Value = terminalYcoords(j)
        nextRow.Cells(j + 3, 3).Value = boundaryPoint
        prepOutput.Cells(1, terminalYcoords(j)).Value = boundaryPoint
    Next j

    'Eliminate duplicate boundary points
    Call DeleteDuplicateRows

    Sheets(''PrepSheet'').Activate

    'Generate special boundary points (corner points)
    rngLastCell = findLastUnusedRow(1)
    Set nextRow = Sheets(GridOutputSheet).Cells(rngLastCell, 1)
    nextRow.Cells(1, 1).Value = 0
    nextRow.Cells(1, 2).Value = 0
    nextRow.Cells(1, 3).Value = boundaryPoint
    prepOutput.Cells(1, 1).Value = boundaryPoint
    nextRow.Cells(2, 1).Value = 0
    nextRow.Cells(2, 2).Value = height
    nextRow.Cells(2, 3).Value = boundaryPoint
    prepOutput.Cells(1, height).Value = boundaryPoint
    nextRow.Cells(3, 1).Value = width
    nextRow.Cells(3, 2).Value = 0
    nextRow.Cells(3, 3).Value = boundaryPoint
    prepOutput.Cells(width, 1).Value = boundaryPoint
    nextRow.Cells(4, 1).Value = width
    nextRow.Cells(4, 2).Value = height
    nextRow.Cells(4, 3).Value = boundaryPoint
    prepOutput.Cells(width, height).Value = boundaryPoint

    'Get number of boundary points
    xDimMax = WorksheetFunction.CountA(Range(''A:A''))
    yDimMax = WorksheetFunction.CountA(Range(''1:1''))
End Sub

Sub GenerateSteinerPoints()
    'Get last unused row in grid output sheet
    rngLastCell = findLastUnusedRow(1)
```

```
    Set nextRow = Sheets(GridOutputSheet).Cells(rngLastCell, 1)

    'Generate Steiner points
    Dim currentCell As Range
    Dim k As Integer
    Dim m As Integer
    Dim x As Integer

    x = 1
    For k = minXCoordVal To maxXCoordVal
        Set currentCell = prepOutput.Cells(k, 1)
        If currentCell.Value = boundaryPoint Then
            For m = minYCoordVal To maxYCoordVal
                Set currentCell = prepOutput.Cells(1, m)
                If currentCell.Value = boundaryPoint Then
                    If Columns(m).Cells(k, 1).Value = ‘‘’’ Then
                        Columns(m).Cells(k, 1).Value = steinerPoint
                        nextRow.Cells(x, 1).Value = k
                        nextRow.Cells(x, 2).Value = m
                        nextRow.Cells(x, 3).Value = steinerPoint
                        x = x + 1
                    End If
                End If
            Next m
        End If
    Next k
    'Tack on GridTangle characteristics...will be used in MATLAB
    nextRow.Cells(x, 1).Value = xDimMax
    nextRow.Cells(x, 2).Value = yDimMax
    nextRow.Cells(x, 3).Value = 0
End Sub

Sub SortGridTangle()
    'Get last unused row in grid output sheet
    rngLastCell = findLastUnusedRow(1)
    Set nextRow = Sheets(GridOutputSheet).Cells(rngLastCell, 1)

    'sort results by y-coord then by x-coord
    Sheets(GridOutputSheet).Activate
    Dim sortRange As Range
```

```
    Dim beginRange As String
    Dim endRange As String

    rngLastCell = findLastUnusedRow(2)
    beginRange = ''A1''
    endRange = ''C'' & rngLastCell
    Set sortRange = Range(beginRange, endRange)
    sortRange.Select
    Selection.Sort Key1:=Range(''B1''), Order1:=xlAscending, Key2:=Range(''A1'') _
        , Order2:=xlAscending, Header:=False, OrderCustom:=1, MatchCase:= _
        False, Orientation:=xlTopToBottom, DataOption1:=xlSortNormal, DataOption2 _
        :=xlSortNormal
    Range(''A1'').Select
End Sub
```

Appendix B. MATLAB® Code

```
% Main File
%
% Author: Umar M. Khan, Maj, USAF
% Student, Dept of Operational Sciences
% Air Force Institute of Technology
% Wright-Patterson Air Force Base, OH
%
% Date: February 14, 2014

clear
clc



% MAIN PROGRAM
%%%%%%%%%%%%%%%%%%%%%%%%%%%%%%%%%%%%%%%%%%%%%%%%%%%%%%%%%%%%%%%%%%%%%%%%%%%%%%%
%                   PART I: PARTITION RECTANGLE                              %
%%%%%%%%%%%%%%%%%%%%%%%%%%%%%%%%%%%%%%%%%%%%%%%%%%%%%%%%%%%%%%%%%%%%%%%%%%%%%%%

% Read in raw data
RAW = xlsread('GridTangleData.xlsm', 'Scenario7');
R = RAW(1:end-1,:);
GridDim = RAW(end, 1:2);
Rdim = RAW(end-1, 1:2);

% Set up variables for binary IP
Grid = GenerateGrid(R);
Terminals = GetTerminalPoints(Grid);
[Neighborhood] = BuildNeighborhood(Grid, GridDim, Rdim);
[SubStructure, Canonicals, Feasibles] = GenerateSubRectangles(Neighborhood, Terminals, GridDim);
FeasibleCompositions = Decompose(Feasibles, Canonicals);
CostStructure = FeasibleRectangleCosts(Feasibles);

%Solve binary IP (Branch and Bound)..solves a series of LP relaxations
%Verifies by also solving LPs
sizeFC = size(FeasibleCompositions, 2);
b = ones(sizeFC, 1);
x = bintprog(CostStructure', FeasibleCompositions', b, FeasibleCompositions', b);
B = full(x);
```

```
Partition = IdentifyPartition(B, Feasibles);

VisualData = GenerateFigure(Terminals, Partition, Rdim);

%%%%%%%%%%%%%%%%%%%%%%%%%%%%%%%%%%%%%%%%%%%%%%%%%%%%%%%%%%%%%%%%%%%%%%%%%%%%
%                        PART II: ASSIGN UAVs                              %
%%%%%%%%%%%%%%%%%%%%%%%%%%%%%%%%%%%%%%%%%%%%%%%%%%%%%%%%%%%%%%%%%%%%%%%%%%%%

MISSION_DURATION = 48; % hours of surveillance - modify as needed
MAX_REVISIT_TIME = 9;   % DM's desired maximum revisit time in hours
U = InitializeUAVs();
Mapping = Match(U, Partition, MISSION_DURATION, MAX_REVISIT_TIME);
Q = PrintMapping(Partition, Mapping);

%-------------------------------------------------------------------------
% CLASSES

classdef GridPoint
    %GridPoint objects are: Terminal, Steiner, and edge points of R
    %   Ref: Meneses and Souza (1998); point objects are used to define
    %   objects of class FeasibleRectangle

    properties
        x
        y
        type
        nXpos = Neighbor;
        nYpos = Neighbor;
        nXneg = Neighbor;
        nYneg = Neighbor;
    end

    methods

        % class constructor
        function p      = GridPoint(c1, c2, t)
            p.x         = c1;
            p.y         = c2;
            p.type      = t;
        end
```

```
    end
end

classdef SubRectangle

    % Class of subrectangles (superset of feasible rectangles)

    properties
        cost              %cost of including rectangle
        ID                %identifier
        TL  = GridPoint;  %top left
        TR  = GridPoint;  %top right
        BL  = GridPoint;  %bottom left
        BR  = GridPoint;  %bottom right
    end

    methods
        % class constructor
        function rect = SubRectangle(bl, tl, br, tr, id)
            rect.BL  = bl;
            rect.TL  = tl;
            rect.BR  = br;
            rect.TR  = tr;
            rect.ID  = id;
        end

        function per = Perimeter(r)
            a    = r.TR.x - r.TL.x;
            b    = r.TL.y - r.BL.y;
            per  = 2*(a + b);
        end

        % cost incurred by anchored rectangles
        function ec = ExtraCost(rangle)

            % parameters of rectangle R
            width = 50;
            height = 40;

            val = 0;
```

```
            if (rangle.TL.x == 0)
                val = val + (rangle.TL.y - rangle.BL.y);
            end

            if (rangle.TL.y == height)
                val = val + (rangle.TR.x - rangle.TL.x);
            end

            if (rangle.TR.x == width)
                val = val + (rangle.TR.y - rangle.BR.y);
            end

            if (rangle.BL.y == 0)
                val = val + (rangle.BR.x - rangle.BL.x);
            end

            ec = val;
        end
    end
end

classdef Neighbor
    %Every GridPoint object has one or two neighbors in the ‘‘up’’ or ‘‘right’’
    %directions on the grid GI(P).

    properties
        N = GridPoint;
    end
end

classdef UAV
    % Creates UAV objects with select properties
    properties
        designation
        speed
        cameraSwath
        turnRate180
        endurance
        radius
```

```
    end

    methods
        % class constructor
        function u = UAV(d, s, cs, tr, e, r)
            u.designation = d;
            u.speed = s;
            u.cameraSwath = cs;
            u.turnRate180 = tr;
            u.endurance = e;
            u.radius = r;
        end
    end
end

classdef Assignment
    % Objects include subrectangles and their assigned UAV types
    % along with how many of each UAV is required for the mission
    % duration.

    properties
        rect = SubRectangle;
        vehicle = UAV;
        count % number of the assigned UAV needed
        revisitTime
    end

    methods
        % class constructor
        function A = Assignment(SubRect, AirVehicle, num, rt)
            A.rect = SubRect;
            A.vehicle = AirVehicle;
            A.count = num;
            A.revisitTime = rt;
        end
    end
end

%-------------------------------------------------------------------------
% FUNCTIONS
```

```
function [P] = IdentifyPartition(B, F)
    % Use output of bintprog to identify feasible rectangles
    % in optimal partition (lowest cost).

    sizeB = size(B,1);
    part = SubRectangle.empty;

    k = 1;

    for m = 1:sizeB
        if (B(m) == 1)
            % Collect partition elements
            part(k) = F(m);
            k = k+1;
        end
    end

    [P] = part;
end

function [PlotValues] = GenerateFigure(T, P, plotDims)
    % Draw a plot of terminals

    numTerminals = size(T, 2);
    terminalList = zeros(numTerminals, 2);
    xMax = plotDims(1);
    yMax = plotDims(2);

    k = 1;

    for m = 1:numTerminals
        terminalList(k, 1) = T(m).x;
        terminalList(k, 2) = T(m).y;
        k = k + 1;
    end

    sizeP = size(P,2);

    figure(1)
```

```
         plot(terminalList(:,1), terminalList(:,2), 'r*')
         axis([0 xMax 0 yMax])

    figure(2)
        plot(terminalList(:,1), terminalList(:,2), 'r*')
        axis([0 xMax 0 yMax])
        hold on
        for n = 1:sizeP
            plot([P(n).TL.x, P(n).TR.x], [P(n).TL.y, P(n).TR.y])
            plot([P(n).TL.x, P(n).BL.x], [P(n).TL.y, P(n).BL.y])
            plot([P(n).BL.x, P(n).BR.x], [P(n).BL.y, P(n).BR.y])
            plot([P(n).TR.x, P(n).BR.x], [P(n).TR.y, P(n).BR.y])
        end

    [PlotValues] = terminalList;
end

function [A] = GenerateGrid(rawData)
    % Pass a list of ordered pairs.
    % Output an array of GridPoint objects (a ``rectangle'').

    rows = size(rawData,1);
    GridPoints = GridPoint.empty;

    for m = 1:rows
       GridPoints(m) = GridPoint(rawData(m,1),rawData(m,2),rawData(m,3));
    end

    [A] = GridPoints;
end

function [T] = GetTerminalPoints(GT)
    % Get list of terminal points

    sizeGT = size(GT,2);
    Terminals = GridPoint.empty;

    k = 1;

    for m = 1:sizeGT
```

```
        if (GT(m).type == 1)
            Terminals(k) = GT(m);
            k = k+1;
        end
    end

    [T] = Terminals;
end

function [N] = BuildNeighborhood(GT, GD, RD)
    % For a given array of GridPoint objects - a ‘‘GridTangle’’ (GT),
    % produce the neighbors - up, right, down, left - of each point.

    sizeGT   = size(GT,2);

    % parameters specific to each rectangle R
    xDimMax  = GD(1);
    width    = RD(1);
    height   = RD(2);

    % up and right neighbors
    for k = 1:sizeGT
        if (GT(k).y == height) && (k < sizeGT)
            GT(k).nXpos = GT(k+1);
            %GT(k).nYpos is null
        elseif (GT(k).x == width) && (k <= sizeGT-xDimMax)
            %GT(k).nXpos is null
            GT(k).nYpos = GT(k+xDimMax);
        elseif (GT(k).x == width) && (GT(k).y == height)
            %do nothing
        else
            GT(k).nXpos = GT(k + 1);
            GT(k).nYpos = GT(k + xDimMax);
        end
    end

    % down and left neighbors
    for z = sizeGT:-1:1
        if (GT(z).y == 0) && (z > 1)
            GT(z).nXneg = GT(z-1);
```

```
            %GT(z).nYneg is null
        elseif (GT(z).x == 0) && (z > 1)
            %GT(z).nXneg is null
            GT(z).nYneg = GT(z-xDimMax);
        elseif (GT(z).x == 0) && (GT(z).y == 0)
            %do nothing
        else
            GT(z).nXneg = GT(z - 1);
            GT(z).nYneg = GT(z - xDimMax);
        end
    end

    [N] = GT;
end

function [S, C, F] = GenerateSubRectangles(N, T, GD)
    % Input some ‘‘GridTangle’’ (N) and output the set of all subrectangles.
    % Output includes infeasible rectangles.

    SR = SubRectangle.empty;
    Canonicals = SubRectangle.empty;
    Feasibles = SubRectangle.empty;

    % parameters - modify for each input rectangle R
    xDimMax = GD(1);
    yDimMax = GD(2);

    chunkSize = yDimMax - 1;
    neighborhoodSize = size(N,2);
    numTerminals = size(T,2);

    id  = 1;
    cid = 1;
    fid = 1;

    % HORIZONTAL SUBRECTANGLE GENERATION
    for t = 1:chunkSize

        maxIndex = neighborhoodSize - t*xDimMax - 1;
```

```
k = 1;
for m = 1:maxIndex

    if (mod(m, xDimMax) == 1) && (m > 1)
        k = k + 1;
    end

    if (mod(m, xDimMax) == 0)
        continue
    else
        bl  = N(m);
        tl  = N(m + t*xDimMax);
    end

    nmax = k*xDimMax - m - 1;

    for n = 0:nmax

        br = N(m + n + 1);
        tr = N(m + n + 1 + t*xDimMax);
        SR(id) = SubRectangle(bl,tl,br,tr,id);
        SR(id).cost = SR(id).Perimeter;

        count = 0;

        if (t == 1) && (n == 0)
            % extract canonicals
            Canonicals(cid) = SR(id);
            cid = cid + 1;
        end

        if (t == 1)
            Feasibles(fid) = SR(id);
            fid = fid  + 1;
        else
            for g = 1:numTerminals
                if (T(g).y >= SR(id).TL.y) || (T(g).y <= SR(id).BL.y) || (T(g).x >= SR(id).TR.x)...
                 || (T(g).x <= SR(id).TL.x)
                    % terminal point is not in interior of SR(id)
                    count = count + 1;
```

```
                    end
                end

                if (count == numTerminals)
                    Feasibles(fid) = SR(id);
                    fid = fid + 1;
                end
            end
            id  = id + 1;
        end
    end

    [S] = SR;
    [C] = Canonicals;
    [F] = Feasibles;
end

function [FC] = Decompose(F, C)
    % take feasible rectangles and associate canonicals
    % a_ij = 0 if feasible rectangle j contains canonical i

    sizeF = size(F,2);
    sizeC = size(C,2);

    FeasibleCompositions = zeros(sizeF, sizeC);

    for m = 1:sizeF

        for n = 1:sizeC

            if (C(n).BL.x >=  F(m).BL.x) && (C(n).BR.x <= F(m).BR.x) && (C(n).BL.y >= F(m).BL.y)...
             && (C(n).TL.y <= F(m).TL.y)
                FeasibleCompositions(m,n) = 1;
            end
        end
    end

    [FC] = FeasibleCompositions;
end
```

```
function [CS] = FeasibleRectangleCosts(F)
    %Collect cost of every feasible subrectangle in a vector

    sizeF = size(F,2);
    CostStructure = zeros(1, sizeF);

    for m = 1:sizeF
        CostStructure(m) = F(m).cost;
    end

    [CS] = CostStructure;
end

function [V] = InitializeUAVs()
    % Create UAV objects

    UAVs = UAV.empty;

    UAVs(1) = UAV('RQ-11 Raven', 48, 1, 1, 1.5, 10);
    UAVs(2) = UAV('RQ-7 Shadow', 185, 3, 1, 6, 125);
    UAVs(3) = UAV('RQ-4 Global Hawk', 640, 10, 1, 32, 10000);

    [V] = UAVs;
end

function [M] = Match(U, Part, missionTime, maxRevisitTime)
    % map a set U of UAVs to a Partition P of an instance of the RGP

    partitionSize = size(Part,2);
    numOfUAVs = size(U,2);
    A = Assignment.empty;
    oneMinute = 1/60;
    t_est = 0;

    for k = 1:partitionSize

        height = Part(k).TL.y - Part(k).BL.y;
        width = Part(k).BR.x - Part(k).BL.x;
```

```
if width >= height

    for r = 1:numOfUAVs

        x = 0;

        if height <= U(r).cameraSwath
            t_est = oneMinute + 2*width/U(r).speed;
        else
            t_est = (2*width*height/U(r).cameraSwath)/U(r).speed ...
               + oneMinute*(2*height/U(r).cameraSwath - 1);
        end

        if t_est <= maxRevisitTime
            numUAVs = ceil(missionTime/U(r).endurance);
            A(k) = Assignment(Part(k), U(r), round(numUAVs), t_est);
            x = x + 1;
            break
        end

    end

    if x == 0   % no UAV meets revisit time criterion
        A(k) = Assignment(Part(k), UAV('None', 0,0,0,0,0), 0, t_est);
    end

else    % height > width

    for n = 1:numOfUAVs

        x = 0;

        if width <= U(n).cameraSwath
            t_est = oneMinute + 2*height/U(n).speed;
        else
            t_est = (2*width*height/U(n).cameraSwath)/U(n).speed ...
               + oneMinute*(2*width/U(n).cameraSwath - 1);
        end

        if t_est <= maxRevisitTime
```

```
                numUAVs = ceil(missionTime/U(n).endurance);
                A(k) = Assignment(Part(k), U(n), round(numUAVs), t_est);
                x = x + 1;
                break
            end

        end

        if x == 0
            A(k) = Assignment(Part(k), UAV('None', 0,0,0,0,0), 0, t_est);
        end

    end

    [M] = A;

end

function [V] = PrintMapping(P, M)
    % Print Mapping Solution

    sizeP = size(P,2);

    for m = 1:sizeP
        [P(m).TL.x P(m).TL.y P(m).BR.x P(m).BR.y]
        width = P(m).TR.x - P(m).TL.x;
        height = P(m).TL.y - P(m).BL.y;
        [width, height]
        M(m).vehicle.designation
        M(m).count
        M(m).revisitTime
    end

    [V] = 1;
end
```

Bibliography

[1] "C-17 Globemaster III Factsheet", 2008. URL http://www.172aw.ang.af.mil/resources/factsheets/factsheet.asp?fsID=12699&page=2.

[2] "Platforms for Persistent Communications, Surveillance and Reconnaissance". Army Science Board Report, 2008.

[3] "FY2009-2034 Unmanned Systems Integrated Roadmap". U.S. Department of Defense, 2010.

[4] "Global Hawk unloading from C-5 Galaxy", 2011. URL http://www.goodfellow.af.mil/news/story.asp?id=123272577.

[5] "Agencies Could Improve Information Sharing and End-Use Monitoring on Unmanned Aerial Vehicle Exports". GAO Report, 2012.

[6] "Gallery of USAF Weapons". Air Force Magazine, 2012.

[7] "JP 2-01: Joint and National Intelligence Support to Military Operations". U.S. Department of Defense, 2012.

[8] "Department of Defense Dictionary of Military and Associated Terms". U.S. Department of Defense Report, 2013.

[9] "JP 2-0: Joint Intelligence". Joint Military Doctrine, 2013.

[10] "UN Starts Drone Surveillance in DR Congo", 2013. URL http://www.bbc.com/news/world-africa-25197754.

[11] "MATLAB® documentation", 2014. URL http://www.mathworks.com/help/optim/ug/binary-integer-programming-algorithms.html.

[12] "MQ-8 Fire Scout", 2014. URL http://www.navair.navy.mil/index.cfm?fuseaction=home.display&key=8250AFBA-DF2B-4999-9EF3-0B0E46144D03.

[13] "RQ-4A/B Global Hawk HALE Reconnaissance UAV, United States of America", 2014. URL http://www.airforce-technology.com/projects/rq4-global-hawk-uav/.

[14] Ahmadzadeh, Ali, Gilad Buchman, Peng Cheng, Ali Jadbabaie, Jim Keller, Vijay Kumar, and George Pappas. "Cooperative control of UAVs for Search and Coverage". Proceedings of the AUVSI Conference on Unmanned Systems. Orlando, FL. August 29–31, 2006.

[15] Ahmadzadeh, Ali, James Keller, Ali Jadbabaie, and Vijay Kumar. "Multi-UAV Cooperative Surveillance with Spatio-Temporal Specifications". 45th IEEE Conference on Decision and Control. San Diego, CA. December 13–15, 2006.

[16] Akella, Mohan, Sharad Gupta, and Avijit Sarkar. "Branch and Price: Column Generation for Solving Huge Integer Programs", 2014. URL http://www.acsu.buffalo.edu/~nagi/courses/684/price.pdf.

[17] Barr, Alistair. "Amazon testing delivery by drone, CEO Bezos says". *USA Today*, 2013. URL http://www.usatoday.com/story/tech/2013/12/01/amazon-bezos-drone-delivery/3799021/.

[18] Carlsson, John. "Dividing a Territory among Several Vehicles", *INFORMS Journal on Computing*, 24:565–577, 2012.

[19] Cavas, Christopher. "Fire Scout UAVs bound for Afghanistan", 2011. URL http://www.navytimes.com/article/20110421/NEWS/104210326/Fire-Scout-UAVs-bound-Afghanistan.

[20] Chepoi, Victor, Karim Nouioua, and Yann Vaxès. "A Rounding Algorithm for Approximating Minimum Manhattan Networks", *Theoretical Computer Science*, 390(1):56–69, 2008.

[21] Choset, Howie. "Coverage for Robotics &Ndash; A Survey of Recent Results", *Annals of Mathematics and Artificial Intelligence*, 31(1-4):113–126, 2001.

[22] Choset, Howie and Philippe Pignon. "Coverage Path Planning: The Boustrophedon Decomposition". 1st International Conference on Field and Service Robotics. Canberra, Australia, 1997.

[23] Erwin, Sandra. "For U.S. Air Force, the Cost of Operating Unmanned Aircraft Becoming Unsustainable", 2011. URL http://www.nationaldefensemagazine.org/blog/Lists/Posts/Post.aspx?ID=523.

[24] Garfinkel, Robert. "An Improved Algorithm for the Bottleneck Assignment Problem", *Operations Research*, 19(7):1747–1751, 1971.

[25] Garfinkel, Robert and George Nemhauser. *Integer Programming*. Wiley, New York, 1972.

[26] Gudmundsson, Joachim, Christos Levcopoulos, and Giri Narasimhan. "Approximating a Minimum Manhattan Network", *Nordic J. Comput*, 8:2001, 1999.

[27] Ha, Taegyun. *The UAV Continuous Coverage Problem*. Master's thesis, Air Force Institute of Technology, 2010.

[28] Hert, Susan and Vladimir Lumelsky. "Polygon Area Decomposition for Multiple-Robot Workspace Division", *International Journal of Computational Geometry and Applications*, 8:437–466, 1998.

[29] Huang, Wesley. "Optimal Line-sweep-based Decompositions for Coverage Algorithms". Proceedings of the 2001 IEEE International Conference on Robotics and Automation. Seoul, South Korea. May 21–26, 2001.

[30] Marwedel, Peter, Lothar Thiele, and Frank Vahid. "Partitioning Algorithms..." compiled lecture notes, n.d.

[31] Maza, Ivan and Anibal Ollero. "Multiple UAV Cooperative Searching Operation using Polygon Area Decomposition and Efficient Coverage Algorithms". School of Engineering, University of Seville, 2006.

[32] de Meneses, Cludio Nogueira and Cid Carvalho de Souza. "Exact Solutions of Rectangular Partitions via Integer Programming". Universidade Estadual de Campinas, Instituto de Computação, Campinas/SP, Brazil, 1998.

[33] Nigam, Nikhil. *Control and Design of Multiple Unmanned Air Vehicles for Persistent Surveillance*. Ph.D. thesis, Stanford University, 2009.

[34] Nigam, Nikhil and Ilan Kroo. "Persistent Surveillance Using Multiple Unmanned Air Vehicles". Proceedings of the IEEE Aerospace Conference. Big Sky, MT. March 1–8, 2008.

[35] O'Rourke, Joseph and Geetika Tewari. "The Structure of Optimal Partitions of Orthogonal Polygons into Fat Rectangles", *Computational Geometry*, 28:49–71, 2004.

[36] Ousingsawat, Jarurat. "UAV Path Planning for Maximum Coverage Surveillance of Area with Different Priorities". The 20th Conference of Mech. Engineering Network of Thailand. Nakhon Ratchasima, Thailand. October 18–20, 2006.

[37] Pohl, Adam J. *Multiobjective UAV Mission Planning using Evolutionary Computation*. Master's thesis, Air Force Institute of Technology, 2008.

[38] Quijano, Humberto and Leonardo Garrido. "Improving Cooperative Robot Exploration Using an Hexagonal World Representation". Electronics, Robotics and Automotive Mechanics Conference. Cuernacava, Morelos, Mexico. September 25–28, 2007.

[39] Rader, David. *Deterministic Operations Research*. Wiley, New Jersey, 2010.

[40] Stone, Andrea. "Drone Program Aims To Accelerate Use Of Unmanned Aircraft By Police", 2012. URL `http://www.huffingtonpost.com/2012/05/22/drones-dhs-program-unmanned-aircraft-police_n_1537074.html`.

[41] Yanmaz, Evsen. "Connectivity Versus Area Coverage in Unmanned Aerial Vehicle Networks". IEEE International Conference on Communications. Ottawa, Canada. June 10–15, 2012.

REPORT DOCUMENTATION PAGE

Form Approved
OMB No. 0704–0188

1. REPORT DATE *(DD–MM–YYYY)*	2. REPORT TYPE	3. DATES COVERED *(From — To)*
27–03–2014	Master's Thesis	Aug 2012 – Mar 2014

4. TITLE AND SUBTITLE

OPTIMAL PARTITIONING OF A SURVEILLANCE SPACE FOR PERSISTENT COVERAGE USING MULTIPLE AUTONOMOUS UNMANNED AERIAL VEHICLES: AN INTEGER PROGRAMMING APPROACH

5a. CONTRACT NUMBER

5b. GRANT NUMBER

5c. PROGRAM ELEMENT NUMBER

6. AUTHOR(S)

Khan, Umar M., Major, USAF

5d. PROJECT NUMBER

5e. TASK NUMBER

5f. WORK UNIT NUMBER

7. PERFORMING ORGANIZATION NAME(S) AND ADDRESS(ES)

Air Force Institute of Technology
Graduate School of Engineering and Management (AFIT/EN)
2950 Hobson Way
WPAFB OH 45433-7765

8. PERFORMING ORGANIZATION REPORT NUMBER

AFIT-ENS-14-M-16

9. SPONSORING / MONITORING AGENCY NAME(S) AND ADDRESS(ES)

Intentionally Left Blank

10. SPONSOR/MONITOR'S ACRONYM(S)

11. SPONSOR/MONITOR'S REPORT NUMBER(S)

12. DISTRIBUTION / AVAILABILITY STATEMENT

Distribution Statement A: Approved for Public Release; Distribution Unlimited

13. SUPPLEMENTARY NOTES

14. ABSTRACT

Unmanned aerial vehicles (UAVs) are an essential tool for the battlefield commander in part because they represent an attractive intelligence gathering platform that can quickly identify targets and track movements of individuals within areas of interest. In order to provide meaningful intelligence in near-real time during a mission, it makes sense to operate multiple UAVs with some measure of autonomy to survey the entire area persistently over the mission timeline. This research considers a space where intelligence has identified a number of locations and their surroundings that need to be monitored for a period of time. An integer program is formulated and solved to partition this surveillance space into the minimum number of subregions such that these locations fall outside of each partitioned subregion for efficient, persistent surveillance of the locations and their surroundings. Partitioning is followed by a UAV-to-partitioned subspace matching algorithm so that each subregion of the partitioned surveillance space is assigned exactly one UAV. Because the size of the partition is minimized, the number of UAVs used is also minimized.

15. SUBJECT TERMS

Set Partitioning, Integer Programming, Persistent Surveillance, Unmanned Aerial Vehicles

16. SECURITY CLASSIFICATION OF:			17. LIMITATION OF ABSTRACT	18. NUMBER OF PAGES	19a. NAME OF RESPONSIBLE PERSON
a. REPORT	b. ABSTRACT	c. THIS PAGE			James W. Chrissis, Ph.D., AFIT/ENS
U	U	U	UU	121	19b. TELEPHONE NUMBER *(include area code)* (937) 255–3636 ext 4606; james.chrissis@afit.edu